EXTENDED AMYGDALA CRH CIRCUITS TRIGGER AVERSIVE RESPONSES

Simon Chang

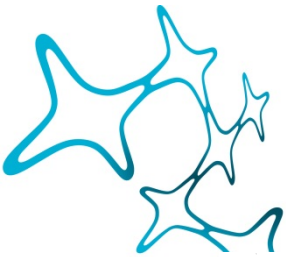

Graduate School of
Systemic Neurosciences

LMU Munich

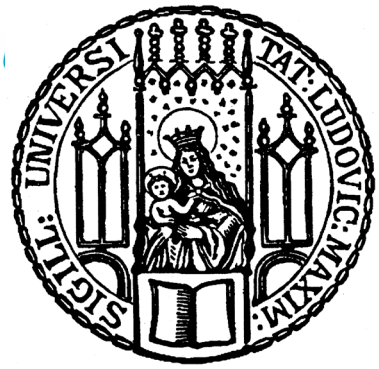

Dissertation at the
Graduate School of Systemic Neurosciences
Ludwig-Maximilians-Universität München

16.12.2020

Supervisor
Dr. Jan Deussing
Molecular Neurogenetics
Max Planck Institute of Psychiatry

First Reviewer: Dr. Jan Deussing
Second Reviewer: PD Dr. Carsten Wotjak
External Reviewer Pro Dr. Valery Grinevich

Date of Submission: 16.12.2020
Date of Defense: 29.04.2021

Contents

Abbreviations iv

Abstract 1

1. Introduction 2

1.1 The battle against mental disorders, where we are? 2

1.2 The Corticotropin-releasing hormone (CRH) system 3

1.2.1 CRH as a neuropeptide in the central nervous system 3

1.2.2 The CRH-family and its receptors 4

1.2.3 CRH and its role in stress 5

1.2.4 CRH receptors and their role in the CNS 6

1.2.5 CRH receptors in psychiatric diseases and clinical implications 8

1.3 Tracing of neurocircuits 11

1.4 Visualizing neurocircuits in the brain 18

1.5 Neurocircuitries of stress focusing on the extended amygdala 22

2. Aim of the thesis 26

3. Material and methods 27

3.1 Animals 27

3.2 Tissue dissection for single nucleus sequencing 28

3.3 Isolation of Nuclei 28

3.4 FACs (Fluorescence activated cell sorting) 28

3.5 Single nuclei RNA sequencing 29

3.6 Tissue collection and immunohistochemistry 29

3.7 CNO administration 30

3.8 R121919 administration 30

3.9 Assessment of animal behaviour 30

3.10 Virus and tracer injections 33

3.11 Optogenetic manipulation 34

3.12 In vivo optogenetic excitation 35

3.13 Real time place preference 35

3.14 CLARITY 35

3.15 iDISCO 36

3.16 Statistical analysis 36

4. Results 38

Towards a biological signature of CRHR1 neurons 38
4.1 Single-nucleus RNA sequencing 38
4.2 Validation of single nucleus sequencing results 42
4.2.1 Confirmation of heterogeneity of CRHR1 expressing cells in the ventral mid brain with immuno-histochemistry 42
Dissecting CRH/CRHR1 neurocircuits 44
4.3 Retrograde tracing 44
4.3.1 Retrograde tracing revealed the main brain regions projecting into the VTA 44
4.3.2 Retrograde tracing of CRH neurons revealed the main brain regions projecting into the substantia nigra (SN) 46
4.4 Anterograde tracing 47
4.4.1 Tracing of extended amygdala CRH efferences 47
4.4.2 Differences in connectivity between CeA and IPACL 51
4.4.3 Establishing tissue (brain) clearing methods 53
4.4.4 The molecular identity of CRH cells in the IPACL 56
4.5 Dissecting SN afferents using rabies virus-mediated retrograde tracing 58
4.5.1 CRH neurons have only minor synaptic contacts with CRHR1 neurons in the SN 58
4.5.2 Rabies virus tracing reveals main brain regions projecting into the SN 58
Functional characterization of CRH/CRHR1-specific neurocircuits 60
4.6 Activation of CRH neurons in IPACL induces aversive responses 60
4.6.1 Validation of chemogenetic tools 60
4.6.2 Activation of CRH neurons in the IPACL contributes to behavioural arousal 62
4.6.3 Activation of IPACL CRH neurons results in increased plasma corticosterone level 64
4.6.4 Activation of IPACL CRH neurons induced conditioned place aversion 65
4.6.5 Validation of optogenetic tools 66
4.6.6 Optogenetic activation confirmed that CRH neurons in the IPACL contribute to place aversion 67
4.6.7 Stimulation of CRH projections from the IPACL into the SN triggered place aversion 69
4.7 Activation of CRHR1 neurons in the SN promotes anxiogenic behaviours 71
4.7.1 Activation of CRHR1 neurons in the SN promotes anxiogenic behaviours 71
4.7.2 CRHR1 is essential for aversive behaviour 74
4.8 Globus pallidus CRHR1 neurons are involved in anxiety circuits 78
4.8.1 CRHR1 is strongly expressed in neurons of the globus pallidus 78

4.8.2 Parvalbumin positive CRHR1 neurons in the globus pallidus project into the SN . 80

4.8.3 Activation of CRHR1 neurons in the GPe contributes to place aversion and increases arousal 81

4.8.4 Activation of terminals of GPe CRHR1 neurons in the SN is sufficient to trigger place aversion 84

5. Discussion 86

References 95

6. Supplements 112

6.1 Curriculum Vitae 112

6.2 List of publications 115

6.3 Acknowledgements 117

6.4 List of contributions 119

6.5 Eidesstattliche Versicherung/Affidavit 120

Abbreviations

AAVs Adeno-associated viral vectors

ACTH Adrenocorticotropic hormone

BABB Benzyl benzoate

BDA Biotinylated dextran amine

BLA Basolateral amygdala

BNST Bed Nucleus of the stria terminalis

BSTLP Bed Nucleus of the stria terminalis, lateral posterior

BSTLD Bed Nucleus of the stria terminalis, lateral dorsal

CAV2 Canine adeno-virus

CCK Cholecystokinin

CeA Central amygdala

CLARITY Clear lipid-exchanged acrylamide-hybridized rigid imaging/immunostaining/in situ hybridization-compatible tissue-hydrogel

CeL Lateral part of the central amygdala

CeM Medial part of the central amygdala

CNO Clozapine N-oxide

ChR Channelrhodopsin 2

CRH Corticotropin-releasing hormone

CRH-BP CRH binding protein

CRHR1 Corticotropin-releasing hormone receptor 1

CSF cerebrospinal fluid

CTB Cholera toxin subunit B

CUBIC clear, unobstructed brain imaging cocktails and computational analysis

3DISCO 3-D imaging of solvent-cleared organs

dG-RV Deletion-mutant recombinant rabies virus

dlBNST Dorsolateral BNST

DREADD Designer receptor exclusively activated by designer drug

DRN Dorsal raphe nucleus

EPM Elevated plus maze

FDISCO DISCO with superior fluorescence-preserving capability

fMRI Functional magnetic resonance imaging

GABA γ-aminobutyric acid

GPe Globus pallidus external

GR Glucocorticoid receptor

GWAS Genome-wide association study

HYP Hypothalamus

HPA-axis Hypothalamic–pituitary–adrenal axis

HPC Hippocampus

HRP Horseradish peroxidase

iDISCO Immunolabeling-enabled three-dimensional imaging of solvent-cleared organs

IO Inferior olive

IPACL Interstitial nucleus of the posterior limb of the anterior commissure, lateral part

LC Locus coeruleus

LDCV Large, dense core vesicle

LH Lateral hypothalamus

MeA Medial amygdala

MB Midbrain

MGM Medial portion of the medial geniculate

MnPO Median preoptic nucleus

MR Mineralocorticoid receptors

NAc Nucleus accumbens

PAG Periaqueductal grey

PET Positron emission tomography

PFC Prefrontal cortex

PHA-L Phytohaemagglutinin-L

Pkcđ Protein kinase C đ

PL Prelimbic cortex

POMC Pro-opiomelanocortin

PTSD Post-traumatic stress disorder

PV Parvalbumin

PVN Paraventricular nucleus of the hypothalamus

PVT Paraventricular nucleus of the thalamus

SN Substantia nigra

SNc SN pars compacta

SNr SN pars reticulata

SNP Single nucleotide polymorphism

sn-RNASeq Single-nucleus RNA sequencing

SOM Somatostatin

SWITCH System-wide control of interaction time and kinetics of chemicals

TH Tyrosine hydroxylase

UCN1 Urocortin 1

UCN2 Urocortin 2

UCN3 Urocortin 3

uDISCO Ultimate DISCO

vHPC Ventral hippocampus

VMH Ventromedial hypothalamus

VTA Ventral tengemental area

WGA Wheat germ agglutinin

Abstract

Corticotropin-releasing hormone (CRH) regulates neuroendocrine functions such as adrenal glucocorticoid release and has a key role in stress-related behaviours. In addition, the corticotropin-releasing hormone receptor 1 (CRHR1) critically controls behavioural adaptation to stress and is causally linked to stress-related emotional disorders. However, there are still unanswered questions. In this study, single-nucleus sequencing was conducted to resolve the heterogeneity of midbrain CRHR1 neurons encompassing dopaminergic, GABAergic and glutamatergic neurons, which was further substantiated by immunostaining. Anterograde and retrograde tracings revealed strong projections of extended amygdala CRH neurons into the VTA and SN. Chemogenetic and optogenetic manipulation demonstrated that activation of CRH neurons in the interstitial nucleus of the posterior limb of the anterior commissure (IPACL), resulted in maladaptive behaviour, arousal and place aversion. Systemic injection of the CRHR1 antagonist R121919 was sufficient to reverses these behaviours indicating a direct role of CRH and CRHR1 in these circuits contributing to the behavioural outcomes. Overall, this study uncovered a novel CRH circuit originating from the IPACL, which is a part of extended amygdala innervating the SN. This circuit is modulated by the CRH/CRHR1-system and is involved in the regulation of arousal and place aversion behaviour.

1. Introduction

1.1 The battle against mental disorders, where we are?

With the dramatic rise in mental disorders and mental illnesses, psychiatry has become one of the fastest growing medical disciplines. For many years, scientists have fought hard in order to find a blink of light in the treatment of psychiatric disorders. On the way of discovery, there were many proposed targets that ultimately failed in clinical trials. This raised the question whether there is a gap in the technology or whether the approach of identifying possible markers or targets has been oversimplified. There are still too many mysteries in the understanding of stress, emotion and the development of psychiatric diseases.

Emotions dynamically integrate internal states and environmental stimuli to enable the rapid selection of situationally appropriate behaviours. There are many faces of emotional responses: ranging from positive to negative ones. Aim of this study is to discuss the dark side of emotions which is a fundamental reason for the development of psychiatric diseases. Throughout life, inevitably, there are stones in the way. Those stones could be any kind of events or circumstances that generated negative feelings. These adverse events are the fire that forges an individual's character. Unfortunately, these adverse events might be too heavy to carry in some cases, and alternatively lead to diseases. To understand the current progress in psychiatric research, one has to travel back in time. In 1921, Kraepelin, regarded as the contemporary father of psychiatry, published the article "Psychological work experiments" establishing 'descriptive psychiatry' and which laid the foundation for modern psychiatry [1]. For the next 3 decades research on psychiatric diseases followed two main research directions: The first focus was on designing different scales for diagnosis of mental disorders [2]. The second focus of the field was on psychopathology and the abnormal morphology of the brain [3-5]. With more and more different rating scales popping up [6-8], scientists also started to better describe the pathology of psychiatric diseases [9-11]. The focus on developing anti-psychotic drugs also emerged with the increasing comprehension of molecular mechanism underlying psychiatric diseases [12,13]. From the end of the second millennium, focus in psychiatric research changed again towards circuits of emotion which currently dominated the main stage. In addition, brain imaging emerged as a new direction of the field [14-17]. In the 21st century, neurogenetics became the star in the psychiatric field, and within this period numerous potential targets for the treatment of psychiatric diseases have been identified by

genome-wide association studies (GWAS) giving new hope to patients [18-23]. Unfortunately, despite enormous efforts invested into the field, until today, we still haven't been able to find resounding biomarkers for complex diseases like major depression or bipolar disorder [24,25]. Now, entering the post-genomic era, newly developed genetic and viral tools, optogenetics and advanced *in vivo* imaging techniques make it possible to characterize the activity, connectivity and function of specific cell types within complex neuronal circuits and to specifically manipulate different neuronal systems within an individual [26-28].

Integration of different regulatory components is important for an individual to appropriately respond to stress and maintain homeostasis. In this regard, the neuropeptide corticotropin-releasing hormone (CRH), expressed and secreted from parvocellular neurons of the paraventricular nucleus (PVN) in the hypothalamus, represents a final common path integrating the neuroendocrine stress response in the brain and therefore plays a critical role in the regulation of stress-related circuits [29,30].

1.2 The Corticotropin-releasing hormone (CRH) system

1.2.1 CRH as a neuropeptide in the central nervous system

Mature CRH or CRF (corticotropin-releasing factor) is a 41 amino acid peptide centrally expressed in the brain. CRH is released from the paraventricular nucleus of the hypothalmus (PVN) travels to the anterior pituitary and triggers the release of ACTH into the general circulation. ACTH further travels to the adrenal cortex which then secrets corticosterone (in rodents) or cortisol (in humans) which travels back to the brain initiating a series of feedback responses. CRH is critically involved in various different stress-related behaviours and the regulation of the HPA-axis [31,32]. Dysregulation of the HPA-axis is reported to be one of the main phenotypes accompanying psychiatric diseases and in particular of depression [33,34]. CRH is related with arousal responses in primates and blocking CRH action by a CRHR1 antagonist in mice attenuates stress responses [35].

1.2.2 The CRH-family and its receptors

The CRH family contains 4 different ligands and 2 different receptors. CRH and its relatives, the urocortins 1–3, which interact with their specific receptors (CRHR1, CRHR2), have emerged as central components of the physiological stress response. Both the CRH cDNA and the gene were characterized in human, sheep, rat, and mouse after the first discovery [36-41]. The CRH gene is located differently between human (chromosome 8) and mouse (chromosome 3). In contrast to many other neuropeptides, no other neuropeptide is encoded by the CRH precursor [42].

CRH paralogues and orthologs were discovered in different species: Sauvagine from the skin of the South American tree frog *Phyllomedusa sauvagei*; urotensin I from the urophysis of the teleost fish species *Cyprinus carpio*. These paralogues and orthologs have been reported to elicit similar biological effects as CRH [43,44]. Urocortin 1 (UCN1), the CRH ortholog in mammals was identified by the Vale group. Similar to CRH, synthetic UCN1 stimulates secretion of ACTH *in vivo* and *in vitro* [45]. Urocortin 3 (UCN3) and urocortin 2 (UCN2) were identified later in 2001. At the first place they have been named stresscopin and stresscopin-related peptide.

CRH or UCNs are difficult to detect as proteins are rapidly sorted into large, dense core vesicles (LDCV) of the peptides and transported to their site of action [46]. The currently most reliable detection with high spatial resolution is on the mRNA level via in situ hybridization. The other way is to inhibit microtubule polymerization via colchicine in order to trap the neuropeptide at the soma of neurosecretory cells.

CRH shows the most widespread expression in the brain compared with the other CRH-related peptides [47-50]. CRH is strongly expressed in the paraventricular nucleus (PVN) of the hypothalamus, where it regulates the activity of the HPA axis. In addition, CRH is expressed in the olfactory bulb, shell of the nucleus accumbens (NAc), the neocortex, piriform cortex, scattered interneurons of the hippocampus, the central amygdala (CeA); mainly the centrolateral division, the interstitial nucleus of the posterior limb of the anterior commissure (IPAC), and different divisions of the bed nucleus of striatal terminus (BNST). In the brain stem, CRH is expressed in Barrington's nucleus, in the laterodorsal tegmental nucleus, in the nucleus parabrachialis, and very strongly in the brain stem inferior olive (IO). CRH expression has also been detected in the cerebellum [51-53]. Until now, the identity of CRH

neurons throughout the CNS has only been partially revealed. In the hippocampus, CRH is exclusively expressed in a population of γ-aminobutyric acid (GABA)-ergic interneurons that innervate CA1 and CA3 pyramidal neurons. Most hippocampal CRH neurons show the appearance of basket cells and co-express parvalbumin (PV) but neither calbindin nor cholecystokinin (CCK) [54]. In the neocortex, CRH neurons appear either as small basket cells, descending basket cells, or double bouquet cells. These cells are also GABAergic but show more diversity with respect to colocalization of markers. The majority of CRH neurons co-express somatostatin (SOM) in a layer-dependent manner. In contrast to the hippocampus, neocortical CRH neurons are largely PV negative. While only few CRH neurons co-express CCK or calretinin [55]. The cell bodies of CRH neurons are relatively large in the CeA and have been reported to be GABAergic. In the periphery, a striking differential expression pattern has been observed in humans and rodents. While the human placenta shows increased levels of CRH expression during gestation, neither rat nor mouse placenta express any CRH [56].

1.2.3 CRH and its role in stress

CRH is thought to be involved in regulating stress responses due to its role as an activator of the HPA axis [57-59]. Perception of physical or psychological stress by an organism is followed by a series of events, including the release of CRH from the PVN. These neurons project via the external zone of the median eminence and release CRH into the hypophysial portal vasculature, which transports the neuropeptide to secretory corticotrope cells of the anterior pituitary. The activation of CRHR1 on these corticotropes stimulates the release of ACTH and other pro-opiomelanocortin (POMC)-derived peptides. ACTH, in turn, triggers the synthesis and release of glucocorticoids from the adrenal cortex (cortisol in humans, corticosterone in rodents). Glucocorticoids then trigger series of physiological responses in order to deal with the stress event. The responses to glucocorticoids include cardiovascular activation, energy mobilization, anti-inflammatory effects and suppression of reproductive and digestive functions [60-62]. To restore the HPA axis to its normal state and to protect it from overshooting, glucocorticoids signal back via glucocorticoid (GR) and mineralocorticoid receptors (MR) at various feedback levels, which ultimately inhibit the secretion of CRH. In humans, Nemeroff and colleagues initially showed increased CRH levels in the CSF of depressed patients, which was confirmed by other studies [63,64]. Besides major depression,

elevated CRH concentration can also be detected in patients with post-traumatic stress disorder (PTSD), which suggested that CRH could serve as a potential biomarker as well [65].

Besides the role of CRH in controlling of HPA-axis, CRH is highly expressed in the extended amygdala and limbic system including the CeA and BNST as well as hippocampus which also implicates the involvement of CRH in the stress responses. Activation of central CRH circuits in rodents elicits behavioural responses similar to those observed following stress. These include increased anxiety-related behaviour, arousal, decreased food-consumption, alterations in locomotion, and diminished sexual behaviour and sleep disturbances [66-70]. In general, central application of CRH was shown to promote primarily anxiogenic effects, as demonstrated in different behavioural tasks, such as the elevated plus maze, acoustic startle response, and social interaction test [71-75]. Specific brain regions expressing CRH might be involved in these behaviours. Administration of CRH into the ventricles or the dorsolateral BNST (dlBNST) in rats generates anxiety-like behaviours. These behaviours are reduced by CRHR1 antagonists injected into the BNST, but not when injected into the CeA [75-78]. A recent study showed that reward is able to inhibit CRH neurons in the PVN which might shed light on the treatment of stress-related disorders [79]. The diverse and broad expression pattern of CRH peptides and receptors, as well as the high level of signalling complexity, allow this circuitry to effectively integrate neuroendocrine, autonomic and behavioural responses of stress. Moreover, another study reported that CRH might be a relevant factor in neurogenesis in rodents, one of the known processes disturbed in stress-related diseases such as depression. This again emphasizes the importance of understanding the role of CRH in contributing to the stress responses [80].

1.2.4 CRH receptors and their role in the CNS

CRH and the urocortins signal through activation of two membrane-bound G-protein-coupled receptors, CRHR1 and CRHR2, which share 70 % amino acid identity [81-83]. CRH shows a much higher affinity for CRHR1 than for CRHR2 while UCN1 displays equal affinities for both receptors. UCN2 and UCN3, on the other hand, appear to be selective ligands for CRHR2 [84,85].

The human CRHR1 gene was mapped to chromosome 17 [86,87] compared to mouse which is located on chromosome 11 in a region of conserved synteny [88]. To date, in humans, 14 exons

encoding CRHR1 have been characterized, which is different from the mouse and rat genes that only have 13 exons. The CRHR1α variant plays a dominant role as a fully functional receptor, but the activity is regulated by the variant CRHR1β, also known as proCRHR1 [89]. This regulation can be achieved either by increased generation of the other splice variants which regulates the availability of the CRHR1α or through dimerization/oligomerization of CRHR1α with these variants, which can change the function of the receptor, for instance, ligand binding, intracellular localization and activity [90]. Furthermore, soluble isoforms can function in a way similar to the CRH binding protein (CRH-BP) and regulate the bioavailability of the CRH-related ligands [91].

CRHR1 mRNA is found throughout the CNS including the olfactory bulb, cerebral cortex, BNST, basolateral amygdala, hippocampus, globus pallidus, reticular thalamic nucleus, caudate putamen, ventral tegmental area, substantia nigra and the cerebellum. It is also highly expressed in the anterior pituitary where it initiates HPA axis activity in response to CRH binding [92,93]. In humans, eight splice variants of the CRHR1 gene have been identified primarily in the skin, placenta, or endometrium [94]. The biological identity of CRHR1 neurons hasn't been revealed systematically so far but appears quite diverse depending on the region where CRHR1 expressing neurons are located.

The human CRHR2 gene has been identified on chromosome 7 and the mouse CRHR2 gene is located on chromosome 6 [95]. CRHR2 is processed differently throughout species. Amphibians only possess the CRHR2α variant [96], whereas primates and rodents have both CRHR2α and CRHR2β [97,98]. Until now, the CRHR2γ variant has been identified in humans only [99]. However, in mouse, a soluble variant of the CRHR2 was identified, which has not been found in other species [100]. The CRHR2 variants are expressed in a tissue-specific, but also species-specific manner. CRHR2 variants are expressed in reverse manner comparing humans and rodents. For instance, CRHR2β and CRHR2γ in human are expressed in neurons of the brain, whereas CRHR2α is expressed in the periphery, such as in the heart, skeletal muscle, and skin [98]. In mouse, CRHR2α is expressed in CNS neurons and CRHR2β in the periphery [91,101]. In addition, human CRHR2α and mouse CRHR2β are expressed in the choroid plexus, which produces cerebrospinal fluid (CSF) [102]. In mice, CRHR2α displays a more confined expression, with high density in the olfactory bulb, BNST, lateral septum, ventromedial hypothalamic nucleus, and the dorsal raphe nucleus [92,101].

1.2.5 CRH receptors in psychiatric diseases and clinical implications

Since its discovery, the CRH system has attracted enormous scientific interest, which is reflected by the multitude of studies applying pharmacological administration of CRH-related peptides and CRHR antagonists either ICV or in a brain region-specific manner [103]. These studies have provided valuable insights into the role of CRH-related peptides and their receptors modulating emotional states and behavioural responses to stress [57].

Human genetic studies also have provided considerable support for the CRH hypothesis of mood and anxiety disorders [59]. Although none of the recent meta-analyses of linkage scans for bipolar disorder provide strong support for linkage to regions containing CRH-system genes [104,105], some individual scans in major depressive or anxiety disorders [106] have reported suggestive evidence for association in some of these regions. Other studies have investigated the phenotype of behavioural inhibition in children of parents with anxiety disorders and found association with a repeat polymorphism of the gene and three single nucleotide polymorphisms (SNPs) of CRH [107-109]. Two of these SNPs were also tested for association with panic disorder in a case–control study in adults, but no significant associations were observed.

Testing association of genetic variation in the CRHR1 gene revealed that particularly SNPs in combination with adverse environmental factors are able to predict risk for the development of stress-related psychiatric disorders. The CRHR1 gene appears to moderate the development of depression after childhood trauma and variation in the CRHR1 gene has been linked to the risk for depression in the presence of childhood maltreatment, predicting increased neuroticism [110,111].

Mainly, the three-allele haplotype of CRHR1 involving the SNPs rs7209436, rs110402, and rs242924 in intron 1 form a haplotype, where the TAT combination protects severely maltreated individuals against developing depression. The presence of the rare TAT haplotype shows a significantly decreased risk for adult depressive symptoms in an additive manner in subjects with a history of child abuse. In addition, the TAT haplotype was associated with heightened levels of neuroticism in children who had experienced one or two types of maltreatment, but not who had experienced three or four types of maltreatments [112]. This finding was confirmed in another study showing that the CRHR1 gene interacts with childhood maltreatment to predict adult depression.

In addition, PTSD subjects with the GG genotype at SNP rs110402 with a history of childhood abuse showed a significant improvement in symptoms when treated with a CRHR1 antagonist compared with placebo [113]. Cortisol response in the dexamethasone/CRH test can be predicted where the SNPs rs110402 and rs242924 shown to significantly interact with childhood maltreatment. Maltreated subjects clearly showed as elevated cortisol response to the test [114]. Moreover, current, adult depressive symptoms can be predicted with individuals carrying risk alleles in both CRHR1 and 5-HT transporter gene (5-HTTLPR). Interaction of the CRHR1 gene with the promoter region of the 5-HTTLPR results in depressive symptoms at less severe levels of child abuse compared with individuals with no or only one of the risk alleles [115].

In addition, CRHR1 SNPs were found to be associated with panic disorder and with the response to antidepressant treatment [116-119]. The CRHR1 SNPs rs1876828, rs242939 and rs242941 were tested with antidepressant treatment in Mexican-Americans. It appeared that only patients in the high-anxiety group showed a significant association with treatment response. Similar results were obtained in Han Chinese patients with major depression. Another study revealed that individuals carrying the G-allele of rs242939 or the haplotype GGT may be highly susceptible to recurrent major depression when exposed to adverse life events [120]. These findings suggest that genetic variation in CRHR1 increase the risk for affective disorders by influencing the function of the neural circuit underlying anxious temperament. Moreover, differences in gene expression or in the protein sequence involving exon 6 may play an important role and suggests that variation in CRHR1 may influence brain function even before any childhood adversity.

So far only a limited number of associations with depression and anxiety-related phenotypes has been reported for CRHR2 [59]. A recent study identified a rare variant of CRHR2 in a family with bipolar disorder, which tracked with the affected status that reduced cell surface expression and altered intracellular signalling [121]. In addition, SNP rs28365143 identified in the CRH-BP gene was predictive with respect to antidepressant treatment in HPA axis responses. Patients homozygous for the G allele had better remission and response rates, as well as reduced symptoms. Patients also had better treatment outcomes with selective serotonin reuptake inhibitors but not for the combined 5-HT and norepinephrine reuptake inhibitors [122].

Preclinical and clinical findings supported that the CRH/CRHR system might be a promising target for the treatment of psychiatric disorders and stimulated the development of CRHR1 antagonists and realization of a significant number of clinical trials [123,124]. NBI-30775/R121919 was used in the first clinical study showing certain efficacy. The compound improved depression symptoms in the Hamilton Depression Rating Scale similar to a serotonergic antidepressant and additionally improved sleep parameters [125,126]. In addition, NBI-30775/R121919 did not have major impact on HPA axis activity when tested in the CRH challenge test [127]. However, the further development of NBI-30775/R121919 was hindered due to the elevation of liver enzyme observed in some healthy controls. Until now, R121919 is the only CRHR1 antagonist that showed efficacy.

There are numerous examples of failed CRHR1 antagonist: CRHR1-specific antagonist CP-316,311 was tested in a subsequent Phase IIb, double-blind, placebo-controlled trial in patients with recurrent major depression. However, the treatment did not improve Hamilton Depression Rating Scale scores compared with a placebo-treated control group and was ended prematurely [128]. Similarly, CRHR1 antagonist pexacerfont (BMS-562086) was unable to demonstrate any therapeutic effect of generalized anxiety disorder [129]. An earlier study using the same antagonist for treatment of major depression was completed without reporting any results [130]. Moreover, the development of several compounds, for instance, ONO-2333Ms, SSR125543, and others, was discontinued due to lack of efficacy in controlled trials for major depression [123,124,131]. Most recently, the first evaluation of a CRHR1 antagonist verucerfont (GSK561679) for the treatment of PTSD also failed [113,132].

The so-called “self-medication” hypothesis, suggested that drug use might be motivated by negative reinforcement mechanisms to relieve depression-like symptoms by the anxiolytic and dysphoria relieving effects. Activation of the CRH system may contribute to the withdrawal/negative effect stage of the addiction cycle. CRH-related circuits may represent a common pathway underlying the observed comorbidity of alcohol dependence and major depression. Therefore, CRHR1 antagonists have the additional indication for drug and particular alcohol dependence [133]. However, CRHR1 antagonists verucerfont and pexacerfont have also been disproven in their efficacy as treatments for stress-induced craving for alcohol [134,135]. Overall, the development of CRHR1 antagonist as a drug has not been successful. In the future, with the help of more circuit associated studies and more genomic studies, CRHR1 antagonist might rise up again as a possible treatment for personalized medical treatments.

1.3 Tracing of neurocircuits

Tracing of neurocircuits: from human to rodent

Human imaging studies using Positron emission tomography (PET) and Functional magnetic resonance imaging (fMRI) have examined differences in regional brain activation in depressed and anxious subjects relative to controls as well as in patients revealing several brain regions that are involved in response of aversive conditions [14]. Since the discovery of temporal lobe structures contributing to emotional behaviours, our understanding of the neural substrates of anxiety largely relied on lesion and inactivation studies. Although these important early works led to the identification of key loci regulating anxiety, including the amygdala, the bed nucleus of the stria terminalis (BNST), the ventral hippocampus (vHPC) and the prefrontal cortex (PFC), we still lack detailed insight into the circuits involved in anxiety.

An increasing number of studies revealed different circuits in the brain involved in animal behaviour. A board range of methods has been applied in different studies. Understanding the pros and cons of these methods will allow us to interpret data accordingly. These tracing methods can be separated into two major types: anterograde and retrograde depending on their travelling direction. On the one hand, there are traditional conventional tracers using different peptides, amines and particles: Horseradish peroxidase (HRP), Biotinylated dextran amine (BDA), Phytohaemagglutinin-L (PHA-L), Wheat Germ Agglutinin (WGA), FluoroGold, Retrobeads and Cholera toxic subunit B. On the other hand, there are viral-based tracers: adeno-associated viral vectors (AAVs), canine adeno-virus (CAV2) and deletion-mutant recombinant rabies virus (dG-RV). This study provides a brief summary of the comparison between different conventional tracers and will put more focus on the newly developed viral-based tracers (Fig. 1 and Table 1).

Horseradish peroxidase (HRP), initially discovered as retrograde tracer possesses both retrograde and anterograde function. HRP is taken up by cell bodies and dendrites at the injection site and transported to axons and their terminals in an anterograde manner. Or can be taken up into neurons non-selectively by passive endocytosis. This tracer will be taken up by both neurons and glia. The disadvantage is that in some systems it is difficult to detect the terminals of injected brain systems. While the axons emanating from labelled cells were always found, in some cases it is hard to find labelled axon terminals [136,137].

Biotinylated dextran amines (BDA), are highly sensitive compounds for anterograde (mainly) and retrograde pathway tracing studies of the nervous system. BDA can be reliably delivered into the nervous system by iontophoretic or pressure injection and visualized with an avidin-biotinylated HRP (ABC) procedure, followed by a standard or metal-enhanced diaminobenzidine (DAB) reaction [138]. Several features of BDA make it advantageous for light microscopy and electron microscopy studies. First, BDA reliably yields anterograde labelling after injection into the nervous system. Secondly, it is easy to make small and well-defined injections of BDA, thereby making it possible to confine the injection to the region of interest and/or study the topographic order to a projection from a given region [139]. Since the discovery of BDA, it has been applied to many tracing studies in different brain regions [140] and it has been recently applied to the tracing of axons in primates' brain [141].

Phytohemagglutinin-L (PHA-L), isolated from the kidney bean, serves as reliable anterograde tract tracers in the CNS [142]. Generally, PHA-L is transported anterogradely with evidence of retrograde transport in some neuronal systems [143,144]. A distinguishing feature of PHA-L is that it provides visualization of the fine morphologic detail of the labelled neurons. The labelling is stable for extended survival periods, which allows for labelling of very long axonal processes [145]. Furthermore, tract tracing with PHA-L could be combined with immunocytochemistry for specific neurotransmitters, neuropeptides, or receptors to further determine the phenotype of the axon terminal or the postsynaptic target [146].

Wheat Germ Agglutinin, WGA is a lectin-based anterograde and retrograde tracer. The specific affinity of WGA for neural membranes makes it an excellent tracer for tracking neural connections in any region of the brain, spinal cord, and peripheral nervous system. It is reliable and versatile, as projections are labelled in the anterograde and retrograde directions. It is robust enough for tracking fine pathways in small animals, and it is stable enough for

long-term tracing of neurons in large species. In some systems, WGA can even travel transynaptically to label the connected neurons.

Fluoro-Gold (FG), introduced as a retrograde tracer, is a fluorescent dye with many advantages. FG is visible in lysosome-like structures allowing for the identification of projection neurons at the ultrastructural level, and remains in the labelled neurons for extended periods of time. Photoconversion and immunostaining for FG, result in a stable, electron-dense reaction product. Thus, the retrogradely labelled cells can be analysed quantitatively in the light- and electron microscope for their structural characteristics and input synapses. The ability to define the extent of the tracer diffusion [147,148], massive axonal FG uptake at the injection site[149], and bright fluorescent back labelling of the parent cell bodies are well-known features of this tracer[150,151].

Rhodamine-labelled fluorescent latex microspheres,' or "beads" have provide as an increasingly powerful tool for analysing the connectivity and cell biology of the vertebrate brain [152]. After injection, the beads show little spreading and provide a sharp and well defined injection site which is a great advantage over other tracers [153]. The beads are relatively stable and non-toxic, so they do not cause necrosis at injection sites or in labelled cells in vivo or in vitro that can be detected over weeks after injection. In addition to their use in pathway tracing studies based on retrograde axonal transport, rhodamine beads have been used to identify specific projection neurons in living [152,154], and fixed brain slices[155], to mark cells in tissue culture [156], to label neurons in transplantation studies [157], and to identify specific groups of cells in conjunction with immunocytochemistry [158]. Disadvantages of the rhodamine beads include their incompatibility with most retrograde tracers and with immunocytochemical and Golgi [159] techniques. However, their long-term persistence in labelled tissues, resistance to fading under fluorescent illumination, and limited diffusion from injection sites made it useful for anatomical studies. Later developed green beads overcame the disadvantage of the rhodamine beads and it is now possible for investigators to use two neuronal tracers that share almost all characteristics, and differ only in fluorescent colour [160].

Historically, the use of the neuroanatomical tracer cholera toxin subunit B (CTB) has been limited to single-labelling techniques using bright-field horseradish peroxidase and DAB staining [161-164]. CTB has now been made available conjugated with Alexa Fluor (AF) fluorescent dyes. This makes reliable multiple pathway tracing possible using fluorescent microscopy. A common issue in most neuroanatomical studies is that fluorescent tracers are

significantly less sensitive than their bright field counterparts [165]. As reported in the study of Alexa Fluro conjugated CTB (AF-CTB), they consistently found highly sensitive retrograde labelling of connections. Of most importance, it has been reported that due to the more sensitive nature of CTB, scientists were able to inject the tracer into a very confined injection site, yet still see extensive labelling patterns. Furthermore, the AF dyes proved to be exceptionally bright and photostable compared with the dyes attached to other neuroanatomical tracers [166]. The properties of these conjugates overcome many of the limitations of other fluorescent tracers. Now with two different colours of CTB available, they provide the freedom for scientists to play around with the combination to have intensive neuronal tracing [167].

Table 1. Summary of conventional tracers for circuit tracing

Conventional Tracers	Time of discovery	Discovered by	Type of tracing	Advantages
Horseradish peroxidase, HRP	1971	Kristensson, Olsson [137]	Retrograde and Anterograde	First retrograde tracer
Biotin dextran amine, BDA	1990	Veenman, Reiner and Honig [139]	Anterograde* and retrograde	Highly sensitive, confined injection site
Phytohemagglutinin-L, PHA-L	1984	Gerfen, Sawchenko [168]	Anterograde	Fine morphologic details, stable for extended survival periods
Wheat germ agglutinin, WGA	1972	Schwab, Javoy-Agid and Agid [169]	Anterograde and retrograd	Increased sensitivity, limited diffusion, longer persistent time in cells, compatible with different fixatives
FluoroGold™	1986	Schmued and Fallon [170]	Retrograde	Brighter fluorescence, less fading of the fluorescence, high sensitivity, reduced leakage out of labelled cells, use in multi-labelling studies, longer survival times
Retrobeads™	1984	Katz, Burkhalter and Dreyer [152]	Retrograde	No obvious cytotoxicity or phototoxicity, minimal diffusion, longer persistence
Cholera toxic subunit B	1977	Stoeckel, Schwab and Thoenen [171]	Retrograde	Highly sensitive, decreased diffusion, high affinity for cell surface, immunohistochemical detection

* Main function

The following paragraphs will focus on viral-based tracers comparing the advantages and disadvantages of them.

The use of adeno-associated viral vectors as tracers started from vectors containing constructs to express GFP or other fluorescent proteins which provided selective anterograde axonal labelling. This allows morphological detail of neuronal structure comparable to those produced with PHA-L. The development of transgenic mouse lines with Cre-recombinase expression directed to specific neuronal cell types [172] combined with AAV vectors harbouring Cre-dependent reporter constructs enable specific labelling of axonal projections in specific neuronal subtypes. With a long history of studying different serotypes of AAV [173,174], a great number of studies successfully used AAV vectors as anterograde tracers [175]. With the advent of technology, new methods have been developed to study neuronal connectivity. These are less neurotoxic and more compatible with other neuroscience methods such as electrophysiological recordings. AAVs have been developed into more improved neuronal tracing tools combining optogenetically or chemogenetically (DREADDs) controlled transgenes, together with conditional transgenic mice, to reveal not only the anatomy of neuronal connections, but to visualize neuron connections that are functionally relevant. Apart from mapping neuronal networks, improved AAV vectors could also be powerful tools for the field of gene therapy if they can reach the affected part of the brain in a less invasive manner [176]. Recombinant adeno-associated viruses (rAAVs) have emerged as an effective platform for in vivo gene therapy, as they mediate high-level transgene expression. They are non-toxic, and evoke minimal immune responses [177]. This emerging new tool gives scientists a good replacement of the classic retrograde tracer like rabies virus and others. rAAVs hold great promise in clinical trials for a range of neurological disorders [178] and they constitute some of the most widespread vectors in neuroscience research [179].

The newly engineered rAAV$_2$-retro offers up to two orders of magnitude enhancement in retrograde transport compared to commonly used AAV serotypes, matching the efficacy of synthetic retrograde tracers in many circuits. The level of transgene expression achieved with rAAV$_2$-retro via retrograde access is useful for interrogating neural circuit function, as well as for targeted manipulations of the neuronal genome. Thus, by enabling selective monitoring and manipulation of projection neurons connecting different brain areas, rAAV$_2$-retro-based tools can provide insights into how large-scale networks enable brain function, and may form the basis for future therapeutic intervention in diseases characterized by progressive largescale network dysfunction [180].

Adenovirus vectors have significant potential for long- or short-term gene transfer. Preclinical and clinical studies using human derived adenoviruses (HAd) have demonstrated the feasibility of flexible hybrid vector designs, robust expression and induction of protective immunity. In the early 1990s, scientists considered the possibility of using non-human vectors and started designing canine adenovirus serotype 2 (CAV2) vectors [181-183], with the hypothesis that vectors derived from non-human adenoviruses would be clinically useful. CAV2 is retrogradely transported in neuronal axons after injection in mice or primates. In vitro, reports suggested that CAV2 trafficking was bidirectional with a preferential retrograde transport, implying coordination between molecular motors of different polarities. Beside the need of clinical usage, the CAV2 vector has been a good transporter of different tools that is useful for neuroscience studies. Combining it with rabies virus and transgenic mouse lines, this provides scientist with the possibility to trace and activate specific circuits of interest [184].

Rabies virus (RV) is a highly neurotropic, enveloped, negative-strand RNA virus with a very broad host range including virtually all mammals and birds. Viral transmembrane glycoprotein (G) is crucial for neurotropism and host range, which mediates attachment to target cells, endocytosis, transport of endocytosed vesicles, and virus–vesicle membrane fusion to release the viral nucleocapsid into the cytoplasm of target cells [185,186]. The typical RV retrograde spread from an infected neuron to presynaptic neurons is exclusively via actual synaptic connections [187,188]. This feature is unique among viruses and makes RV a true trans synaptic tracer [189-191]. The resulting pseudo type viruses infect cells according to the receptor specificity of the heterologous env protein [192]. The receptor for EnvA is TVA, a small avian protein not present in mammalian cells [193]. Infection of TVA-expressing mammalian neurons by EnvA pseudotype virions is, therefore, highly specific with little background [194]. This combination is ideal for monosynaptic tracing experiments such as those pioneered by Callaway and colleagues: Neurons expressing TVA and G by standard transgene approaches are selectively infected by RV (EnvA) pseudotype viruses such as SAD ΔG-eGFP (EnvA) [188,195]. RV vectors allow sufficient gene expression in probably all types of neurons and yet cause limited neuronal damage so they do not destroy the connections required for viral spreading to and within the central nervous system. Nevertheless, neurons infected with full-length virus or SAD ΔG viruses will continuously accumulate and produce viral RNA and proteins, which ultimately (within a couple of days) will lead to damage [196].

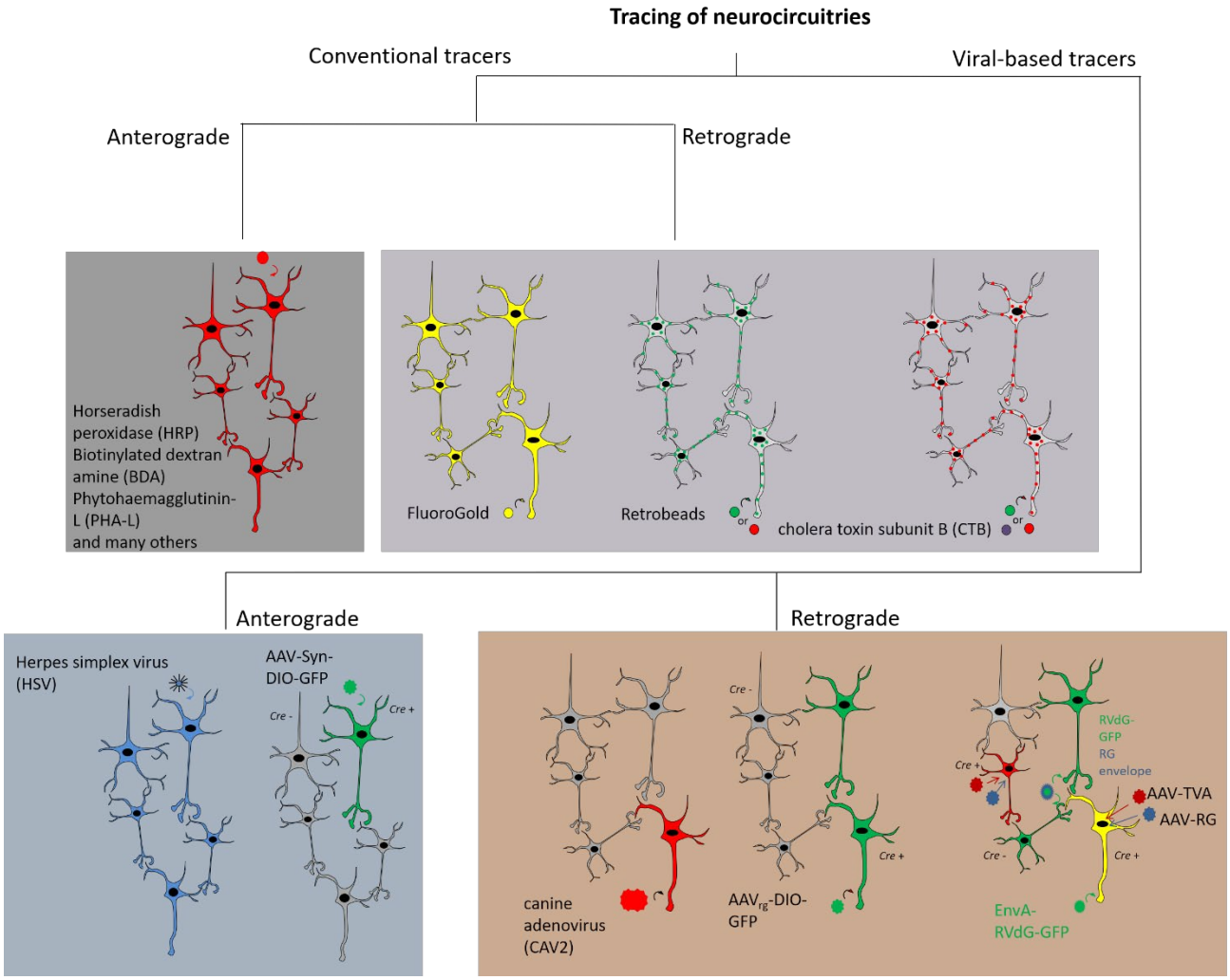

Fig. 1 Methods of neuronal tracing

Generally neuronal tracers are separated into two main groups: conventional and viral-based tracers. These can be further separated into anterograde and retrograde tracers depending on how they are taken up. Different tracers also have different labelling properties as the tracers will fill the entire soma of a neuron, in case of most of the anterograde conventional tracers and FluoroGold. In addition, some viral based tracers such as AAVs (depends on the viral construct) also filled the entire soma. In case of some other tracers only puncta will be seen on the membrane, e.g. Retrobeads, CTB and viral-based tracers with membrane-labelling reporter proteins. Rabies virus was modified to only infect user-defined starter cell types by using EnvA-pseudotyped RV, and only expressing the EnvA receptor (TVA) in user-defined cells. Monosynaptic spread is achieved by modifying the wild-type RV genome, which encodes a single envelope protein called rabies glycoprotein (G).

1.4 Visualizing neurocircuits in the brain

The traditional way of visualizing neurocircuits in the brain is to apply neuroanatomy by sectioning brain tissues. This provides access to different structures and with the help of microscopy allows quantifying and understanding the neurocircuits. The advantage of this approach is that the time required for getting the result is relatively short in terms of tissue preparation and processing. However, if one would like to visualize the result in 3D manner, the time for reconstruction of images is enormously increased. The biggest disadvantage of this method is the lack of consistency between different tissue preparations. For instance, two different people will not be able to prepare 100% identical brain slices let alone the quality of tissues and other manipulations. The other disadvantages is related to the difficulty of tracking an entire circuit. With the increasing need of visualizing the brain as a whole, different tissue clearing techniques emerged. In the following currently available clearing methods will be summarized and compared.

The main function of tissue clearing is to reduce light scattering for deeper imaging and subsequent three-dimensional reconstruction of tissue structures. Combined with optical imaging techniques and diverse labelling methods, these clearing methods have significantly adavnced the development of neuroscience. Tissue clearing methods have been developed to tansparentize large-volume brain tissues, using physical or chemical strategies. These clearing methods can be roughly divided into two categories: solvent-based and aqueous-based clearing methods. The first group depends on using different organic solvents in order to remove lipids contained in the brain. Methods in this category including benzyl alcohol and benzyl benzoate (BABB) [197], 3-D imaging of solvent-cleared organs (3DISCO) [198,199], immunolabeling-enabled three-dimensional imaging of solvent-cleared organs (iDISCO) [200], ultimate DISCO (uDISCO) [201], DISCO with superior fluorescence-preserving capability (FDISCO) [202] and so on, usually go through dehydration, lipid removal and refractive index matching with reagents. The latter category can further be divided into three types: simple immersion, such as see deep brain (SeeDB) [203], Clear^{T2} (a detergent- and solvent-free clearing method) [204]; hyperhydration, such as Scale (an aqueous reagent that renders biological samples transparent) [205], clear, unobstructed brain imaging cocktails and computational analysis (CUBIC) [206-208], and hydrogel embedding, such as Clear lipid-exchanged Acrylamide-hybridized rigid imaging/immunostaining/in situ hybridization-compatible

tissue-hYdrogel (CLARITY) [209,210], passive CLARITY technique (PACT) [211-213], system-wide control of interaction time and kinetics of chemicals (SWITCH) [214] and so on (Fig 2).

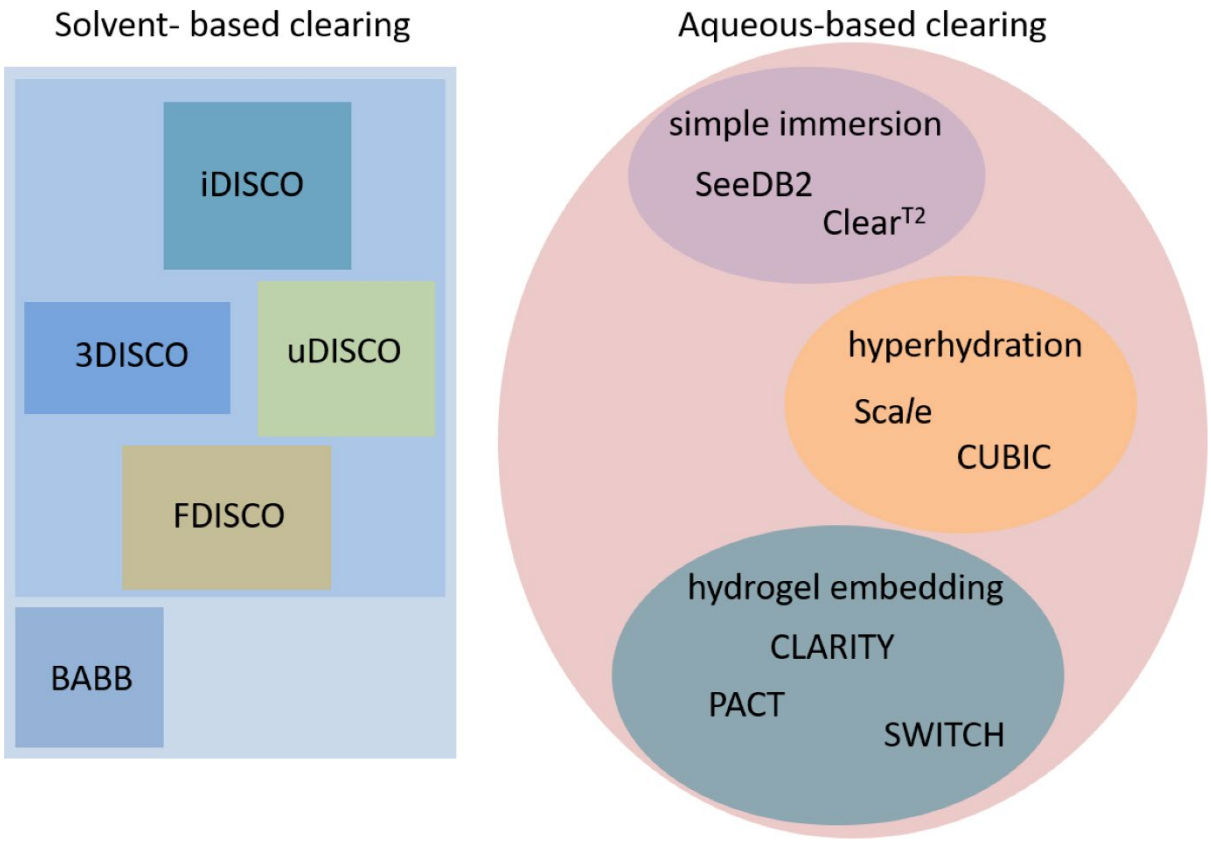

Fig 2. Summary of current methods on tissue clearing

Tissue clearing methods can be separated into two main groups: solvent– and aqueous-based methods. Solvent-based methods included BABB and the DISCO family. Aqueous-based methods can be further divided into three categories: simple immersion (SeeDB2, Clear^{T2}), hyperhydration (Sca*l*e, CUBIC) and hydrogel embedding (CLARITY, PACT, SWITCH).

For comparison 4 methods were selected covering the two categories that we used in this study. The methods used in this study are: iDISCO, FDISCO and CLARITY which will be compared with 3DISCO as a reference. 3DISCO is the first DISCO method that has been developed with the usage of Tetrahydrofuran (THF) as an agent for dehydration and lipid removal, Dibenzyl Ether (DBE) as the index matching buffer. With increasing concentrations of THF, the tissue will turn transparent as well as the endogenous fluorescence fading away at the same time. The time needed for this method is relatively short. It requires about 3 days

to obtain a fully transparent brain. The most similar method to 3DISCO is FDISCO, which applied as a small change to the protocol of 3DISCO changing the pH of THF and the incubation temperature. With this small modification, it is claimed that FDISCO is able to preserve endogenous fluorescence better than 3DISCO. The time required for this method is the same as for 3DISCO. iDISCO implemented many changes compared to the 3DISCO protocol as it is an immunostaining-based method. First of all, the protocol contains dehydration steps by using methanol and dichloromethane (DCM). In addition, it includes a bleaching step with H_2O_2. After dehydration and bleaching, there is no endogenous fluorescence left. In order to visualize the signal, it requires immunostaining before processing with the tissue clearing steps. Since the entire staining steps requires passive diffusion of the antibody, the protocol takes way longer than the previous mentioned two protocols. iDISCO requires at least two and a half weeks until the tissue is fully cleared. The last method that we used is CLARITY, it also requires more time than the other methods due the passive replacement of lipid in the brain. The protocol starts from hydrogel embedding, incubation with clearing solution until the brain is cleared (Fig 3).

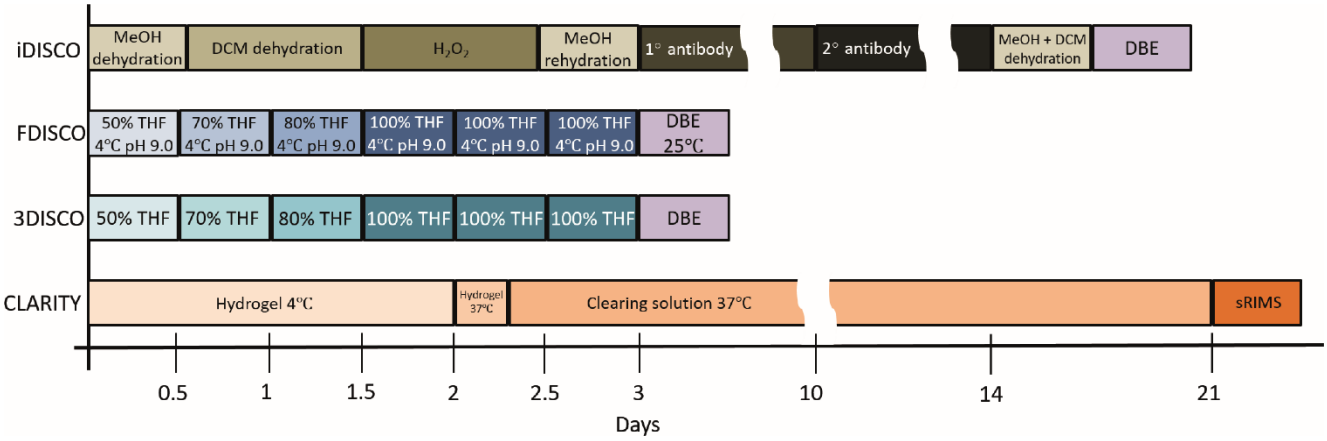

Fig 3. Comparison of protocols of different tissue clearing methods

Four methods including 3 methods that were used in this study were selected to provide a comparison of the different reagents involved and also the time line of each protocol.

Next, we compare the imaging depth and the possibility of fluorescence preservation of each protocol. From the literature and also our own experiences we are able to place CLARITY with in the middle of the comparison that have almost equal capacity of tissue transparency

and fluorescence preservation. iDISCO as mentioned above, has no possibility for fluorescence preservation but has very good tissue transparency due to the bleaching step. As for 3DISCO and FDISCO, these two protocols have the same level of tissue transparency but 3DISCO has less preservation of fluorescence than CLARITY. On the other hand, FDISCO has the best preservation of fluorescence among all [215]. The other factor that determines the quality of a given tissue clearing protocol is the imaging depth. The imaging depth is also affected by the tissue transparency. In this regard 3DISCO is the worst as it shows less transparency and low preservation of fluorescence. iDISCO has good fluorescence intensity after staining and has with good tissue transparency the same efficacy as CLARITY during imaging. Finally, FDISCO having good fluorescence preservation and fluorescence intensity is performing the best in this comparison (Fig 4). Of course, there are still many different factors that will affect the quality of the imaging, for instance, the age of the animals is a crucial factor that affects the effect of tissue clearing. The older the animal the more time is required for tissue clearing, which is due to the increase of white matter in the brain. Due to the replacing of lipid and different reagents used in the protocol; changes in tissue dimension are observed during the process. CLARITY shows expanding of tissue size, whereas the other three protocols result in shrinking sample size. The difference between tissues shrinking is not significantly different between the methods [202,215].

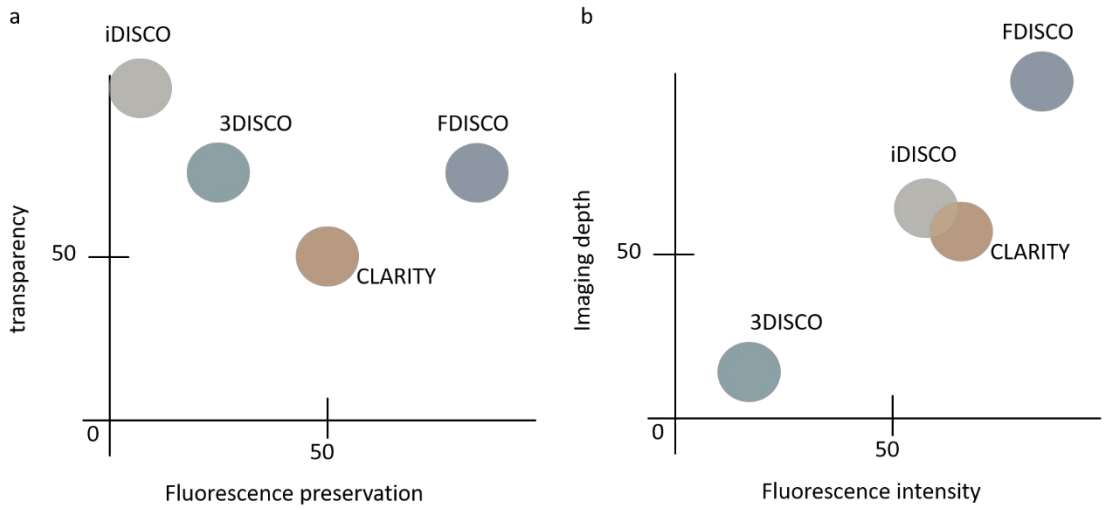

Fig 4. Comparison of clearing capacity of different methods using whole brain tissue

(a) Comparison of tissue transparency and capacity of fluorescence preservation. CLARITY was set as having equal capacity of both factors and is compared with the other methods. In this comparison iDISCO has the worst

fluorescence preservation but the best tissue transparency, 3DISCO has slightly better fluorescence preservation than iDISCO but less transparency. FDISCO preserves a good amount of fluorescence and has good tissue transparency. (b) Comparing imaging depth and fluorescence intensity during imaging using different clearing methods. 3DISCO has the worst imaging depth and fluorescence intensity, iDISCO is performing similar to CLARITY and FDISCO shows the best performance.

1.5 Neurocircuitries of stress focusing on the extended amygdala

In order to understand the response of an individual facing an adverse event, it is important to identify the brain region that responds to the event. With the application of different imaging methods, the amygdala has been identified as one of the key regions involved in the regulation of fear and anxiety [14,216,217]. Fear and anxiety often occur together; however, they have fundamental difference between each other based on the context. According to Diagnostic and Statistical Manual Of Mental Disorders, Fifth Edition (DSM-5), fear relates to a known or understood threat, whereas anxiety follows from an unknown, expected, or poorly defined threat. The extended amygdala receives main input from the basolateral amygdala (BLA) and cortical regions such as the insular cortex. In addition, divisions of the prefrontal cortex (PFC) such as medial PFC (mPFC) and infralimbic PFC (ilPFC) key regions for fear recognition, consolidation and extinction, also send inputs into the extended amygdala [218-220]. Different methods like opto- and pharmacogenetic interventions have been proposed as tools to interrogate the function of neurocircuits of anxiety [221]. Amygdala and extended amygdala regions, which include the central (CeA) and medial (MeA) nuclei of the amygdala and the bed nucleus of the stria terminalis (BNST) are thought to be the central circuits modulating anxiety-like behaviours in the rodent is susceptible to stress [222,223].

A study showed decreased freezing to a tone that predicts a shock following inactivation of the central-medial nucleus of the amygdala (CeM) proving the crucial role for the CeA in mediating behaviours induced by threatening stimuli [224]. Although the CeA receives input from CRH positive projections originating in the paraventricular nucleus and the bed nucleus of the stria terminalis [225], CRH function in the CeA is also driven by a local microcircuitry [226]. For example, the CeL inhibits the CeM, which is the main output of the amygdala [14,227]. Furthermore, CRH and GABA are co-localized within CeA neurons [228], and CRH has been shown to regulate GABAergic neurotransmission in this brain region. Exogenous application of CRH to CeA slices increases presynaptic GABA release in a CRHR1 dependent manner

[229]. In a recent study on feeding suppression, genetic targeting of CeL:PKCδ$^+$ neurons was used to selectively express inhibitory DREADDs to allow for reversible neuronal inhibition of the activity of CeL:PKCδ$^+$ neurons. This inhibition was found to block decreased feeding stimulated by sickness or unpalatable tastes. Conversely, optogenetic excitation of CeL:PKCδ$^+$ neurons dramatically decreased feeding in both hungry and sated mice, and this was not a confound of reduced activity or increased anxiety. These results indicate that CeL:PKCδ$^+$ neurons suppress feeding in response to anxiogenic stimuli [230,231].

In addition to the CeA, the BNST is also crucial in regulating anxiety-like behaviours. It has been shown that chronic stress leads to a hypertrophy of the BNST, increased activation of the anterior BNST and also alterations in the expression of genes associated with the CRH, GABA and glutamatergic systems [232,233]. Stimulation of the Gq-coupled receptor 5-HT$_2$CR in the BNST is sufficient to elevate anxiety-like behaviour in an acoustic startle task [234].

The CeA and the BNST are highly interconnected, although the amygdala is thought to be more associated with fear and the BNST with anxiety, studies using excitotoxic lesions show the involvement of the CeA in the development of stress-induced anxiety. CRH, which is highly expressed in the CeA has been shown as the modulator of anxiety behaviour. Knockdown of CRH in the CeA attenuated stress-induced anxiety behaviour and at same time affected the expression of CRH in the BNST demonstrating the importance of the communication between CeA and the BNST in modulating stress responses [235]. Experiments in rats also showed that CeA CRH projections onto BNST CRH neurons work together in modulating anxiety-like behaviour. In this study, anxiety-like behaviours driven by CRH neuron activation in the CeA were dependent on CRH neurons in the BNST being active at the same time, supporting a cooperative role of the CeA and the BNST in stress-induced anxiety [236]. Another study also demonstrated a role for CRH projections from the CeA to the BNST in fear conditioning in the rat, where optogenetic silencing of these neurons during acquisition of conditioned fear suppressed freezing at later time points during retention testing, either due to impaired consolidation of long-lasting components of fear memory or acceleration of fear extinction [237]. A recent study demonstrated that activation of CeA-projecting BNST neuron terminals by optogenetic stimulation increased anxiety-like behaviours. In contrast, the photostimulation of LH- and VTA-projecting BNST neurons suppresses anxiety-like behaviours [238,239]. Different sub-regions of the BNST also have projections back to the CeA which are involved in anxiety responses. For example,

GABAergic projections from the oval nucleus reach the CeA, VTA and the lateral hypothalamus [240-242].

Evidence showed that inactivation of CRH in GABAergic projection neurons that target CRHR1 on dopaminergic VTA neurons modulate emotional behaviour by regulating dopaminergic neurotransmission [243]. Another study which combined celltype-specific optogenetic targeting with the assessment of multiple behaviours demonstrated that PVN CRH neurons orchestrate a complex repertoire of behaviours after acute stress. The behavioural repertoire does not require CRH signalling, but relied on an excitatory, glutamatergic projection to a subset of neurons of the LH. Furthermore, activation of CRH neurons can over-ride the environmental cues, resulting in behaviours that appeared mismatched to the context. This study suggested that animals de-escalate their behaviours after stress in a specific pattern that is influenced by the environment and the activity of PVN CRH neurons [244].

In summary, multiple lines of evidence have shown that both CeA and BNST have the potential of shaping the behavioural outcomes when an individual faces an aversive event. Further studies focusing on the connectivity of this region will be important in order to further investigate the mechanism involved in the regulation of stress-related diseases. The investigation in this study focuses on CRH projection neurons belonging to the extended amygdala aiming at understanding the importance of CRH involved in stress-related behaviours.

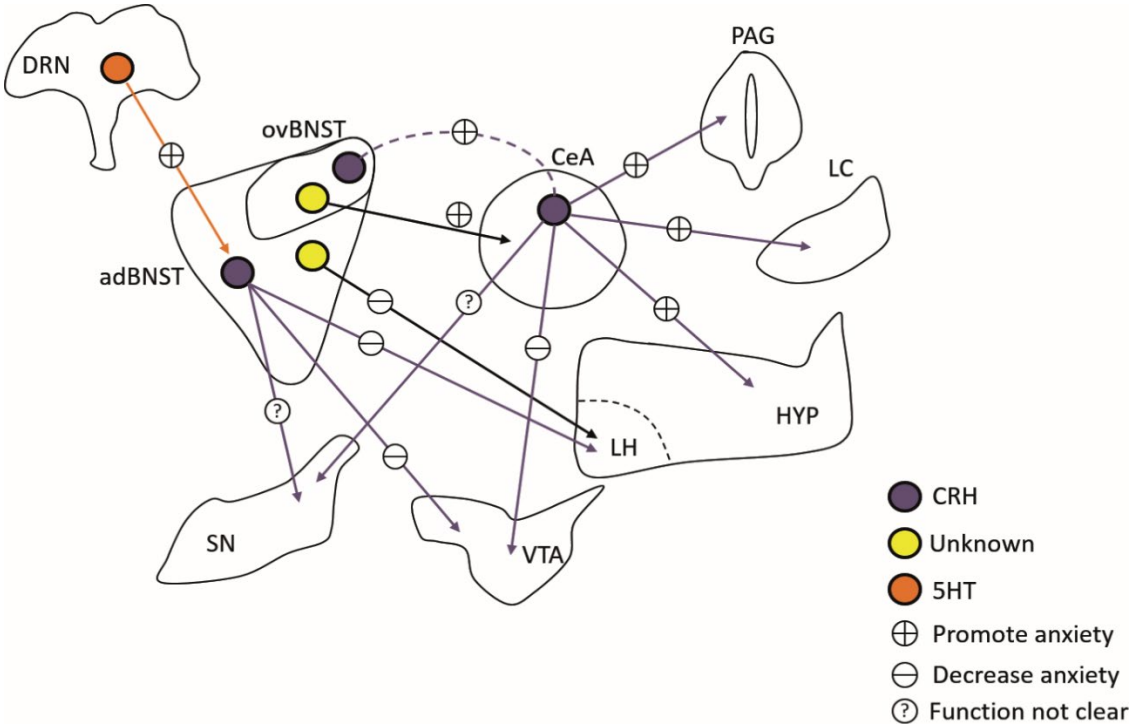

Fig 5. Stress-related neurocircuits of the extended amygdala

Summary of extended amygdala circuits involved in anxiety-related behaviour. On the one hand, CeA CRH neurons promote anxiety through projections into PAG, LC, HYP and co-activation of CRH neurons in the BNST. On the other hand, CRH neurons from CeA projecting to the VTA suppress anxiety behaviour. BNST, projections into the CeA also promote anxiety but projections into LH and VTA have opposite effects. Serotoninergic projections from DRN into BNST also promote anxiety. BNST, bed nucleus of the stria terminalis; CeA, central amygdala; DRN, dorsal raphe nucleus; Hyp, hypothalamus; LC, locus coeruleus; LH, lateral hypothalamus; PAG, periaqueductal gray; SN: substantia nigra; VTA, ventral tegmental area.

2. Aim of the thesis

This study focuses on the interaction of two elements in order to understand how an individual copes with stress. The first element is the brain circuits that regulate the behavioural responses of stress. The orchestra of circuits in different brain structures coordinate the barrage of signals received by an individual. Environmental stimuli which are as important as genetic factors, one integrated by different brain circuits and turned into experience that directs the behavioural responses [245]. The second element is the neuroendocrine in stress responses with the main focus on the CRH/CRHR1 system. To cope with various stressors and maintain homeostasis, individual requires adaptive responses involving changes in the central nervous and neuroendocrine systems [246,247].

There are several questions aimed to be addressed in this study: First, what is the biological identity of the CRHR1 neurons in the ventral midbrain. Second, what is the identity and connectivity of CRH/CRHR1-specific neurocircuits focusing on the extended amygdala. Third, what is the function of these circuits upon activation.

3. Material and methods

3.1 Animals

All animal experiments were conducted with approval and in accordance with the Guide of the Care and Use of Laboratory Animals of the government of upper Bavaria, Germany. Mice (2–3 months old) were grouped housed under standard lab conditions (22 ± 1°C, 55 ± 5% humidity) and were maintained under a 12 h light- dark cycle with food and water ad libitum. At weaning, mice were numbered by ear-punching with a piece of tail collected for genotyping. Mice were single housed one week prior of behaviour testing (Table 2).

Table 2. List of animal usage in this study

Animals	First description	Treatment	Sex
CRH-iCre	Taniguchi et al., 2011 [53]	DREADD in IPACL CORT measurement ChR2 in IPACL Activation SN R121919	Male
CRH-Cre::Ai9	Madisen et al [248]	Anterograde tracing Retrograde tracing Tissue clearing	Mixed
CRHR1-Cre	Dedic et al [243]	DRAEDD in SN Tracing in GPe DRAEDD in GPe ChR2 in GPe	Male*
CRHR1-Cre::INTACT	This study, Mo et al., 2015 [249]	Sn-RNAseq Staining validation	Male
CRH-Cre::CRHR1$^{\Delta EGFP}$	This study, Refojo et al., 2011 [250]	Anterograd tracing	Mixed
PV-Cre	Hippenmeyer et al., 2005 [251]	Rabies tracing	Mixed
Dat-CreER^{T2}	Engblom et al., 2008 [252]	Rabies tracing	Mixed

* Tracing with mixed gender animals.

3.2 Tissue dissection for single nucleus sequencing

Mice were sacrificed at age of 2 months by cervical dislocation. Brains were collected in ice cold PBS and processed for tissue dissection. The target region (ventral midbrain) was collected by subjecting brains to a brain matrix. Brains were cut into 1 mm thick chunks in order to cover the entire region of interest. Cortex was removed and tissues were processed to the next step immediately.

3.3 Isolation of Nuclei

Tissues (fresh mouse brain) were homogenized in 2 ml of lysis buffer (0.32 M sucrose, 10 mM Tris pH 8.0, 5 mM $CaCl_2$, 3 mM Mg acetate, 1 mM DTT, 0.1 mM EDTA, 0.1% Triton X-100) by douncing 10-50 times in a 7-ml dounce homogenizer. Lysate was transferred to a 4 ml ultracentrifugation tube (Beckman; 14 × 95 mm; 344061), and 2 ml of sucrose solution (1.8 M sucrose, 10 mM Tris pH 8.0, 3 mM Mg acetate, 1 mM DTT) was pipetted directly to the bottom of the tube. Ultracentrifugation was carried out at 24,400 rpm for 2.5 h at 4 °C (Beckman; L8-70 M; SW80 rotor). After centrifugation, the two layers of solution were removed by aspiration. Each nuclei containing pellet was resuspended in PBS with 0.1% FBS.

3.4 FACs (Fluorescence activated cell sorting)

After isolation of nuclei, samples were processed to FACs immediately. FACS analysis was performed with a FACS Melody (Beckton Dickinson) in BD FACS Flow TM medium, with a nozzle diameter of 100 μm. Debris and aggregated nuclei were gated out by forward scatter, sideward scatter. Single nuclei were gated out by FSC-W/FSC-A. Gating for fluorophores was done using isolated nuclei containing membrane GFP.

3.5 Single nuclei RNA sequencing

Single nuclei sequencing was performed by using 10x genomics kit and following the instructions of the manufacture (10x Genomics). In brief, nuclei were mixed with solutions containing barcoded beads and partitioning oil. To achieve single cell resolution, cells were delivered at a limiting dilution. After the first step, the gel bead was dissolved, primers were released, and any copartitioned cell is lysed. Primers were mixed with the cell lysate and a master mix containing reverse transcription (RT) reagents. This produced barcoded, full-length cDNA from poly-adenylated mRNA. After incubation, products were broken and pooled fractions were recovered. Silane magnetic beads were used to purify the first-strand cDNA from the post RT reaction mixture, which includes leftover biochemical reagents and primers. Barcoded, full-length cDNA was amplified via PCR to generate sufficient mass for library construction. Enzymatic fragmentation and size selection were used to optimize the cDNA amplicon size. A Chromium single cell 3' gene expression library comprises standard Illumina paired-end constructs which begin and end with P5 and P7. The 16 bp 10x barcode and 12 bp UMI are encoded in read 1, while Read 2 is used to sequence the cDNA fragment. Sample index sequences are incorporated as the i7 index read. TruSeq Read 1 and TruSeq Read 2 are standard Illumina sequencing primer sites used in paired-end sequencing.

3.6 Tissue collection and immunohistochemistry

Mice were sacrificed by an overdose of isoflurane and subsequently perfused. Mice were first perfused with 20 ml PBS then perfused with 20 ml 4% PFA. Dissected brains were fixed in 4% paraformaldehyde overnight at 4℃. All sections for staining were sliced at a thickness of 50 μm. Slices were rinsed in PBS, and incubated overnight at 4℃ with primary antibody (concentration adjusted according to different antibody requirements). Slices were then incubated with suitable fluorescence secondary antibody (1: 250 Alexa fluoro, Invitrogen) and then washed with PBS. Slides were cover slipped with mounting medium (Fluoromount-G, SouthernBiotech) and left to either air dry or cooled to -20°C for photo shooting. (Table 3)

Table 3. List of antibodies

Antibody	Specie and manufacture	Concentration
GFP	Chicken, Aves	1:500
TH	Rabbit, Millipore	1:1000
PV	Mouse, Swant	1:500
RFP	Rabbit, Rockland	1:500
cFOS	Rabbit, Abcam	1:1000
NeuN	Millipore	1:400
GFAP	Rabbit, Abcam	1:1000
Wfs1	Rabbit, St John's Laboratory	1:200
Calbindin	Mouse, Sigma	1:500
SOM	Rabbit, Peninsula, Laboratories International	1:500
Calretinin	Rabbit, SYSY	1:1000
Pkcd	Mouse, BD Bioscience	1:200

3.7 CNO administration

CNO dihydrochloroid was dissolved in 0.9% saline in a concentration of 2.5mg/ml. CNO was administrated 15 min before mice entered the behavioural chambers by i.p. injection of a final concentration of 5 mg/kg.

3.8 R121919 administration

R121919 hydrochloroid was dissolved in 0.9% saline with 10% of ethanol at the concentration of 1.25 mg/ml. R121919 was administrated 30 min prior of behavioural tests by i.p. injection of a final concentration of 10 mg/kg.

3.9 Assessment of animal behaviour

To assess anxiety behaviour, mice were subjected to the open field, elevated plus maze, dark light box, marble burying test, forced swim test, conditioned place preference and novelty suppressed feeding tests. The movement of animals was tracked using Any-maze software (Stoelting). There was a one-day rest between each test, except for the conditioned place

preference test. Mice were single housed for a week and entered the respective test apparatus in random order. All mazes are made by plastic glass; there is no bedding in the maze during the test.

Open field test

Mice were transferred into the arena (40 x 40 cm) and allowed to explore freely for 30 min. The distance of moving, time in the centre zone and entries into centre zone were recorded. Centre zone illumination was 15 lux.

Locomotor activity

Mice were allowed to explore freely for 30 min before the administration of CNO, and after CNO administration mice were exploring the arena for 60 min. Distance of moving were recorded. Same illumination as open field test.

Elevated plus maze

Mice were subjected to the elevated plus maze (20 cm both open and closed arms, 15 cm height from floor) and allowed to freely explore for 15 min. Distance of moving, time spent in open arms and entries into open arms were recorded. Open arms illumination was more than 20 lux, with illumination less then 15 lux in the closed arms.

Dark light box

Mice were subjected to dark light box for 10 min. Mice will enter lit compartment through the tunnel connecting with the dark compartment. Time spent in the lit zone and entries into the lit zone were recorded. Lit zone illumination was more than 400 lux.

Marble burying test

10 marbles were placed in the cage with thick bedding (5 cm), mice were allowed to explore freely in the cage for 90 min. The number of marbles buried was registered. Illumination is 15 lux.

Forced swim test

Mice were subjected to a beaker containing 15 cm of water for 6 min and the time mice spent floating, struggling and swimming was recorded. Water temperature was kept at 25°C.

Conditioned place preference

The CPP apparatus (T shape) consists of a starting box and two conditioning boxes (40(l) x 40(w) x 35(h) cm) made of black acrylic boards. Conditioning compartments are 18(l) x 20(w) x 35(h) cm, separated by a smaller compartment (10(l) x 20(w) x 35(h) cm) in the middle. Left compartment contains mosaic walls and smooth flooring, the right one with black walls and thin-grid flooring.

The experiment consists of 3 phases (5d): preconditioning, conditioning and post-conditioning phases. During preconditioning phase (pretest trial) (d1), each mouse is subjected to the middle compartment with free access to all compartments for 10 min. The conditioning phase (d2 to d4) consists of six 30 min training sessions that are carried out during morning and afternoon training sessions; CNO (5 mg/kg, i.p.) is always paired with the preferred compartment in the afternoon. On d2, mice are treated with saline (10 ml/kg, i.p.) in the morning training session and immediately paired with the less preferred compartment with access blocked for 30 min. In the afternoon, mice are treated with CNO and immediately paired with preferred compartment for 30 min. The morning and afternoon training sessions were repeated for 3d in total from d2-d4. In post-conditioning phase (acquisition trial) (d5), each mouse is subjected to the middle compartment with free access to all compartments in the absence of treatments for 10 min.

Novelty suppressed feeding

Mice were fasted overnight before the start of the experiment. The next day mice were placed in a novel environment (Type 2 mouse cage) with a food pallet presented in the middle of the arena together with strong light on top. Mice were allowed to explorer the arena for 15 min, the first latency to eat and time spent on eating was recorded. Illumination more than 400 lux.

3.10 Virus and tracer injections

Mice were anesthetized for surgery with isoflurane (1.5–2%) and placed in a stereotaxic frame (Kopf Instruments). Body temperature was maintained with a heating pad. A systemic anesthetic (Metacom 5 mg/kg bodyweight) was administered. CRH-*Cre*::Ai9, CRHR1-*Cre* and CRHR1-GFP animals were used for anterograde and retrograde tracing. For retrograde tracing, 0.5 ul of retrograde tracer were injected unilaterally in the region of interest, VTA (AP: -3, ML: 0.6, DV: -4.5) and SN (AP: -3, ML: 1.65, DV: -4.13). For anterograde tracing 0.5 ul of virus were injected into BSTLD (AP: 0.14, ML: 0.9, DV: -3.9), BSTLP (AP: 0.14, ML: 0.9, DV: -4.3), CeA (AP: -1.22, ML: 2.8, DV: -4.7), IPACL (AP: 0.26, ML: 2, DV: -5) and striatum (AP: 0.38, ML: 1.5, DV: -3). All tracers were incubated for 2 weeks before the animals were sacrificed. For the DREADD experiment, 0.5 ul of virus were injected bilaterally into target regions (IPACL, SN or GPe) of CRH-*iCre* and CRHR1-*Cre* animals (coordinates as previous described). Then mice were rested for two weeks before entering behavioural experiments. For rabies virus tracing, we first injected helper virus into SN of CRH-Venus, CRHR1-*Cre*, PV-*Cre* or Dat-*Cre*ERT^2 mice. Two weeks afterward, we injected rabies virus in the same region. (Table 4)

Table 4. Virus and tracers

Virus/ Tracers	Manufacture	Usage
FluoroGold	Fluorochrome	1%
Green Retrobeads^{TM} IX	Lumafluro	Undiluted
AAV-CMV-DIO-Synaptophysin-GFP	Grinevich lab	~10^8 vg/mL
AAV_9-CMV-Synaptophysin-DIO-mCherry	Addgene	~10^8 vg/mL
AAV_8-hSyn-DIO-hM3Dq-mCherry	Addgene	~10^8 vg/mL
AAV_8-hSyn-DIO-mCherry	Addgene	~10^8 vg/mL
AAV_1-CBh-DIO-TVA-t2A-GFP-OG	Götz lab	~10^{12} vg/mL
SAD-EnVA-dG	Conzelmann lab	Undiluted

3.11 Optogenetic manipulation

Adult (25–30g) CRH-*iCre* male mice were grouped housed until surgery. Mice were bilaterally injected with 0.5 µL of AAV_5-Ef1a-DIO-ChR2-EYFP or AAV_5-Ef1a-DIO-EYFP virus (~10^{12} vg/mL, UNC Vector Core) into the IPACL or GPe (coordinates from Bregma: 0.26 AP, ± 2 ML, −5 DV, -0.34 AP, ±1.8 ML, -4 DV). Two weeks after virus injection the optic fiber (200µm core, 0.39 NA, 1.25 mm ferrule, Thorlabs) were implanted above the IPACL (−4.7 mm ventral) or SN (-3.8 mm). Implants were secured with cyanoacrylic glue, and the exposed skull was covered with dental acrylic (Paladur). optogenetic manipulation took place two weeks after the implantation.

3.12 In vivo optogenetic excitation

For photoactivation experiments, 10-ms, 473-nm light pulses at 20 Hz and 10 mW were used. The laser was triggered on the basis of the location of the animal by using Bonsai data-streaming software and Arduino microcontrollers.

3.13 Real time place preference

Mice were placed in a place preference chamber (as described above) for 20 min. One counterbalanced side of the chamber was assigned as the stimulation side. In the photostimulation experiments, mice received a 473-nm stimulation of 20 Hz in the photostimulated side of the arena, which was randomly assigned. The laser was triggered on the basis of the location of the animal by using primmax software and controllers. Behavioural data was recorded via a CCD camera interfaced with Ethovision software (Noldus Information Technologies).

3.14 CLARITY

Perfused mouse brains were fixed in 4% PFA overnight then been transferred into 1% hydrogel solution for 48 hr. The samples were degassed (nitrogen replacing oxygen, using 50ml caps with tubing for 30 minutes) and polymerized (4-5 hours at 37°C) in a 50ml tube. The brains were removed from hydrogel and washed with 200mM NaOH-Boric buffer (pH=8.5) containing 8% SDS for 6-12 hours at 37°C (no shaking) to remove residual PFA and monomers. Brains were transferred to a flow-assisted clearing device using a temperature-control circulator. 100mM Tris-Boric Buffer (pH=8.5) containing 8% SDS was used to accelerate the clearing (at 37-40°C). After clearing, the brains were washed in PBST (0.2% Triton-X100) for at least 48 hours at 37°C to remove residual SDS. Then brains were incubated in sRIMS for several days at room temperature. After sRIMS incubation, the brains were for imaging.

3.15 iDISCO

Perfused mouse brains were fixed in 4% PFA overnight then washed in PBS 30 min three times at room temperature. The samples were dehydrated with methanol/H_2O series: from 20% to 100%, 1h each. Samples were washed further with 100% methanol for 1h and then chilled at 4°c. Overnight incubation of samples with shaking in 66% DCM/ 33% methanol at room temperature. Next day samples were washed twice in 100% methanol at room temperature and then chilled at 4°c. Samples were bleached in chilled fresh 5% H_2O_2 in methanol overnight at 4°c. Samples were rehydrated with methanol/H_2O series: 80%, 60%, 40%, 20%, PBS; 1h each then washed in PTx.2 (0.2% Triton in PBS) at room temperature twice. Samples were incubated in permeabilization solution (PTx.2+1% DMSO+Glycin), 37°C for 2 days (max. 2 days). Then blocked in blocking solution,37 °C, for 2 days (max. 2 days). Samples were incubated with primary antibody in PTwH (0.2% Tween 20 in PBS+10mg Heparin) +5% DMSO+3% goat Serum, 37° for 7 days. After incubation, washed in PTwH for 4-5 times until the next day. Samples were incubated with secondary antibody in PTwH+ 3% goat serum, 37° for 7 days then washed in PTwH for 4-5 times until the next day. Samples were dehydrated in methanol/H_2O series: 20%, 40%, 60%, 80%, 100%, 100%; 1hr each at RT (can be left optionally overnight at RT at this point). 3h incubation with shaking, in 66% DCM/33% Methanol at RT. Incubate in 100% DCM(Sigma 270997-12X100ML) 15 minutes twice (with shaking) to wash the MeOH. Incubate in Di-Benzyl Ether (DBE, Sigma 108014-1KG) (no shaking). The tube should be filled almost completely with DBE to prevent the air from oxidizing the sample. Before imaging, invert the tube a couple of time to finish mixing the solution.

3.16 Statistical analysis

The mean ± SEM was determined for each group. Figure generation and statistic calculation were conducted by Graphpad Prism software. Student's t test was performed with comparison between two groups with one variation. Two-way ANOVA was performed with two groups with multiple variations, Bonferroni's post-hoc test was used for multiple comparisons. Two-way ANOVA with repeated measures was performed with two groups

with continuous variations (time). Bonferroni's post- hoc test was used for multiple comparisons. Differences were considered significant when p was less than 0.05

4. Results

Towards a biological signature of CRHR1 neurons

4.1 Single-nucleus RNA sequencing

In order to investigate the biological identity of midbrain CRHR1 neurons, single-nucleus RNA sequencing (sn-RNASeq) was conducted as an unbiased approach. Since the endogenous expression of CRHR1 gene is quite low, another reporter system is required to provide assist and act as a reference. CRHR1-*Cre*::INTACT animals were introduced for this purpose. This mouse expresses a GFP reporter on the nuclear membrane upon *Cre* recombination which enables fluorescent active cell sorting (FACS). CRHR1-*Cre*::INTACT animals were sacrificed and the ventral midbrain was isolated. Nuclei were isolated from the tissue and immediately sorted by FACS. GFP-positive nuclei were then processed following the custom protocol of sn-RNASeq provided by 10x Genomics. After sequencing, the data was analysed with the python package scanpy [doi: 10.1186/s13059-017-1382-0]. Following quality controls including cell QC and gene QC were carried out on the raw dataset: number of unique molecular identifiers (UMIs), the number of expressed genes and the fraction of mitochondrial genes (Fig 6a-f). Of the 492,928 cells and 31,053 genes in the raw dataset, 16,665 cells and 13,439 genes remained for further analysis after QC. R package scran [doi: 10.12688/f1000research.9501.2] was used to normalize feature and gene counts. 4,000 highly variable genes were selected after data normalization (Fig 6h). The clusters are visualised with the UMAP algorithm. We checked for doublets using the python package scrublet [doi: 10.1016/j.cels.2018.11.005] and ensured there were few doublets and cells do not cluster by the cell cycle phases (Fig 6g). A Welch t-test was performed for differential gene expression between clusters and cluster-specific marker genes were used to annotate each cluster.

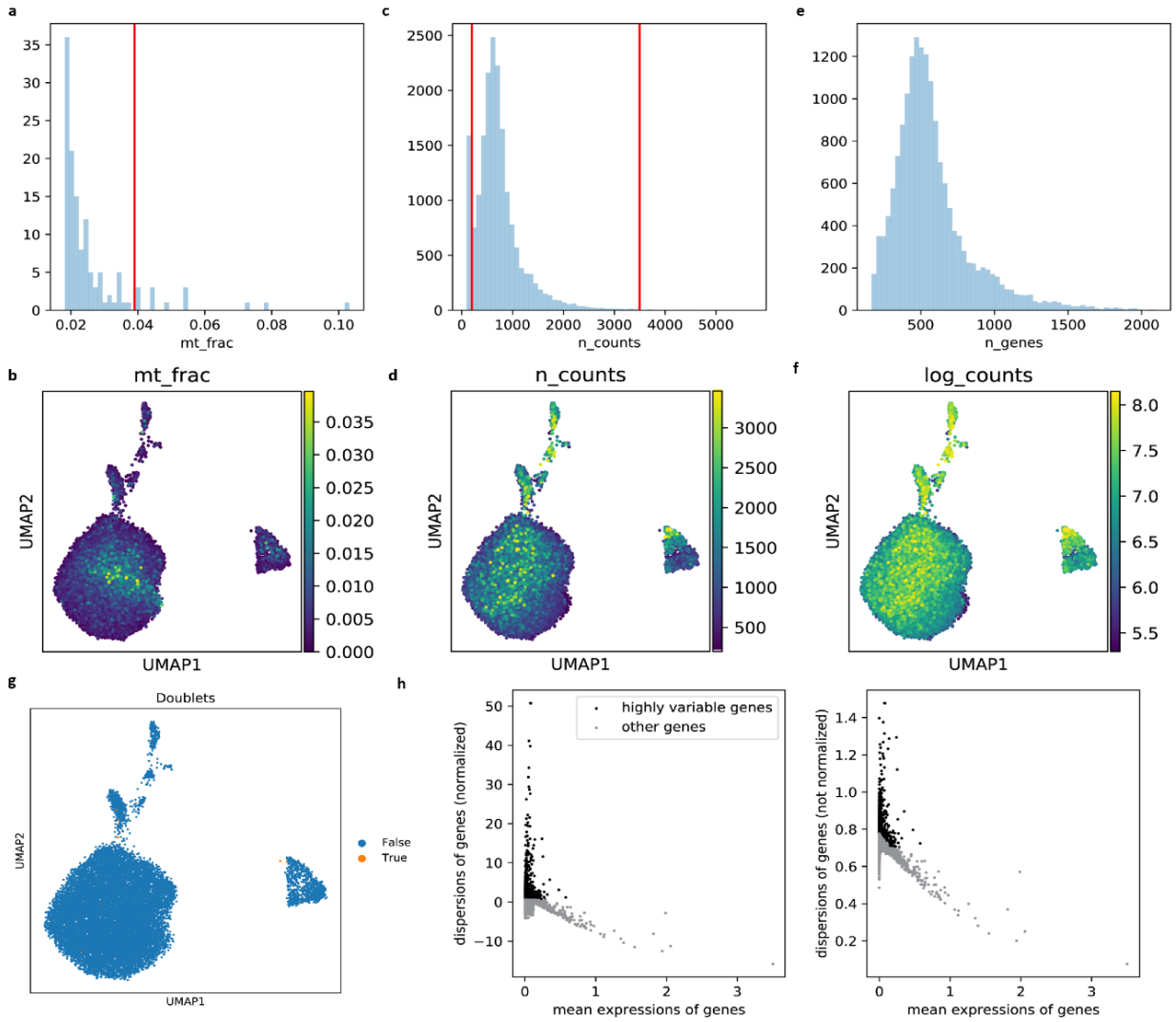

Fig 6. Quality control of the Sn-RNASeq data

(a) Threshold for mitochondria fraction (mt_fraction). (b) UMAP showing the distribution of mt_fraction in the cluster. (c)(d) Quality control for UMI counts of the clusters. (e)(f) Number of genes expressed in the clusters. (g) There are very small numbers of doublets been detected in the clusters. (h) Selection of highly expressed gene from the raw data.

CRHR1 nuclei were separated into 9 clusters, to determine the annotation of each cluster, top 20 expressed genes per cluster were selected. Top 20 genes were determined by their expression level compared to all genes and and compared to the other clusters (Fig 7c). The top 20 genes were manually analyzed and searched for their expression in different cell types in the midbrain using publicly available data at Mouse Brain Atlas (mousebrain.org), for instance dopaminergic (DA), GABAergic and glutamatergic (Glu) neurons. Next, the mean expression representing each cell type was compared and the cluster was assigned to the cell type if the expression was the highest compared to the other clusters.

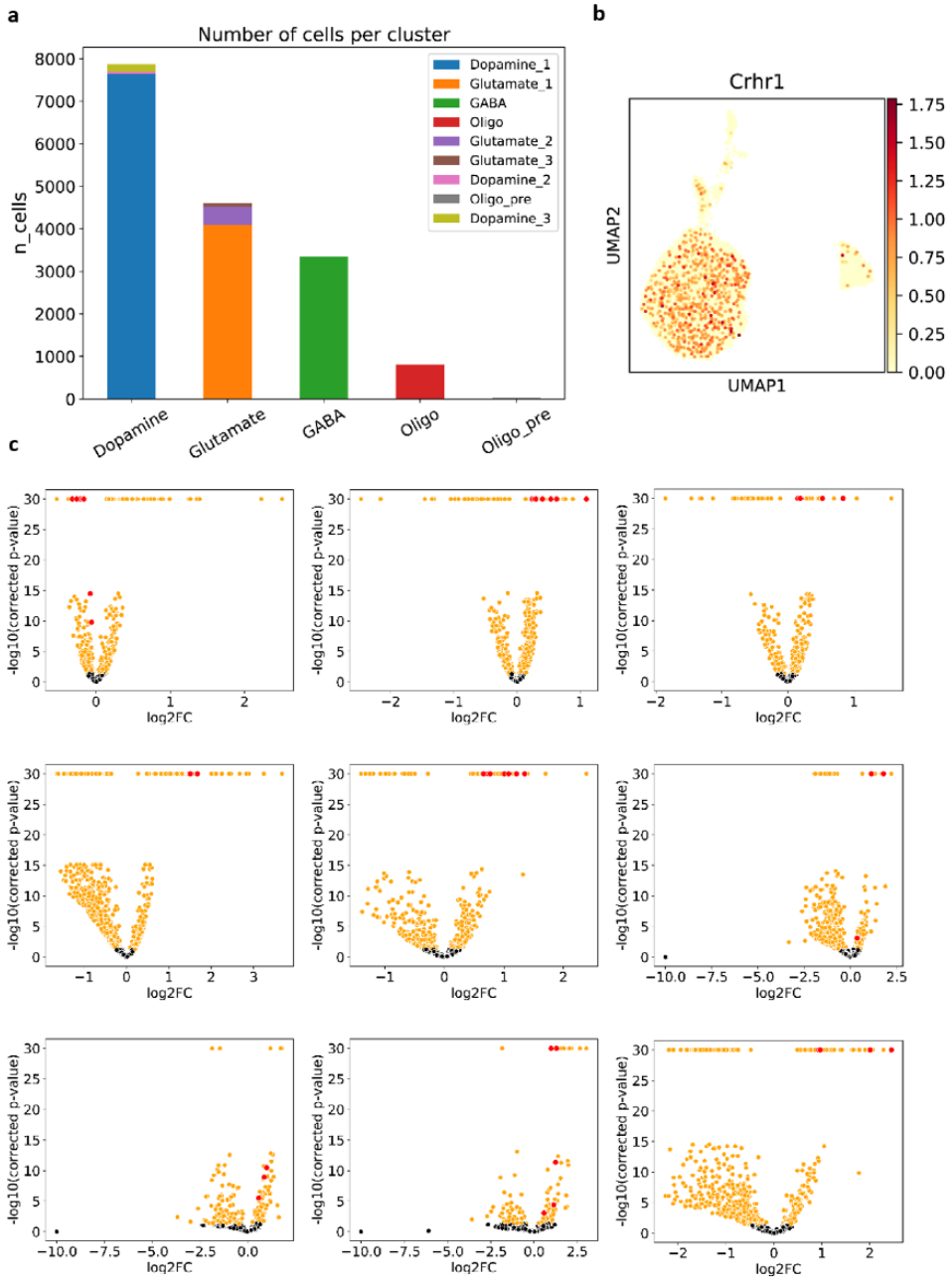

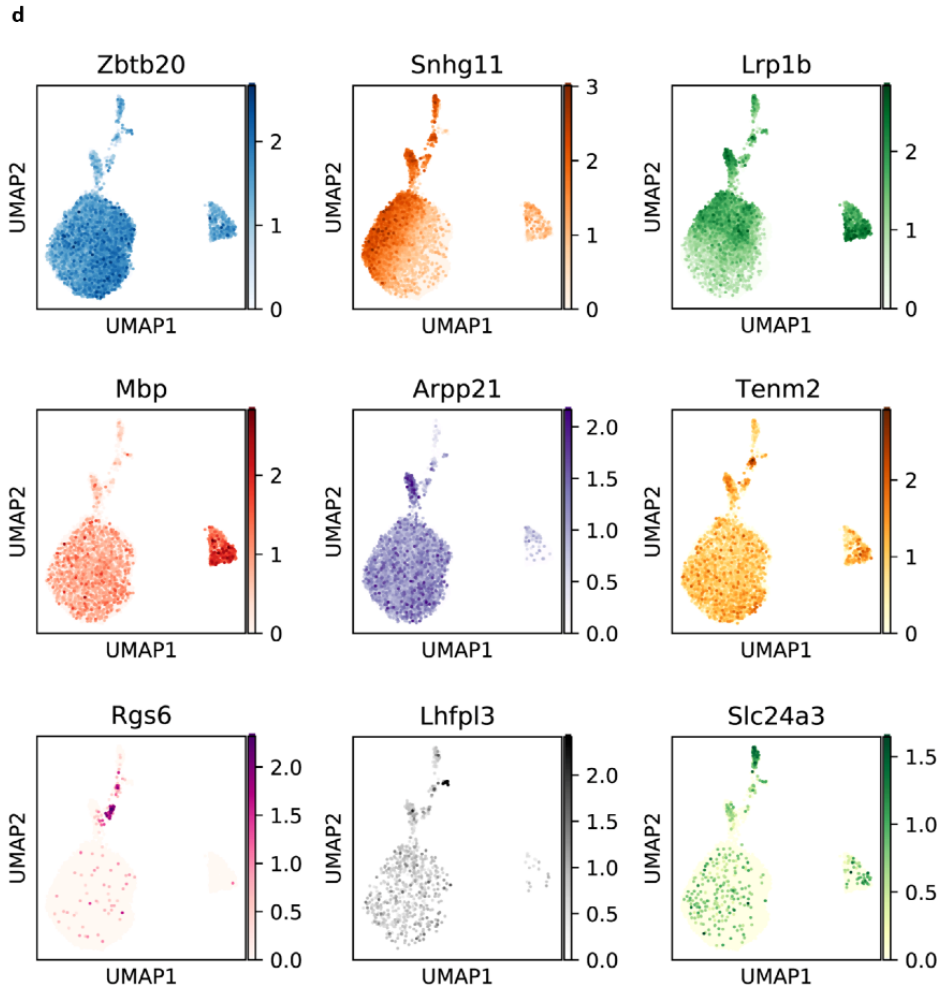

Fig 7. Determination of clusters of midbrain CRHR1 neurons

(a) Number of cells belonging to different cell types. (b) Distribution of CRHR1 neurons within the clusters based on endogenous CRHR1 gene expression. (c) Volcano plots depicting the determination of marker genes in each cluster. (d) Distribution of marker genes for each cluster.

The analysis of Sn-RNAseq data revealed three main clusters of CRHR1 neurons: DA (47%), Glu (25%) and GABA (20%) neurons. In addition, there are 4.9% of oligodendrocyte (Oligo) and 0.2% of oligodendrocyte precursor cells (OPCs) (Fig 7a and 8a).

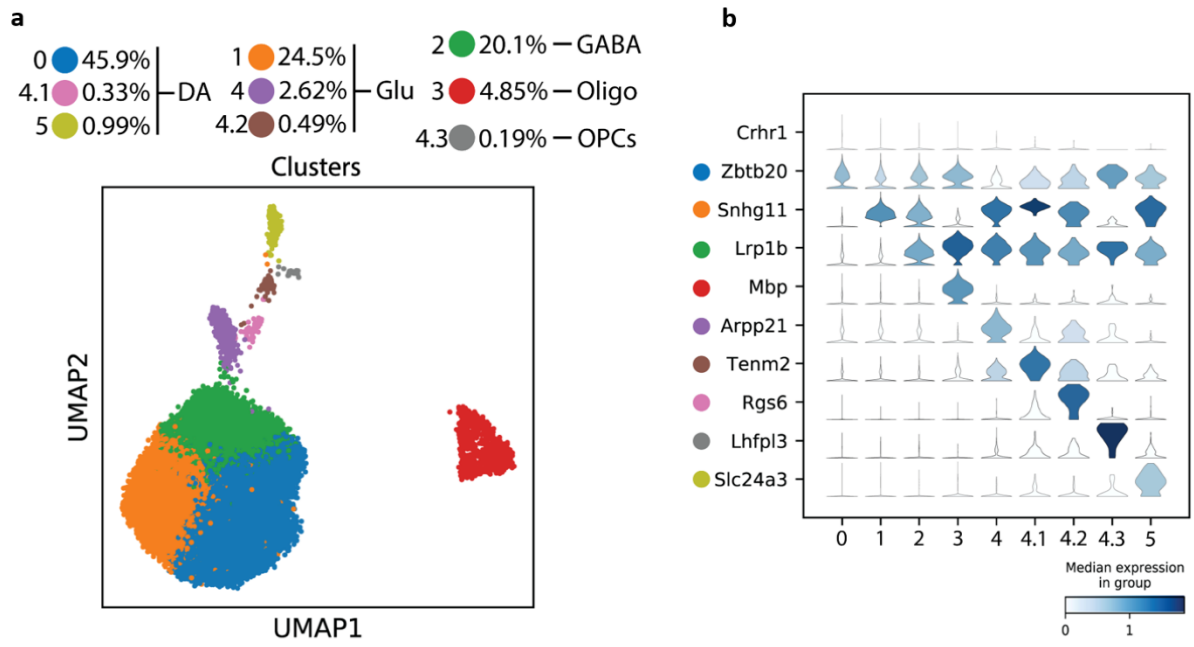

Fig 8. Distribution of CRHR1 expressing cell populations in the ventral midbrain

(a) UMAP depiciting 9 clusters of midbrain CRHR1 neurons which can be specified into main clusters: dopaminergic (DA), glutamatergic (Glu) and GABAergic (GABA) CRHR1 neurons as well as oligodendrocyte (Oligo) and oligodendrocyte precursor cells (OPCs). (b) Expression of marker genes for each cluster are indicated as violin plots.

4.2 Validation of single nucleus sequencing results

4.2.1 Confirmation of heterogeneity of CRHR1 expressing cells in the ventral mid brain with immuno-histochemistry

To validate the single-nucleus sequencing result, CRHR1-*Cre* mice crossed with INTACT mice were used. GFP signals were analyzed throughout different brain sections comparing to the typical CRHR1 expression pattern (Fig 9 a, b). Staining for GFP (CRHR1 positive nuclei), TH (dopaminergic neurons) and PV (GABAergic neurons) were done using brain slices containing the ventral midbrain (Fig 9 c-e). Quantification of cells expressing respective markers in the SN showed that 40% of CRHR1 neurons are dopaminergic, 30% are GABAergic and 30% of the rest are likely glutamatergic neurons (Fig 9 f, g). The number

of cells in SN pars compacta (SNc) and SN pars reticulata (SNr) were separately quantified. CRHR1 neurons are equally distribute between both regions whereas in the SNc there are 80% colocalized with dopaminergic neurons, in contrary, SNr contains 80% of the GABAergic-CRHR1 neurons (Fig 9 h, i). These numbers are consistent with the snRNA-Seq results, confirming the heterogeneity of CRHR1 neurons in the ventral midbrain (Fig 9).

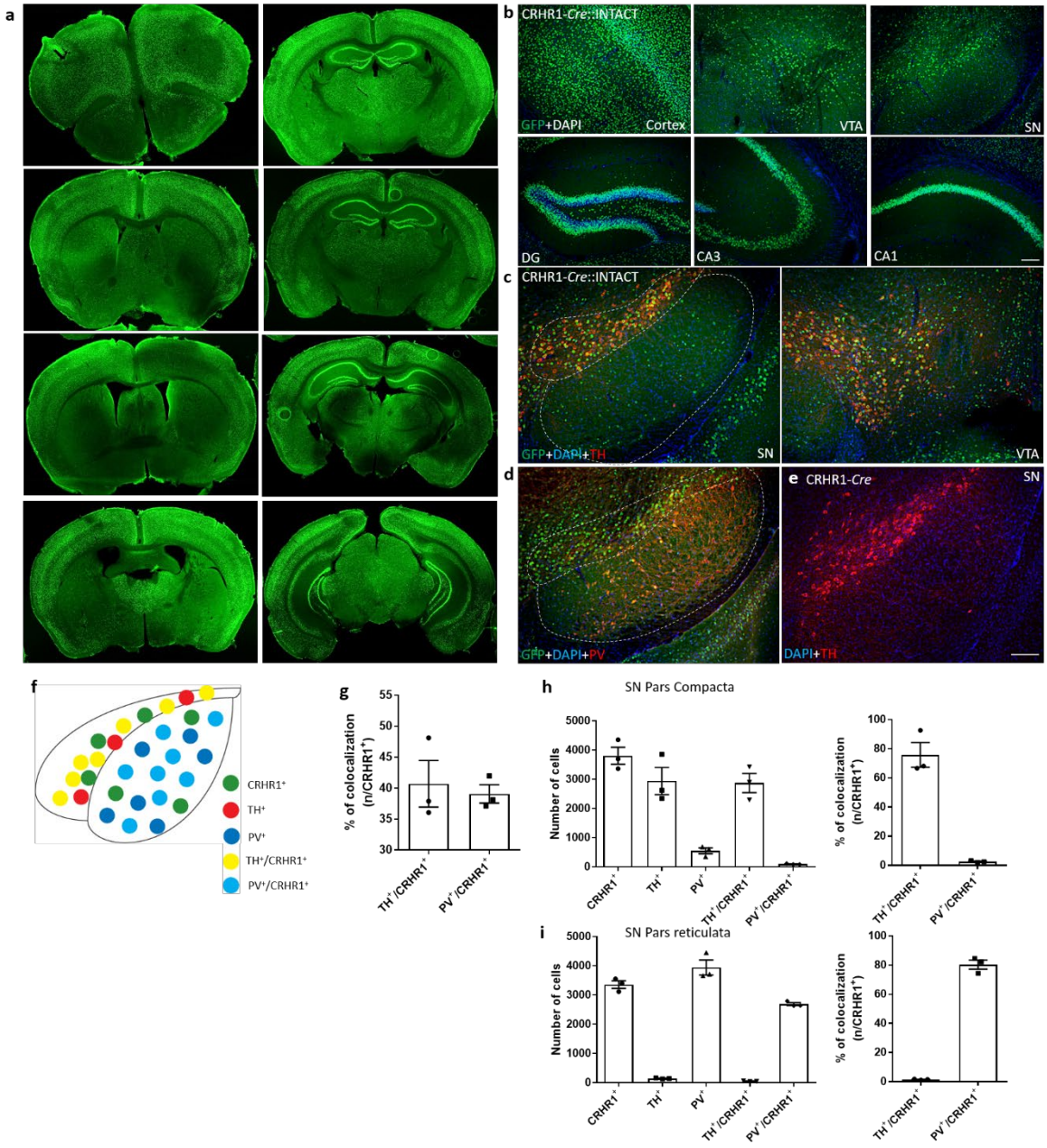

Fig 9. Specification of CRHR1 neuron identity in the SN

(a)(b) GFP staining of nuclei of CRHR1 neurons in different brain regions of CRHR1-*Cre*::INTACT mice showed that the expression of INTACT-GFP matched the expression pattern of endogenous CRHR1. (c)(d) Co-staining of CRHR1 nuclei with markers of dopaminergic (TH) and GABAergic (PV) neurons in the SN. (e) Staining of TH and GFP in the VTA and the SN of CRHR1-*Cre* animals showed the specificity of INTACT-GFP. (f) Distribution of CRHR1 neurons within the SN. (g) Quantification of CRHR1 nuclei in the SN demonstrated equal numbers of dopaminergic and GABAergic CRHR1 positive neurons. (h)(i) Dopaminergic CRHR1 neurons are located mainly in the SN pars compacta (SNc), GABAergic CRHR1 neurons are predominately located in the SN pars reticulata (SNr). Value represent mean ± SEM, Scale bar = 200μm.

Dissecting CRH/CRHR1 neurocircuits

4.3 Retrograde tracing

4.3.1 Retrograde tracing revealed the main brain regions projecting into the VTA

In order to understand the CRH and CRHR1-specific neurocircuits I performed retrograde tracing experiments in the VTA and SN. We chose Fluorogold and retrobeads as tracers for retrograde tracing due to the advantage of strong expression and reliability. I injected 0.5 ul of tracers into the VTA of CRH-*Cre*::Ai9 animals and sacrificed the mice two weeks later. I then checked through the entire brain for the respective fluorescent signals. I quantified the number of cells that got labelled in different regions and the number of cells colocalized with CRH neurons labelled by tdTomato. From the result using fluorogold I found that the main afferents are coming from nucleus accumbens (NAc), central amygdala (CeA), lateral hypothalamus/ ventral medial hypothalamus (LH/VMH), bed nucleus of striatal terminals (BNST) and medial preoptic nucleus (MPO) (Fig 10 a, b and e). In general, similar results were obtained with retrobeads but there were also slight differences between the two groups (Fig 10 c, d and f). This might be due the distribution of the two tracers and the accuracy of injections. Combining results from both tracers revealed that the BNST is the main nucleus from where CRH neurons projection into the VTA.

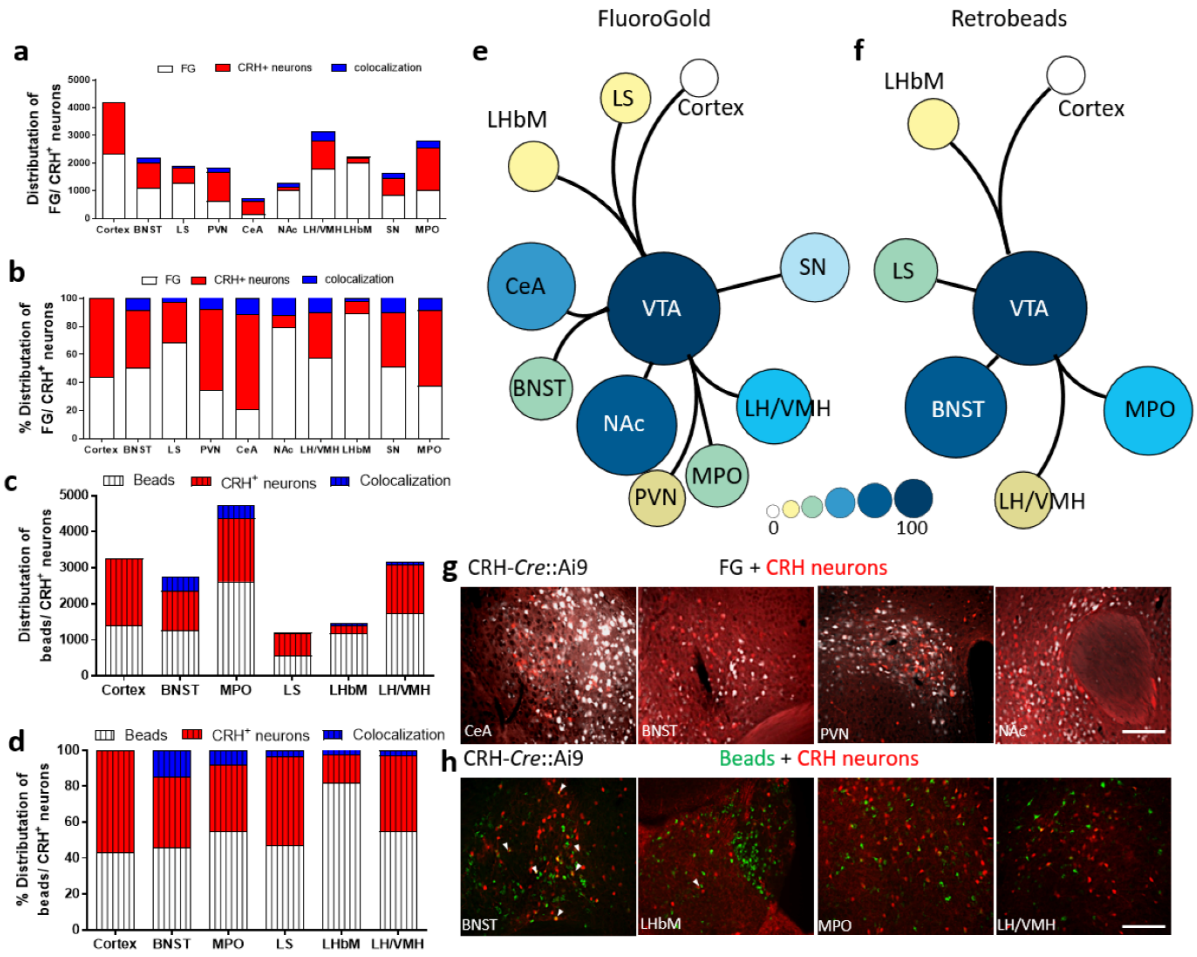

Fig 10. Retrograde tracing of CRH neurons projecting into the VTA

(a)(b) Quantification of the number of CRH neurons colocalizing with FluoroGold and the percentage of colocalization in different brain regions. (c)(d) Quantification of CRH neurons colocalizing with retrobeads and the percentage of colocalization in different brain regions. (e)(f) Circle plots demonstrating that main projections. Colours and size of the circles represent the percentage of colocalization. (g)(h) Representative photos of different brain regions in CRH-*Cre*::Ai9 mice showing tdTomato positive CRH neurons and labelling by Flurogold or retrobeads. Scale bar = 200 μm.

4.3.2 Retrograde tracing of CRH neurons revealed the main brain regions projecting into the substantia nigra (SN)

To identify CRH neurons projecting into the SN, we followed the same procedure as for the VTA and checked labelled cells throughout the brain. Interestingly, we observed strong labelling of cells in the CeA and interstitial nucleus of posterior limb of anterior commissure, lateral part (IPACL). There were also projections detected coming from the BNST which are in accordance with previous studies. (Fig 11).

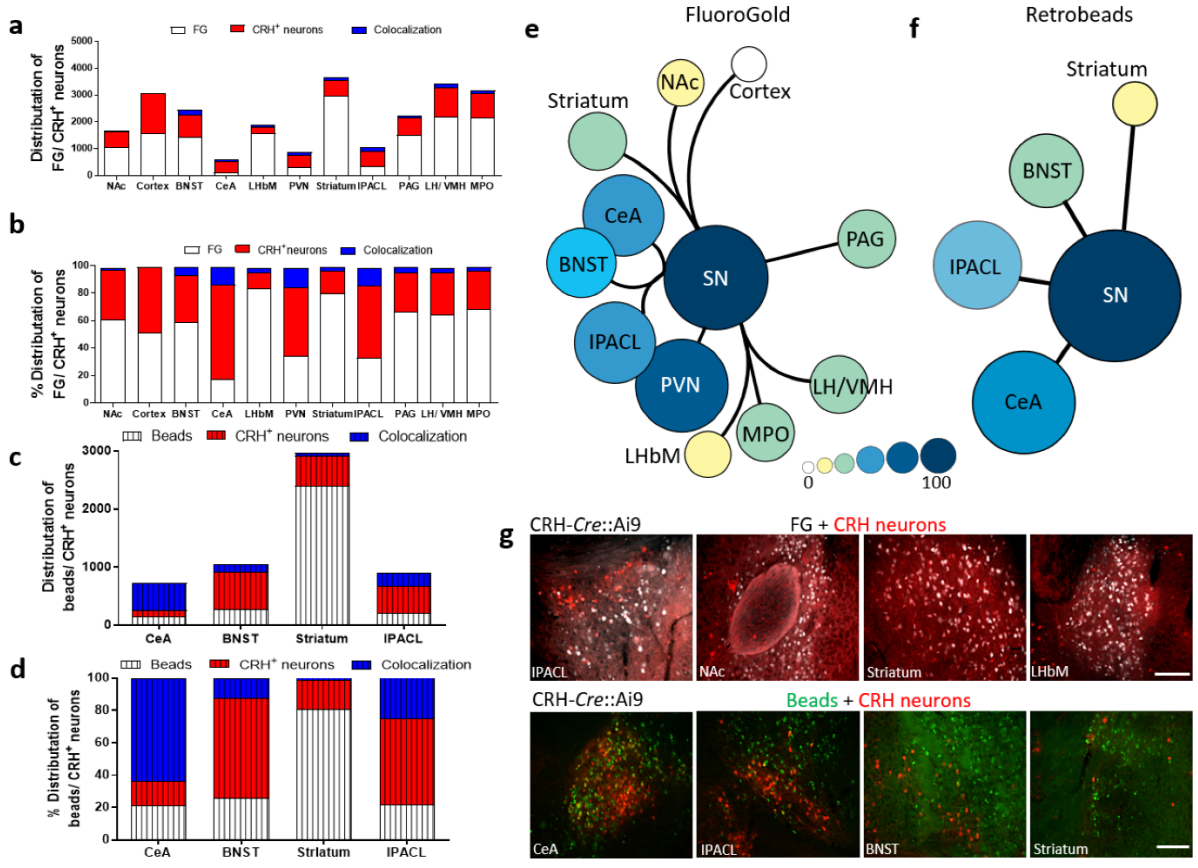

Fig 11. Main projections of CRH neurons into the SN

(a)(b) Quantification of the number of CRH neurons colocalizing with FluoroGold and the percentage of colocalization in different brain regions. (c)(d) Quantification of CRH neurons colocalizing with retrobeads and the percentage of colocalization in different brain regions. (e)(f) Circle plots demonstrating the main projections into the SN. Colours and size of the circles represent the percentage of colocalization. (g)(h) Representative photos of different brain regions in CRH-*Cre*::Ai9 mice showing tdTomato positive CRH neurons and labelling by Flurogold or retrobeads. Scale bar = 200 µm.

4.4 Anterograde tracing

4.4.1 Tracing of extended amygdala CRH efferences

To confirm the results of the retrograde tracing and also have a finer dissection of the identified brain regions I performed AAV-based anterograde tracing. Therefore, I injected AAV-Ef1a-DIO-Syp-GFP in 4 different regions of the extended amygdala of CRH-*Cre*::Ai9 animals: BSTLP, BSTLD, CeA and IPACL (Fig 12). These are regions comprising the extended amygdala that have previously been linked to stress-related or anxiety-like behaviours.

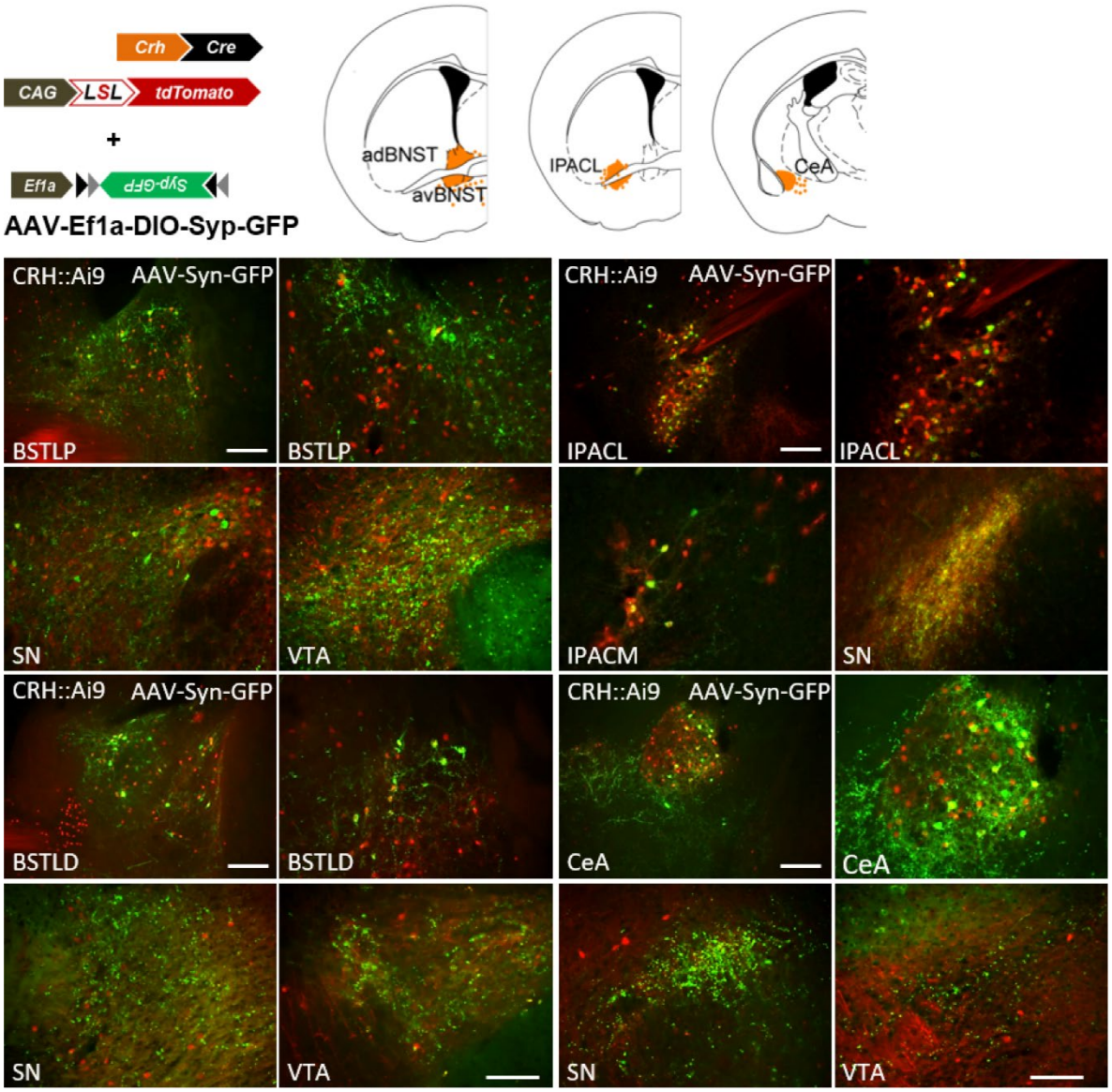

Fig 12. Injection of anterograde tracing virus and demonstration of virus expression

AAV-Ef1a-DIO-Syp-GFP virus was injected as an anterograde tracer into CRH-*Cre*::Ai9 mice. We injected the virus in region of the extended amygdala: BNST, CeA and IPACL. Pictures show the expression of virus and the axon terminals in the regions of interest. CRH neurons are labelled by tdTomato in red and anterograde tracer is with GFP reporter. Images show the injection sites in different magnifications and the projections sites. Scale bar = 200 μm.

Two weeks after virus injection, mice were sacrificed and the projection strength was quantified throughout the brain. The projection strength was set from 0-5, with the injection site as 5 (highest expression level), 0 represent regions with undetectable expression. The projection strength was calculated by comparing the fluorescence strength of each brain region to the injection site then normalized to relative numbers (Fig 13). Afterward, Pearson association tests were performed to identify the associated connectivity between regions. Our result revealed that the BSTLP connected the most with the VTA followed by CeA and BSTLD. Interestingly, the IPACL has the highest correlation with the SN followed by the CeA and the other regions (Fig 14).

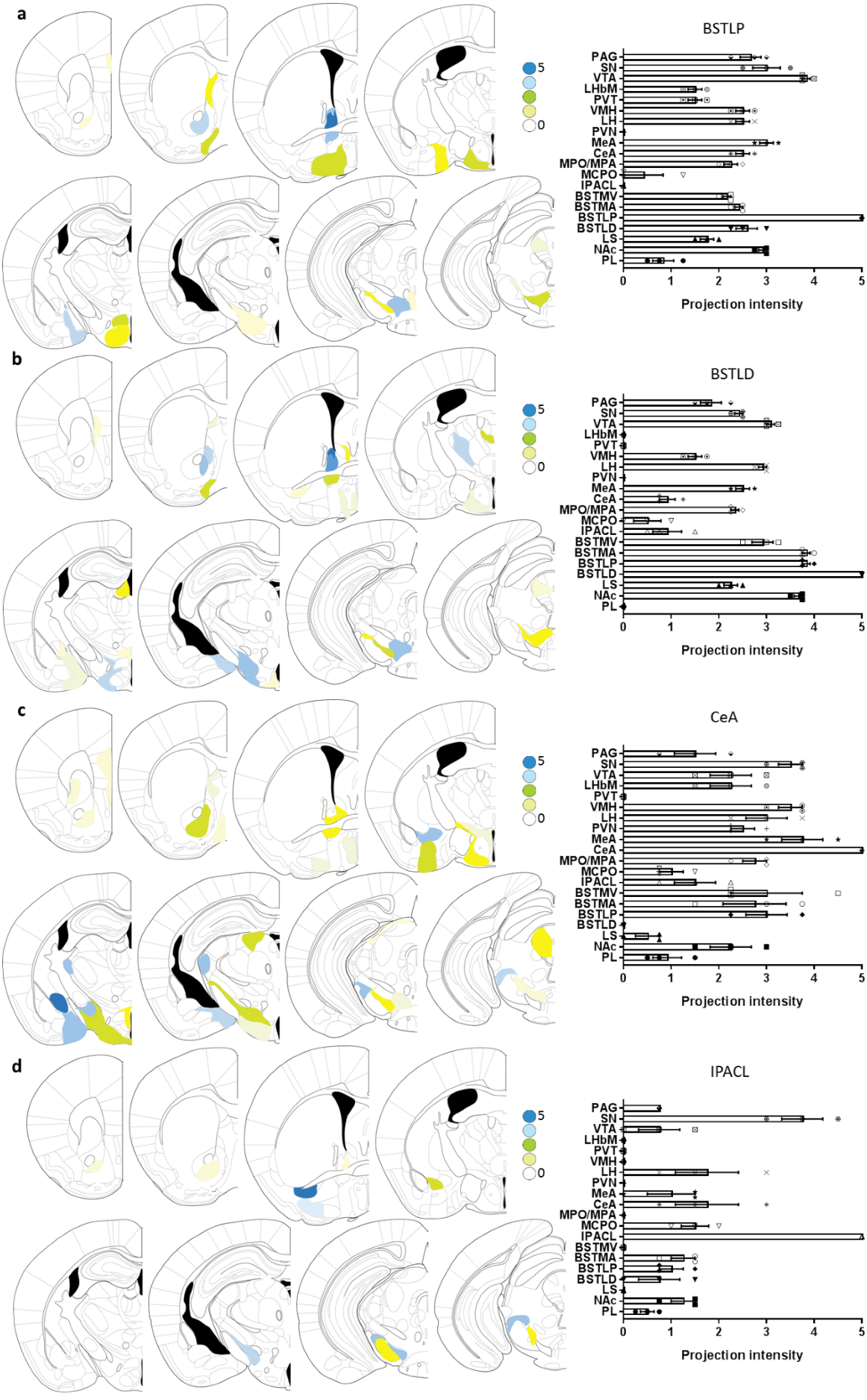
a
5
0
BSTLP
PAG
SN
VTA
LHbM
PVT
VMH
LH
PVN
MeA
CeA
MPO/MPA
MCPO
IPACL
BSTMV
BSTMA
BSTLP
BSTLD
LS
NAc
PL
0 1 2 3 4 5
Projection intensity
b
5
0
BSTLD
PAG
SN
VTA
LHbM
PVT
VMH
LH
PVN
MeA
CeA
MPO/MPA
MCPO
IPACL
BSTMV
BSTMA
BSTLP
BSTLD
LS
NAc
PL
0 1 2 3 4 5
Projection intensity
c
5
0
CeA
PAG
SN
VTA
LHbM
PVT
VMH
LH
PVN
MeA
CeA
MPO/MPA
MCPO
IPACL
BSTMV
BSTMA
BSTLP
BSTLD
LS
NAc
PL
0 1 2 3 4 5
Projection intensity
d
5
0
IPACL
PAG
SN
VTA
LHbM
PVT
VMH
LH
PVN
MeA
CeA
MPO/MPA
MCPO
IPACL
BSTMV
BSTMA
BSTLP
BSTLD
LS
NAc
PL
0 1 2 3 4 5
Projection intensity

Fig 13. Quantification of CRH projections into different brain regions

(a) Projection strength of CRH neurons in the BSTLP was quantified. Data showed that BSTLP has highest connection with the VTA, NAc and other BNST sub-regions. (b) BSTLD also has strong projection into the VTA, NAc and other BNST regions. In addition, BSTLD also projects into LH with high projection intensity. (c) CeA projects to the SN, BNST, VMH, LH and other regions. (d) IPACL projects with highest intensity into the SN compared to other regions. The regions with projections were showed on the left and the expression level was showed on the right side of images. Value represent mean ± SEM.

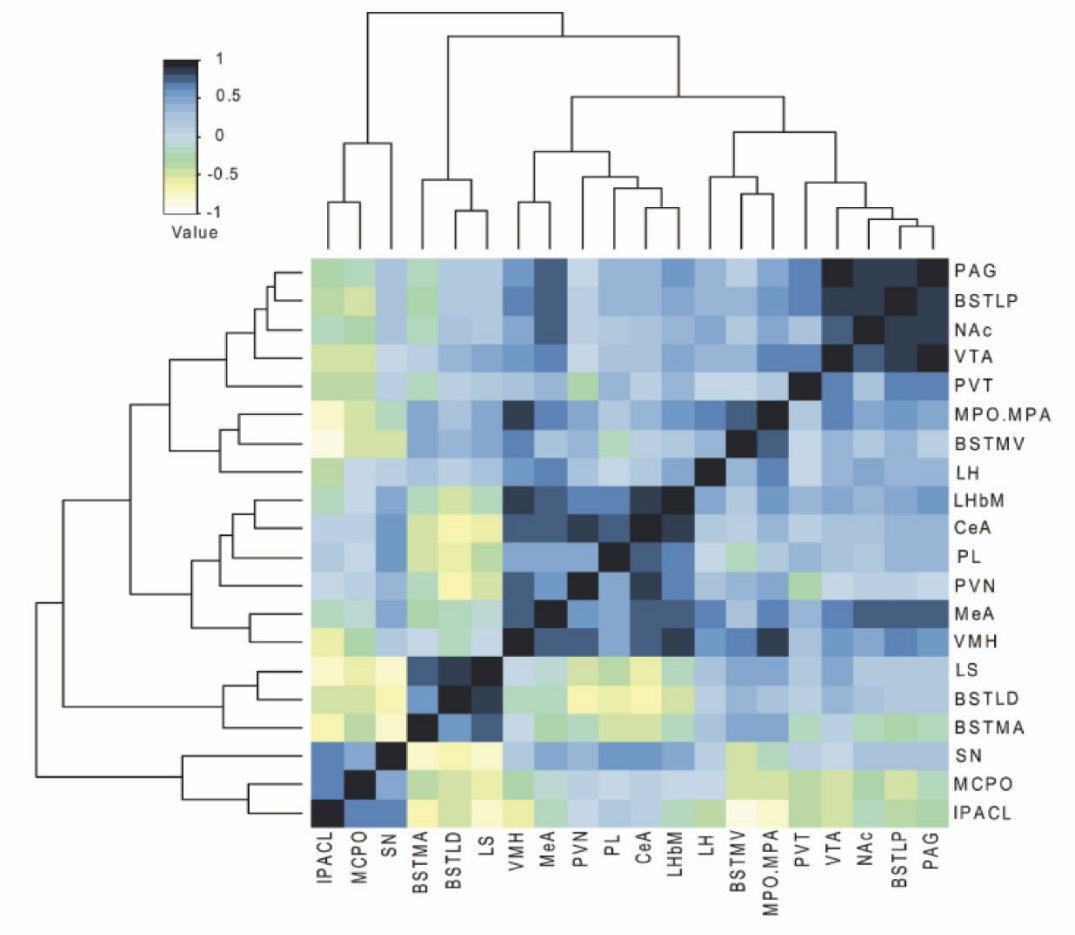

Fig 14. Association of brain connectivity

We quantified the strength of anterograde projections from different brain regions and performed a Pearson assembly test in order to find brain regions highly correlated with respect to connectivity.

4.4.2 Differences in connectivity between CeA and IPACL

To further determine which region will be the main target for subsequent behavioural manipulations, CeA and IPACL were compared. It turned out that the IPACL has a very focused projection almost exclusively innervating the SN. On the other hand, the CeA also has strong projections towards the SN but at the same time projects also to many other regions throughout the brain (Fig 13c and d).

To investigate the anatomical difference between IPACL and CRH projections to the SN, tracing with two differently coloured tracers (AAV-Ef1a-DIO-Syp-mCherry was injected in the IPACL and AAV-Ef1a-DIO-Syp-GFP was injected in the CeA) was conducted in CRH-*Cre*::CRHR1-GFP mice. Result showed that IPACL projections were observed in the medial and lateral part of the SN while the projections originating from the CeA were mainly observed in the lateral part but not in the medial part (Fig 15).

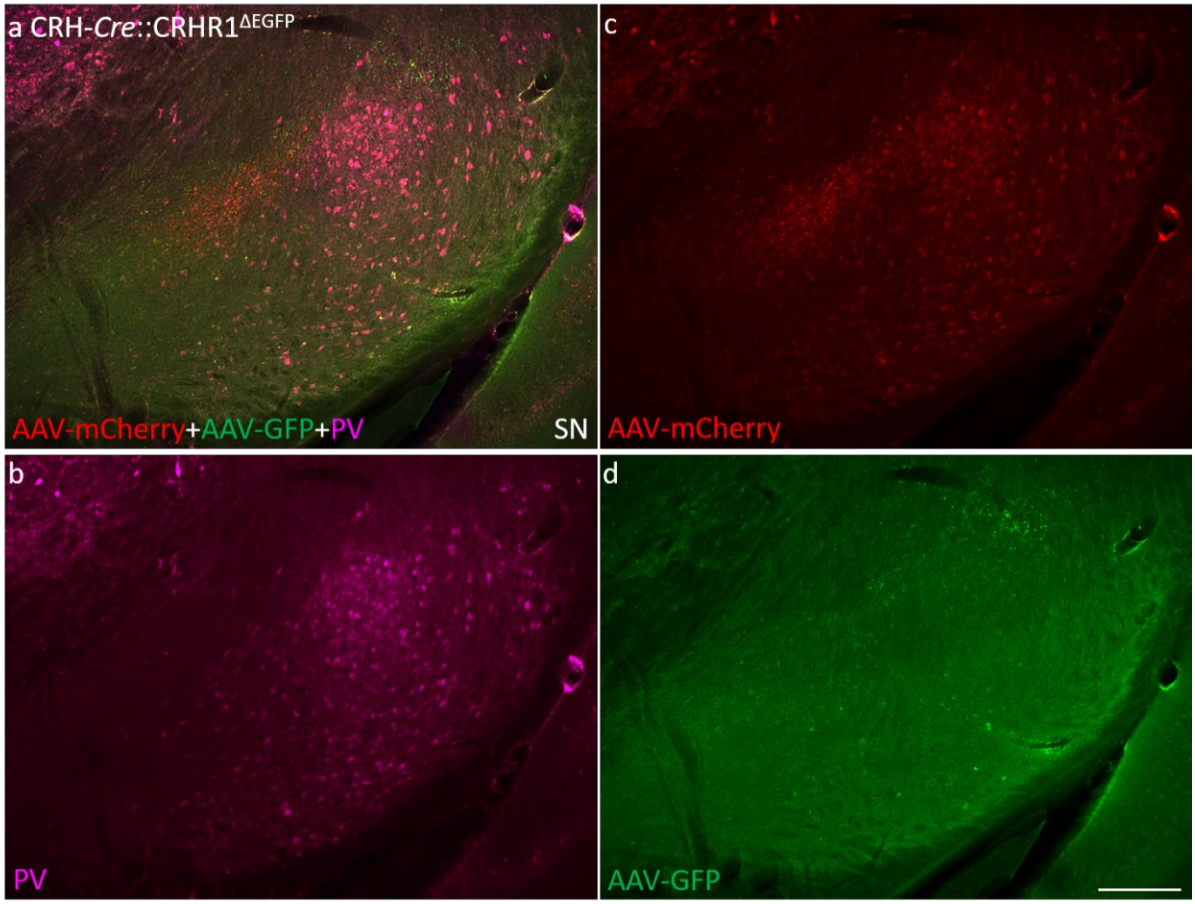

Fig 15. Double tracing reveals spatial segregation of IPACL and CeA in projections in the SN

(a) IPACL and CeA send strong projections into the SN a region which shows enrich of PV positive neurons. (b) Staining of PV positive neurons labelled the region of the SN which contains projections from both IPACL and CeA CRH neurons. (c) Projections from IPACL are located in both medial and lateral part of the SN. (d) Projections for CeA are only located in the lateral part which contains mainly PV neurons. Scale bar = 200 µm.

Furthermore, the IPACL CRH projection in the SN was found to innervate both dopaminergic and GABAergic neurons (Fig 16). Based on this comparison, we screened the large collection of studies in the CRH field but did not find any description of the role of IPACL in anxiety-related behaviours. Therefore, and to better understand its physiological role the IPACL was chosen as a main target for subsequent behavioural manipulations.

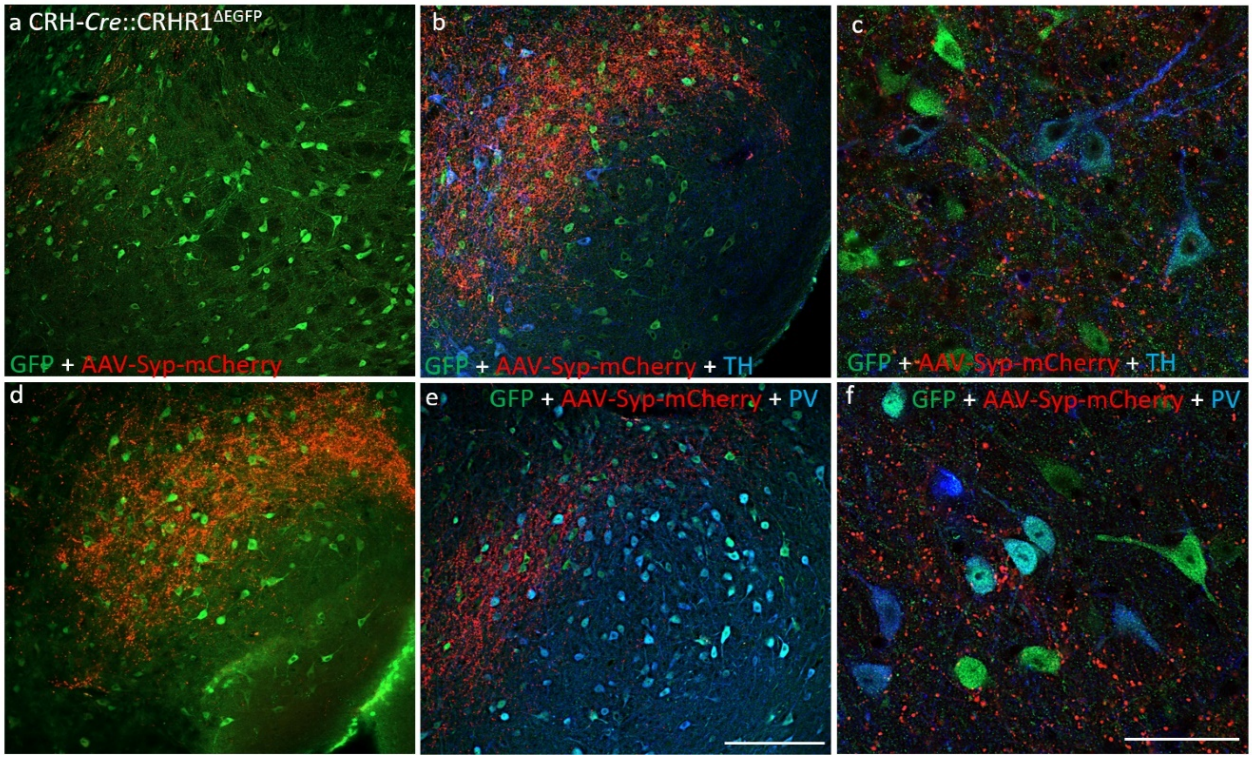

Fig 16. IPACL CRH neurons projecting to both dopamine and PV neurons in the SN

(a)(d) Anterograde tracing with AAV-Syp-mCherry in CRH-*Cre*::CRHR1$^{\Delta EGFP}$ mice showed expression of fluorescence in the SN. (b)(e) Staining of CRHR1 neurons (GFP) with DA (TH) or GABA (PV) neurons showed CRH projections from the IPACL innervating both cell types. (c)(f) Images of higher magnification showed CRH axon terminals innervating local neurons in the SN. Scale bar = 200 µm.

4.4.3 Establishing tissue (brain) clearing methods

In order to reveal the connectivity of CRH neurons in the brain, different tissue (brain) clearing methods were applied in this study. Results of three brain clearing methods: CLARITY, iDISCO and FDISCO (see comparison in the introduction and procedure in material and methods) on CRH-*Cre*::Ai9 animals showed different resolution of CRH neuronal expression in the brain. CLARITY preserved the endogenous tdTomato expression and had least background autofluorescence which served the best for the purpose of tracking neurocircuits in the brain (Fig 17a). iDISCO was able to amplify the soma of neurons with staining but also increased the background signal during imaging (Fig 17b). More optimizations are required in order to maximize the strength of iDISCO in tissue clearness and multiply labelling of different markers. FDISCO, had the weakest expression of tdTomato expression which did not serve as a good method for the purpose (Fig 17c).

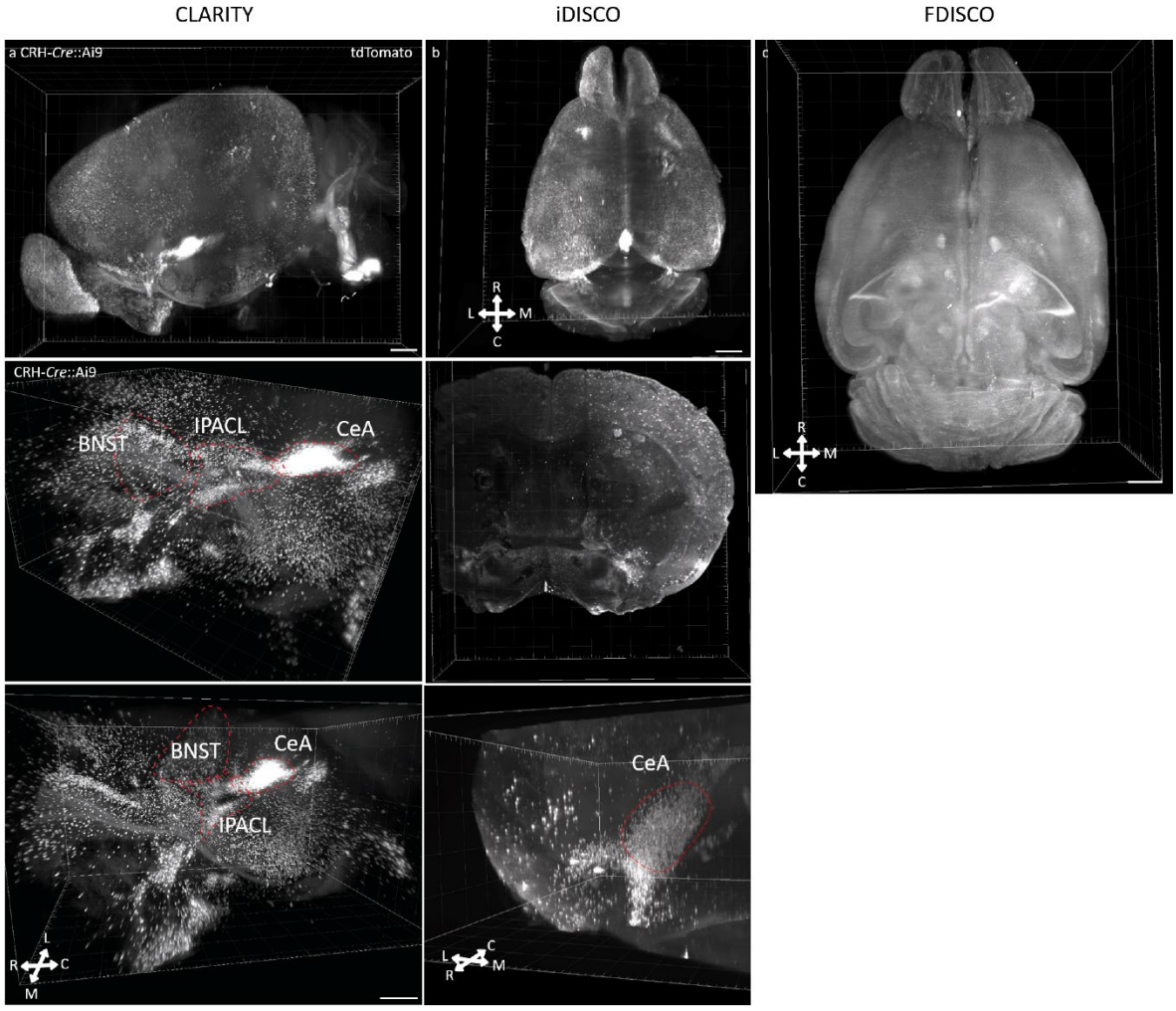

Fig 17 Tissue (brain) clearing methods revealing CRH neuronal expression in the brain

(a) Images presenting full-brain expression of CRH neurons in CRH-*Cre*::Ai9 animal and the expression in the extended amygdala using CLARITY. (b) Full-brain, thick slice and zoomed in images of CRH-*Cre*::Ai9 animal with RFP staining using iDISCO clearing. (c) Full-brain image of CRH-*Cre*::Ai9 animal with FDISCO clearing. Scale bar = 500 μm.

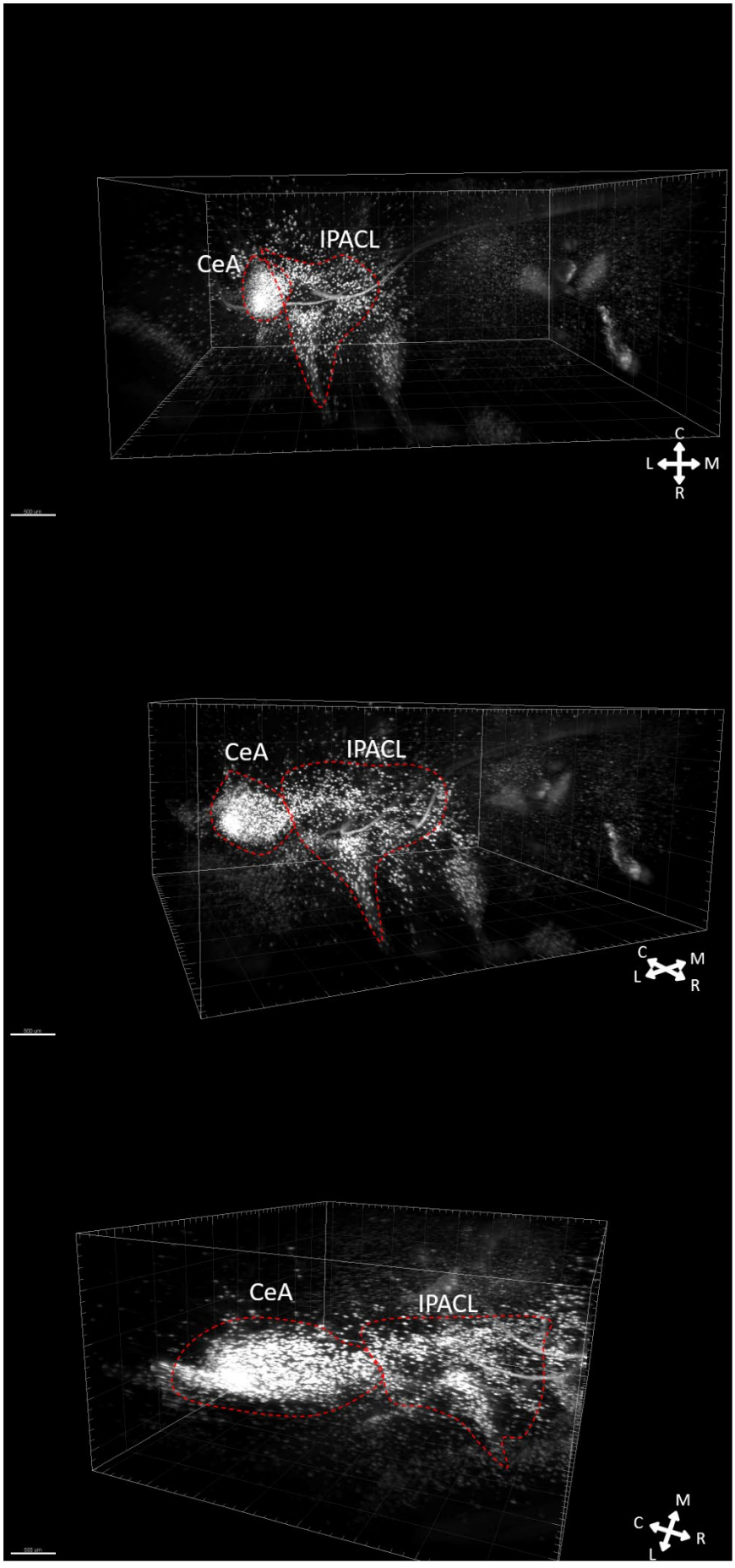
IPACL
CeA
C
L
M
R
CeA
IPACL
C
L
M
R
CeA
IPACL
M
C
R
L

Fig 18. Interconnection of CRH neurons between CeA and IPACL

Images showed CRH neurons labelled with tdTomato (white) in the IPACL are interconnected with CRH neurons in the CeA revealing the IPACL as part of the extended amygdala. Scale bar = 500 μm.

4.4.4 The molecular identity of CRH cells in the IPACL

Once decided that the IPACL will be the main target for behavioural manipulations, the biological identity of CRH cells in the IPACL was investigated. Different immunostainings were conducted in order to further specify the identity of those CRH cells in the IPACL. From previous reports we already know that CRH neurons in the the IPACL are mainly GABAergic, therefore we assessed different GABAergic markers including Wolframin ER transmembrane glycoprotein (Wfs1), somatostatin (SOM) parvalbumin (PV), calbindin, calretinin and protein kinase C-delta (PKCδ). First of all, CRH cells in the IPACL were neurons but not astrocyte (Fig 19a). Second, CRH neurons in the IPACL were co-expressed WFS1, calbindin and SOM but not calretinin or PV. (Fig 19b-g). With quantification, 60% of the CRH neurons in the IPACL are Wfs1 positive, 30-40% are calbindin positive and with 1% of SOM positive (Fig 19h-k).

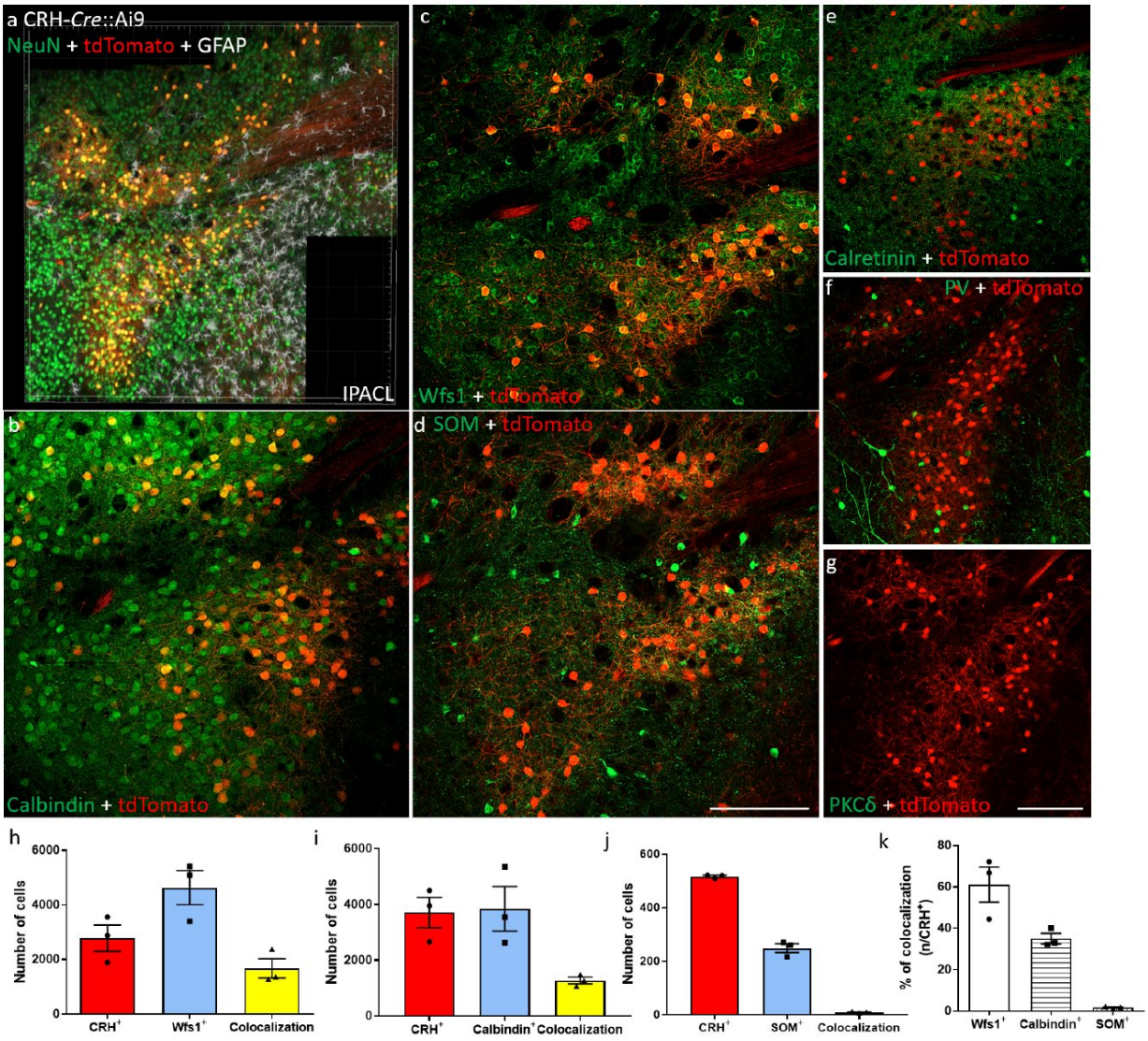

Fig 19. Characterization of IPACL CRH cells

(a) IPACL CRH cells are neurons revealed by their co-labelling with NeuN (green) but not GFAP (white). (b)(c)(d) IPACL CRH neurons are co-labelled with markers of GABAergic neurons: calbindin, Wfs1 and somatostantin (SOM). (e)(f)(g) IPACL CRH neurons do not show any co-labelling with calretinin and PV. There is no expression of PKCδ in the IPACL. (h)(i)(j)(k) Quantification of CRH neurons co-labelling with different markers of GABAergic markers. Value represent mean ± SEM, scale bar = 200 µm

4.5 Dissecting SN afferents using rabies virus-mediated retrograde tracing

4.5.1 CRH neurons have only minor synaptic contacts with CRHR1 neurons in the SN

To understand whether there is a direct synaptic connection between CRHR1 neurons in the SN and the projecting neurons from IPACL, monosynaptic tracing was conducted using rabies virus. I first injected AAV_1-CBh-TVA-GFP-OG virus (helper virus) in the SN of CRHR1-*Cre* mice, two weeks later I injected pseudotyped rabies virus in the same region. After two weeks of incubation mice were sacrificed and the entire brain was screened for retrogradely labelled cells. In general, only a limited number of cells was identified throughout the brain indicating that comparably few cells have direct connections to SN CRHR1 neurons. Labelled cells were partially detected in the CeA and BNST but not in the IPACL.

4.5.2 Rabies virus tracing reveals main brain regions projecting into the SN

Since we found only limited synaptic connections between SN CRHR1 neurons and CRH neurons, we switched our attention toward the two main neuronal populations in the SN, dopaminergic (TH) and GABAergic (PV) neurons. I injected helper virus (AAV_1-CBh-DIO-TVA-GFP-OG) into the SN of PV-*Cre* and Dat-*Cre*ERT^2 animals. Two weeks afterwards I injected the rabies virus in the same region. One week after the injection of rabies virus mice were sacrificed and subjected to detailed anatomical studies. Quantification of the labelled cells showed that the main input into SN PV neurons originated in the striatum and globus pallidus (GP). In addition, there were also projections coming from the CeA, PAG and the IPACL (Fig 20a and c). In case of dopaminergic neurons, they are receiving projections from the striatum, GPe, CeA, BNST and IPACL. These results demonstrate that striatal and extended amygdala regions are providing the main input of the SN. Moreover, there is a reasonable amount of projections from the CeA (Fig 20b and d). However, the IPACL doesn't seem to have strong synaptic connections with these two cell types. Together with the result of CRHR1-Cre animals, we can conclude that IPACL CRH neurons have minimum synaptic connections with the main types of neurons present in the SN.

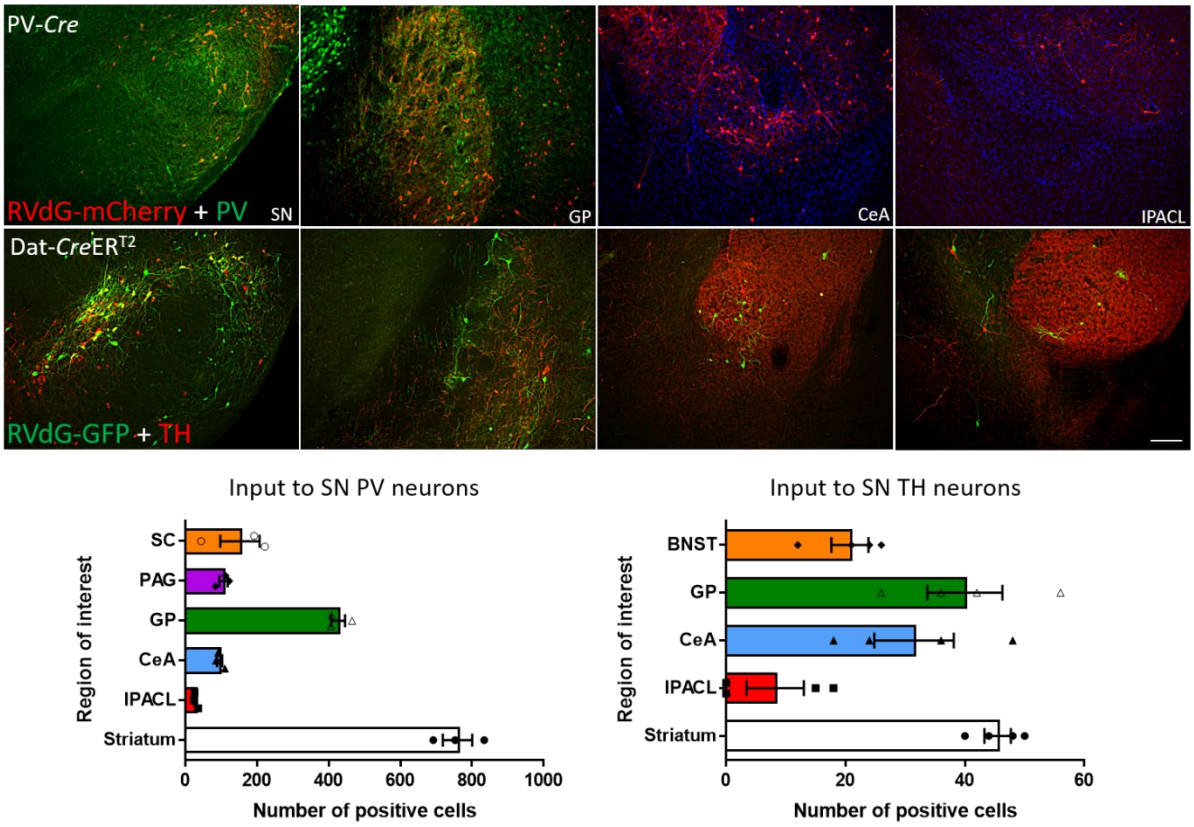

Fig 20. Rabies virus tracing revealed direct connections of extended amygdala with the SN

Rabies virus was injected into the SN of PV-*Cre* and Dat-*Cre*ERT^2 mice. One week after injection virus expression was assessed throughout the brain. I was able to find the cells in SC, PAG, GPe, CeA, IPACL and striatum of PV-*Cre* mice. In Dat-*Cre*ERT^2 mice labelled cells were observed in the BNST, GPe, CeA, IPACL and striatum. Value represent mean ± SEM, scale bar = 200 µm. SC= superior colliculus

Functional characterization of CRH/CRHR1-specific neurocircuits

4.6 Activation of CRH neurons in IPACL induces aversive responses

4.6.1 Validation of chemogenetic tools

Before starting chemogenetic manipulation of the circuits of interest, the experimental setup was validated. To this end, AAV_8-hSyn-DIO-hM3Dq (DREADD) and AAV_8-hSyn-DIO-mCherry (Control) virus were injected bilaterally into the IPACL. Two weeks afterward, mice were subjected to an open field for 90 min. There was no difference between control and DREADD mice in the first 30 min without CNO administration. Ten minutes after the administration of CNO, DREADD mice started to show hyperactivity until the end of the test (Fig 21d). Mice were sacrificed afterwards and the number of cFos positive cells in the IPACL was assessed as a marker for neuronal activation. Both viruses showed similar spreading when comparing control and DREADD mice (Fig 21a). With CNO administration, DREADD mice showed an increased number of cFos positive cells in the IPACL (Fig 21b, c and e).

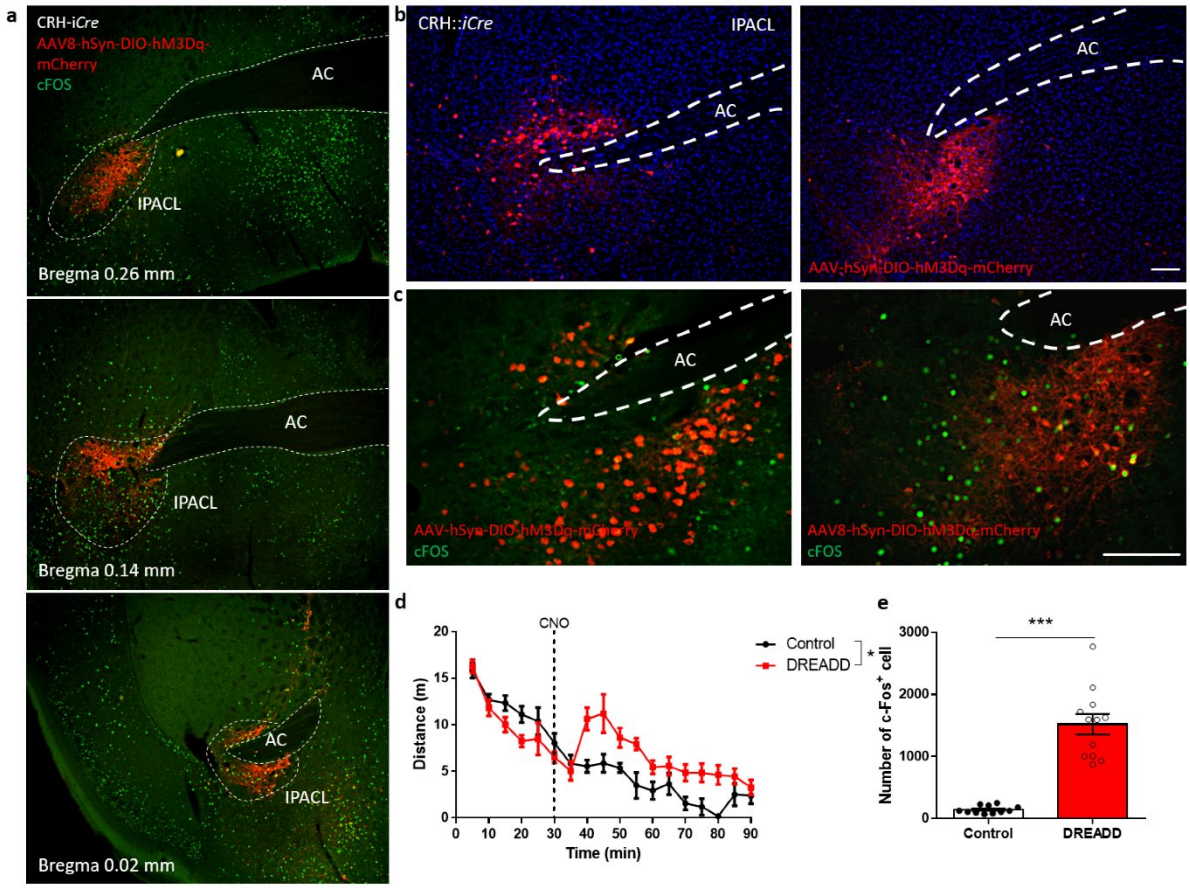

Fig 21. Functional validation of DREADD activity in the IPACL

(a) Representative images of coronal brain sections of CRH-iCre animals injected with AAV_8-hSyn-DIO-hM3Dq-mCherry virus in the IPACL. (b) Images of virus injection comparing control and DREADD-expressing animals. (c) cFos staining demonstrates more activated cells been in the DREADD-expressing animals after CNO administration. (d) 90 min open field test with CNO administration at 30 min showing increased locomotor activity in DREADD-expressing animals (Repeated measures two-way ANOVA, main effect of DREADD, $F_{1,7} = 6.28$, $p = 0.04$). (e) DREADD-expressing animals showed significantly more cFos cell numbers in the IPACL compared to the control animals ($p < 0.0001$, t = 8.04). Values represent mean ± SEM, scale bar = 200 μm, *** $p < 0.0001$.

4.6.2 Activation of CRH neurons in the IPACL contributes to behavioural arousal

After functional validation of the DREADD activation I started to evaluate the behavioural changes after chemogenetically activating CRH neurons in the IPACL. I subjected mice to the open field, elevated plus maze, dark light box, marble burring and novelty suppressed feeding test. DREADD-expressing mice showed maladaptation to the novel environment in the open field and arousal as indicated by hyperlocomotor activity and more entries into the centre zone without spending more time in the centre zone (Fig 22a). In the elevated plus maze, DREADD-expressing mice showed significantly increased activity with more distance travelled. Due to the increase of activity, they also spent more time in the open arms and made more entries into the open arms (Fig 22b). DREADD-expressing mice showed more entries into the lit compartment of the dark light box but without spending longer time in the lit compartment, a phenotype which matches the result of the open field (Fig 22c). To understand whether the behavioural changes are due to generally altered locomotor activity or changes in arousal behaviours, we subjected mice to marble burring and novelty suppressed feeding tests. These tests showed that DREADD-expressing mice buried more marbles compared with control mice (Fig 22d). Moreover, the first latency to approach food was increased while they spent less time on eating (Fig 22e). These findings suggest that the main behavioural changes arise from hyperarousal behaviour. The forced swim test was conducted as an indicator of coping behaviour in our study. Our results showed that there is no difference between control and DREADD-expressing mice with respect to the parameter of swimming, struggling and floating time, suggesting no effect on coping-like behaviour after activation of CRH neurons in the IPACL (Fig 22f).

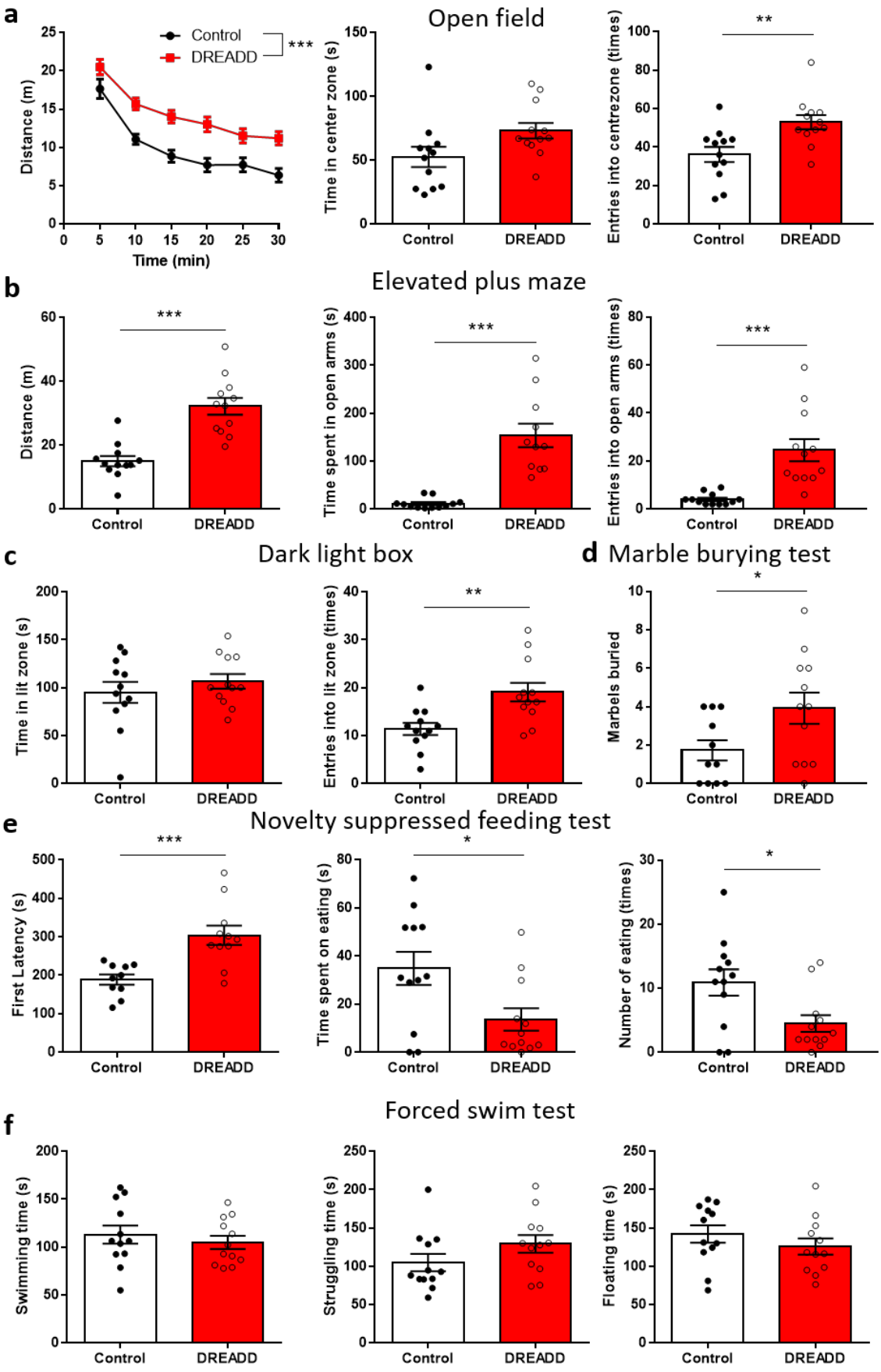
a
Open field
Control
DREADD
***
Distance (m)
Time (min)
Time in center zone (s)
Entries into centrezone (times)
**
b
Elevated plus maze
Distance (m)
Time spent in open arms (s)
Entries into open arms (times)
c
Dark light box
Time in lit zone (s)
Entries into lit zone (times)
d
Marble burying test
Marbels buried
*
e
Novelty suppressed feeding test
First Latency (s)
Time spent on eating (s)
Number of eating (times)
f
Forced swim test
Swimming time (s)
Struggling time (s)
Floating time (s)

Fig 22. Activation of CRH neurons in the IPACL triggers arousal behaviours

(a) DREADD mice showed hyperactivity and delayed habituation in the open field (Repeated measure two-way ANOVA, $F_{1,22} = 17.49$, $p = 0.0004$). They showed more entries ($p = 0.005$, t = 3.1) without spending more time in the centre zone ($p = 0.5$, t = 2.1). (b) DREADD mice showed hyperactivity in the elevated plus maze with more distance travelled ($p < 0.0001$, t = 5.6), more time in the open arms ($p = 0.0002$, t = 4.4) and more transitions into the open arms (p < 0.0001, t = 6.03). (c) DREADD mice entered the lit zone of the dark light box more often ($p = 0.003$, t = 3.3) without spending there more time ($p = 0.4$, t = 0.85). (d) DREADD mice buried more marbles compared with control mice ($p = 0.03$, t = 2.2). (e) DREADD mice approached the food later than control mice in the novelty suppressed feeding test ($p = 0.0009$, t = 3.9). They also spent less time on eating ($p = 0.01$, t = 2.56) and reduced number of approaching the food ($p = 0.01$, t = 2.63). (f) No difference between DREADD and control animals in coping behaviour. There is no difference in time of swimming, struggling and floating after activation of IPACL CRH neurons. Value represent mean ± SEM, * $p < 0.05$, ** $p < 0.01$, *** $p < 0.0001$.

4.6.3 Activation of IPACL CRH neurons results in increased plasma corticosterone level

To further investigate the hyperarousal state of the DREADD-expressing mice we collected blood from control and DREADD-expressing mice from different time points after CNO applications to measure plasma corticosterone. We detected no difference between two groups during basal condition. However, DREADD-expressing mice showed significantly higher plasma corticosterone concentration 30 and 90 min after the administration of CNO indicating a higher state of arousal of mice following activation of CRH neurons in the IPACL (Fig 23).

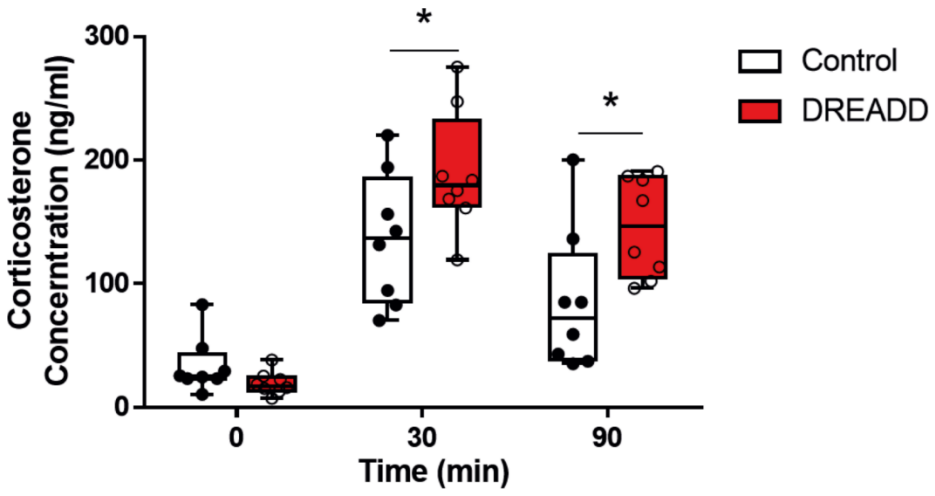

Fig 23. Plasma corticosterone levels following activation of IPACL CRH neurons

Plasma corticosterone levels were measured under basal condition (0), following 30 and 90 min of CNO administration indicating elevated plasma corticosterone levels after CNO injection (Repeat measure two-way ANOVA, $F_{2,42} = 42.7$, $p < 0.0001$). The DREADD-expressing mice show significantly higher plasma corticosterone level compared to control mice 30 and 90 min after CNO administration ($F_{1, 42} = 7.39$, $p = 0.0095$). Value represent max to min, * $p < 0.05$.

4.6.4 Activation of IPACL CRH neurons induced conditioned place aversion

We hypothesized that activation of CRH neurons in the IPACL will have aversive effects. Therefore, DREADD-expressing and control animals were subjected to a conditioned place preference test using CNO to stimulate IPACL CRH neurons. After testing the initial preference of the mice, the preferred side was assigned to CNO administration. The three-day conditioning protocol in the chamber is followed by a preference test without administration of CNO (Fig 24a). DREADD-expressing animals showed conditioned place avoidance behaviour by avoiding the chamber paired with CNO while control animals kept the initial preference (Fig 24b and c). This result provides evidence that activation of CRH neurons in the IPACL contributes to arousal and place avoidance behaviours.

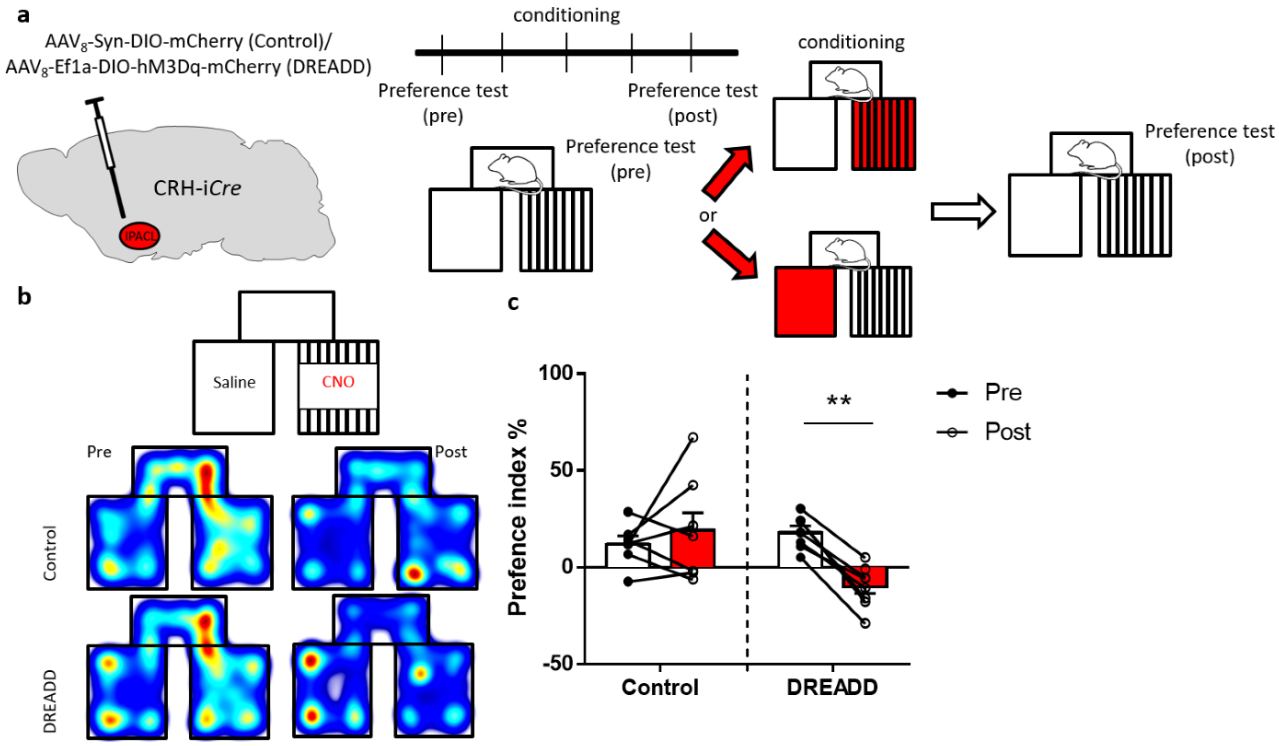

Fig 24. Activation of CRH neurons in the IPACL triggers place aversion

(a) Experimental scheme indicating virus injection and conditioned place preference paradigm. (b) Heatmap showing the time spent in a particular chamber of the first apparent. DREADD-expressing animals avoided the CNO-paired chamber in the preference test. (c) DREADD-expressing mice showed avoidance of the CNO paired chamber following activation of CRH neurons in the IPACL indicating place aversion behaviour (Two-way ANOVA, Bonferroni's multiple comparison test, $p = 0.006$, $t = 3.70$). Value represent mean ± SEM, ** $p < 0.01$.

4.6.5 Validation of optogenetic tools

DREADDs are tools enabling rather local activation or inhibition of neurons. In contrast, optogentic tools provide better access to interrogate a system on the circuit level. At the first place, the proper surgical and validation procedure was established (Fig 25a). Four weeks after the virus injection (IPACL) and optic fibre implantation (IPACL), mice were sacrificed 90 min after light stimulation (473nm, 20Hz, 5 min light on, 5 min light off for 3 times). cFos expression was assessed as an indicator of neuronal activation. The analysis showed that there is increased cFos expression in AAV-hSyn-DIO-ChR2(H134R)-EYFP injected mice but not in control mice following light stimulation (Fig 25b).

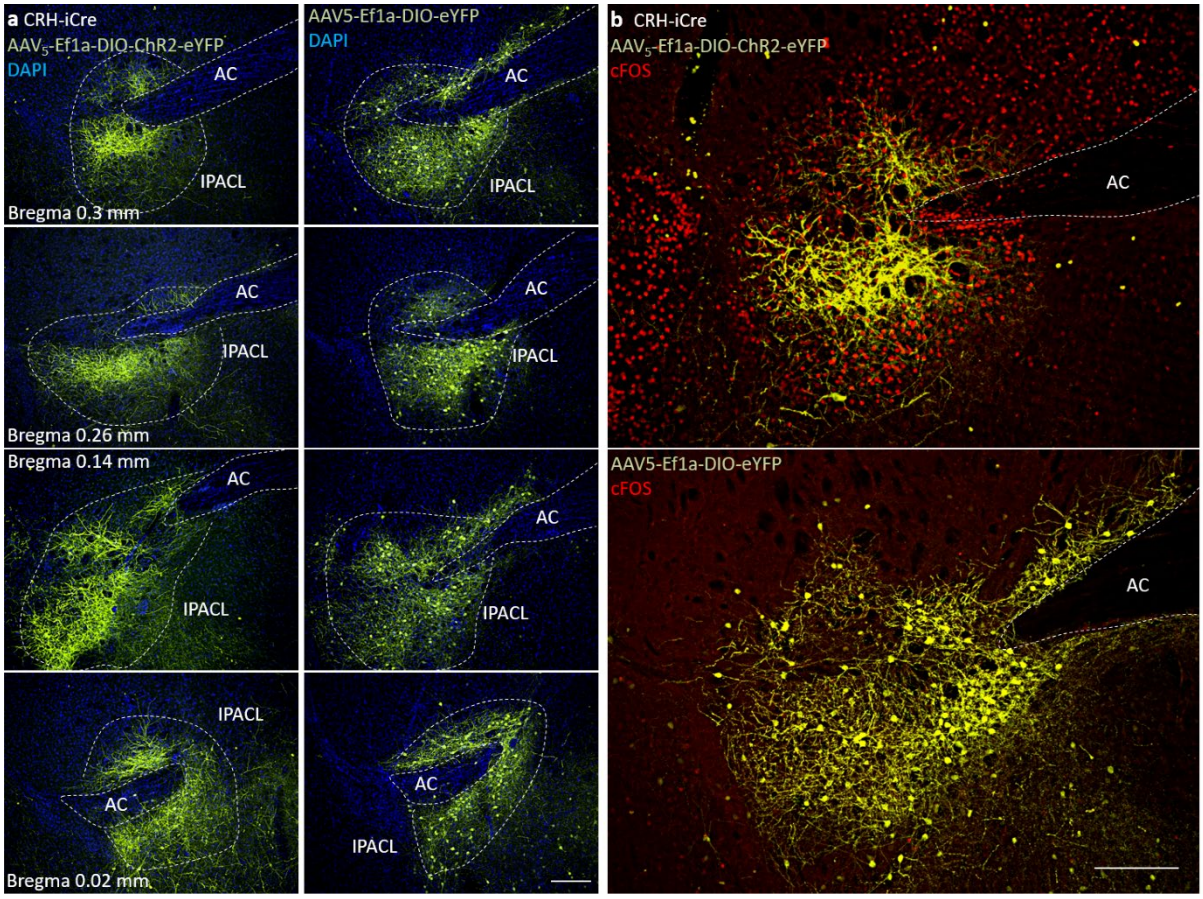

Fig 25. Expression of channelrhodopsin and activation of cFos following optogenetic stimulation

(a) Representative images of coronal brain sections of CRH-iCre animals injected with AAV_5-Ef1a-DIO-ChR2-EYFP and AAV_5-Ef1a-DIO-EYFP virus in the IPACL. (b) ChR2 animals showed significantly more cFos positive cells in the IPACL compared to the control animals. Scale bar = 200 µm.

4.6.6 Optogenetic activation confirmed that CRH neurons in the IPACL contribute to place aversion

After validation of optogenetic tools, mice were subjected to a real time place preference test (RTPP). First, the initial preference of the mice without light (Inactive) was assessed. Then the preferred chamber was assigned as light activation chamber. Once mice enter the light activation chamber, they will receive 473nm light with a frequency of 20 HZ (Active). Light will switch off automatically once the mice entered the other chamber (Fig 26a). There was no difference in terms of preference toward the two chambers without light stimulation. Accordingly, one chamber was randomly assigned as the light stimulation chamber and the

other as neutral. Throughout the test a difference was observed when comparing between stimulus and non-stimulus chambers in ChR2 mice. ChR2 mice avoided the chamber paired with light indicating place avoidance behaviour which is similar to the result observed by DREADD-based activation of CRH neurons in the IPACL (Fig 26b-d). In addition, there was no difference between in distance travelled between control and ChR2 mice. This rule out the possibility that this difference is affected by increased locomotor activity (Fig 26e).

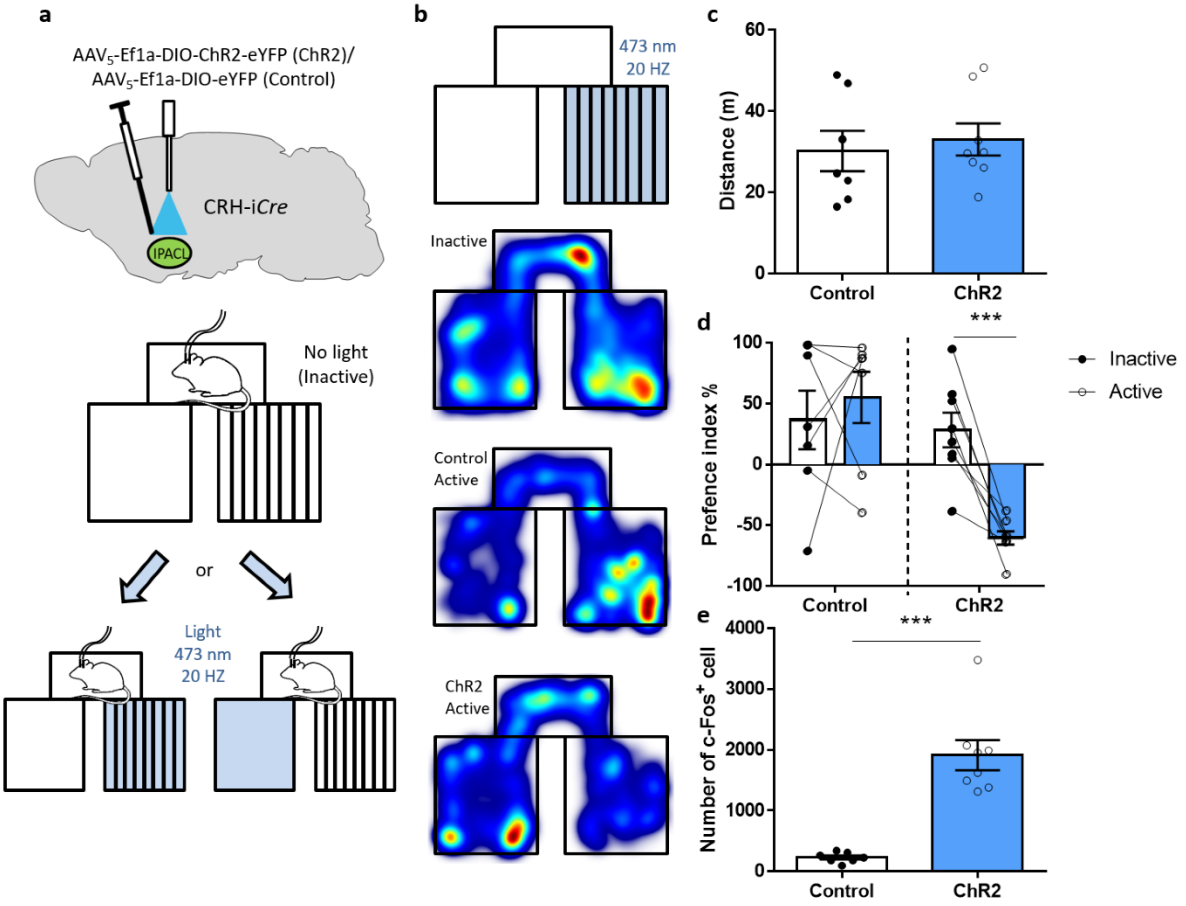

Fig 26. Optogenetic activation of CRH neurons in the IPACL triggers place aversion

(a) Scheme displaying virus injection and composition of real time place preference paradigm. ChR2 or control virus were injected in the IPACL followed by the implantation of optic fibres. (b) Heatmap visualization of the cumulative presence of animals in the test compartments. Both groups of mice showed preference to the mosaic chamber which we assigned as the light chamber. After light activation the control group maintained the same preference but animals of the ChR2 group showed place aversion avoiding the light chamber. (c) No difference in locomotor activity was observed between both groups (p = 0.66, t = 0.45). (d) The ChR2 group avoided the light chamber indicating place aversion behaviour after activation of the CRH neurons in the IPACL (Two–way ANOVA, Bonferroni's multiple comparison, $p < 0.0001$, t = 3.86). (e) In ChR2 animals significantly more cFos

positive cells were detected in the IPACL after light activation ($p < 0.0001$, t = 6.32). Values represent mean ± SEM, *** $p < 0.0001$.

4.6.7 Stimulation of CRH projections from the IPACL into the SN triggered place aversion

The activation of CRH neurons in the IPACL triggered place aversion behaviour raising the question whether projections of CRH neurons from IPACL into the SN contribute to the behavioural outcomes. Therefore, we injected ChR2 virus in the IPACL and implanted the optic fibres in the SN enabling manipulation of axon terminals of CRH projecting neurons (Fig 27a). When mice were subjected to RTPP, ChR2 mice showed strong place aversion compared with control mice (Fig 27b-d). General locomotor activity was not affected. After light activation mice were sacrificed cFos expression in the SN was quantified. Mice of the ChR2 group showed a significant increase of cFos positive cells in the SN compared to control mice. This indicates that activation of terminals of IPACL CRH neurons in the SN was able to trigger place aversion behaviours (Fig 27e).

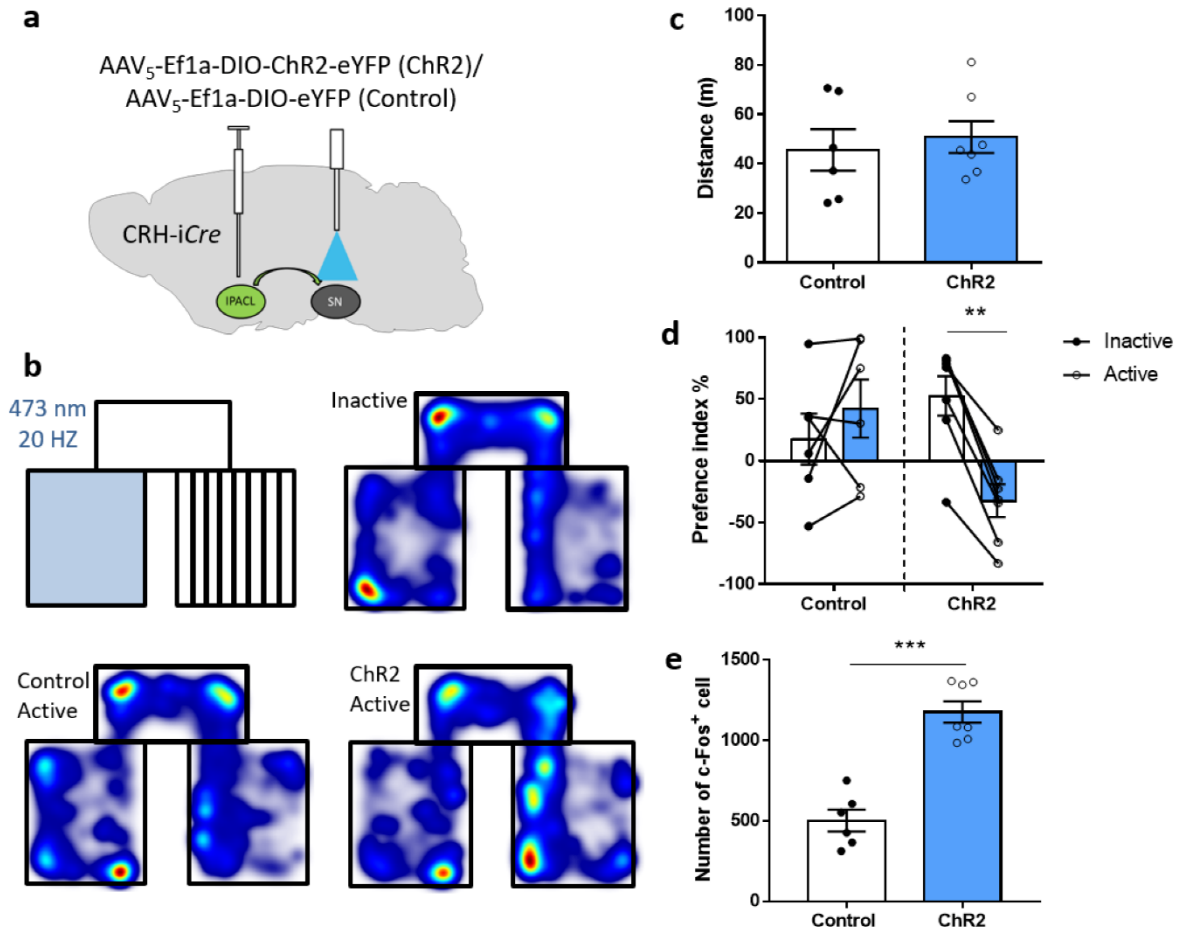

Fig 27. Activation of terminals of IPACL CRH neurons in the SN is sufficient to trigger place aversion behaviour

(a) Scheme displaying virus injection and placement of optic fibres. ChR2 or control virus were injected in the IPACL followed by the implantation of the optic fibres in the SN. (b) Heat map showing the initial preference (Inactive) of the mice. Both groups preferred the chamber without light stimulation. The ChR2 animals showed place aversion by avoiding the light chamber while the control animals maintained the initial preference. (c) No difference in locomotor activity was observed between both groups ($p = 0.62$, t = 0.49). (d) The ChR2 animals avoided the light chamber indicating place aversion after activating the terminals of IPACL CRH neurons in the SN (preference index: two-way ANOVA, Bonferroni's multiple comparison test, $p = 0.008$, t = 3.7). (e) There were significantly more cFos positive cells in the SN of the ChR2 animals demonstrating the successful activation of neurons with light ($p < 0.0001$, t = 7.13). Value represent mean ± SEM, ** $p < 0.01$, *** $p < 0.0001$.

4.7 Activation of CRHR1 neurons in the SN promotes anxiogenic behaviours

4.7.1 Activation of CRHR1 neurons in the SN promotes anxiogenic behaviours

Our results revealed that the IPACL strongly projects into the SN. From previous anatomical studies we understand that there is little to none CRH expression in the SN. This leads to the interesting question: where does CRH released from IPACL CRH neurons axon terminals act? From previous studies, we know that CRHR1 is highly expressed in the SN and we hypothesized that this is the site where CRH released from projections might act. To test our hypothesis, we use again chemogentics as a method to activate local CRHR1 neurons. After 2 weeks of virus injection, we subjected mice to the same behavioural test batteries. To our surprise, there was neither difference in locomotor activity between control and DREADD-expressing mice nor any other difference in the open field (Fig 28a). Similar results were observed in the elevated plus maze with a slight trend pointing toward anxiogenic behaviour (Fig 28b). In the dark light box, DREADD-expressing mice spent less time spent in the lit compartment and had fewer entries to the lit compartment (Fig 28c). In the marble burying test, DREADD-expressing mice buried more marbles in comparison with control mice. In the novelty suppressed feeding test DREADD-expressing mice showed a longer latency before starting to eat (Fig 28d and e). Together, these results indicate that activation of CRHR1 neurons in the SN promotes a slight increase of anxiety-like behaviours. We also checked the cFos expression after administration of CNO confirming the CRHR1 neurons were activated by CNO (Fig 29).

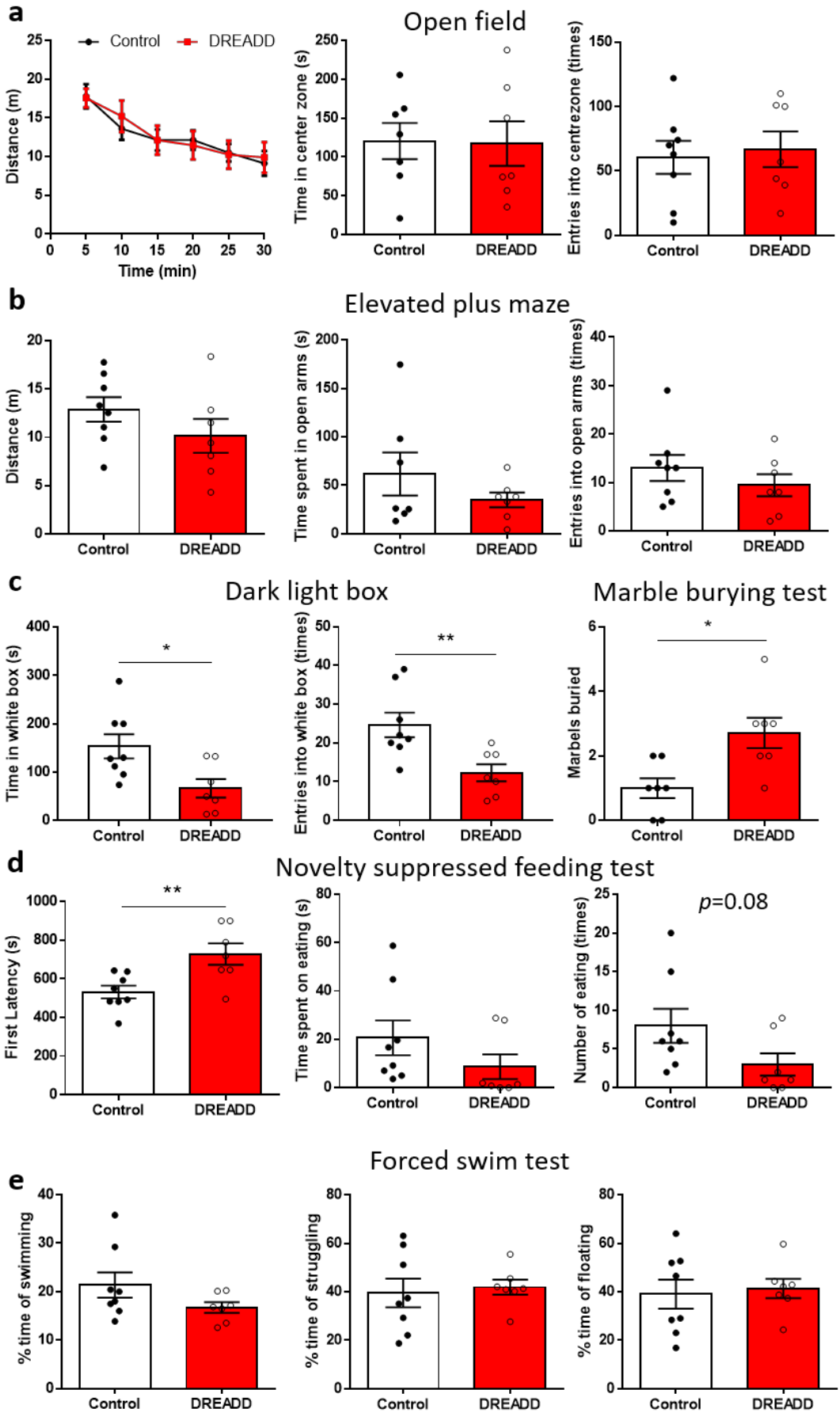
a
Open field
Control
DREADD
Distance (m)
Time (min)
Time in center zone (s)
Entries into centrezone (times)
b
Elevated plus maze
Distance (m)
Time spent in open arms (s)
Entries into open arms (times)
c
Dark light box
Marble burying test
Time in white box (s)
Entries into white box (times)
Marbels buried
d
Novelty suppressed feeding test
First Latency (s)
Time spent on eating (s)
Number of eating (times)
p=0.08
e
Forced swim test
% time of swimming
% time of struggling
% time of floating

Fig 28. Activation of CRHR1 neurons in the SN promotes increased anxiety-like behaviour.

(a) No difference between DREADD-expressing mice and the control group was observed with regards to the distance travelled ($F_{1,14}$ = 0.01, p = 0.92) the time spent in the centre zone (p = 0.93, t = 0.08) or in the entries into the centre zone (p = 0.74, t = 0.33) of the open field. (b) No difference was observed in the elevated plus maze with respect to distance travelled (p = 0.22, t = 1.28), time spent in open arms (p = 0.27, t = 1.13) or entries into open arms (p = 0.33, t = 0.99) comparing DREADD-expressing mice and control mice. (c) DREADD-expressing mice spent less time (p = 0.018, t = 2.68) and have less entries into the lit compartment (p = 0.008, t = 3.09) of the dark light box. (d) DREADD-expressing animals buried more marbles compared to the control group (p = 0.01, t = 3.03). (e) DREADD-expressing animals had a longer first latency to eat (p = 0.007, t = 3.13) without differences in time spent on eating (p = 0.21, t = 1.31) and times approaching food (p = 0.08, t = 1.83). Value represent mean ± SEM, * $P < 0.05$, ** $P < 0.01$.

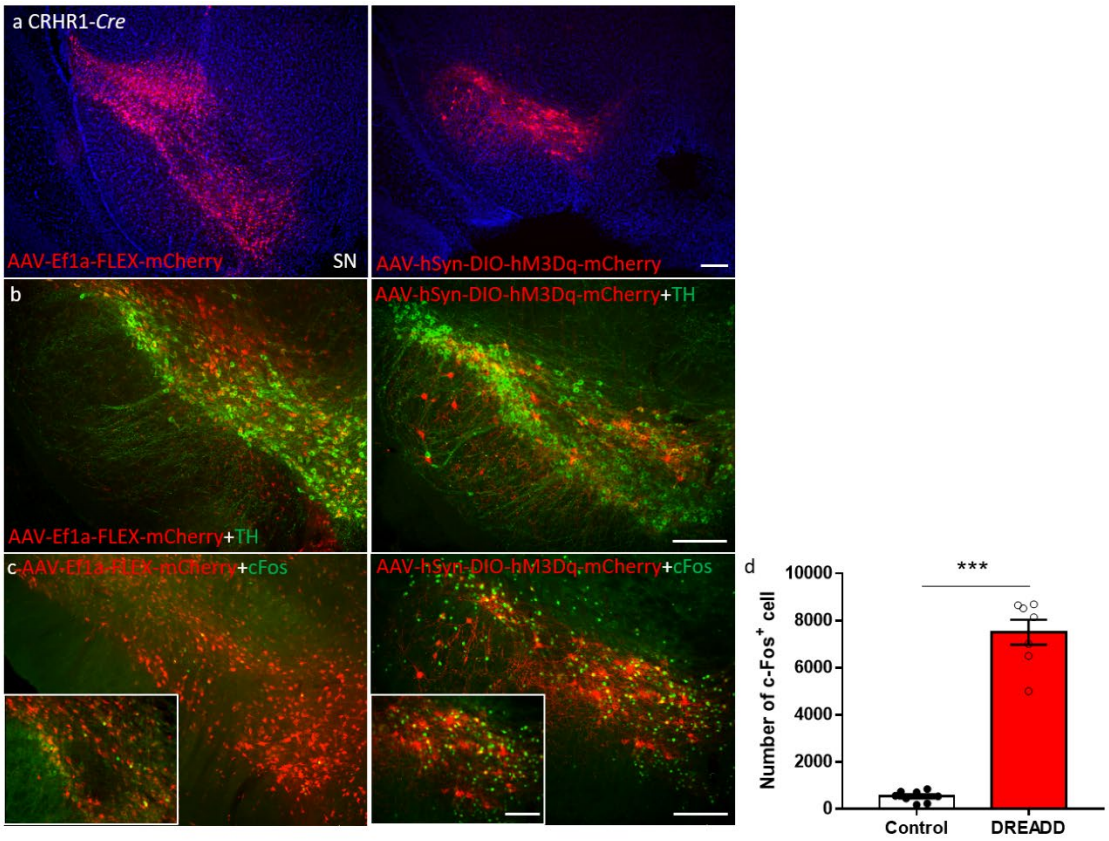

Fig 29. Virus and cFos expression in CRHR1-*Cre* mice

(a) Representative images of AAV_8-Ef1a-Flex-mCherry and AAV_8-hSyn-DIO-mCherry injected into the SN. (b) Virus distribution in the SN with TH staining delineating the structure of the SN. (c) cFos staining showing CRHR1 neurons are activated following the administration of CNO. (d) Quantification of cFos positive cells in the SN demonstrating significant difference between DREADD-expressing mice and control mice ($p < 0.0001$, t = 11.73). Value represent mean ± SEM, *** $p < 0.0001$. Scale bar = 200 μm.

4.7.2 CRHR1 is essential for aversive behaviour

Previous results demonstrate that activation of CRH neurons in the IPACL triggers aversive responses in mice. As a next step, it was of interest to test whether CRH as a peptide activating CRHR1 plays a role in this process or if the effect is rather triggered at the level of circuit communication. To answer this question, DREADD virus was injected in two experimental groups of animals: 1. CNO administration (CNO) and 2. CNO together with systemic administration of the selective CRHR1 antagonist R121919 (CNO + R121919, i.p. 10 mg/kg). Mice were subjected to the same behavioural paradigms used in previously experiments. I observed similar behavioural effects in the group receiving CNO only as in previous experiments (e.g. hyperlocomotor activity and arousal). In case of R121919 administration, the antagonist significantly blunted the effects of activation induced by CRH neurons in the IPACL. The differences were first observed in the 90 min open field (Fig 30).

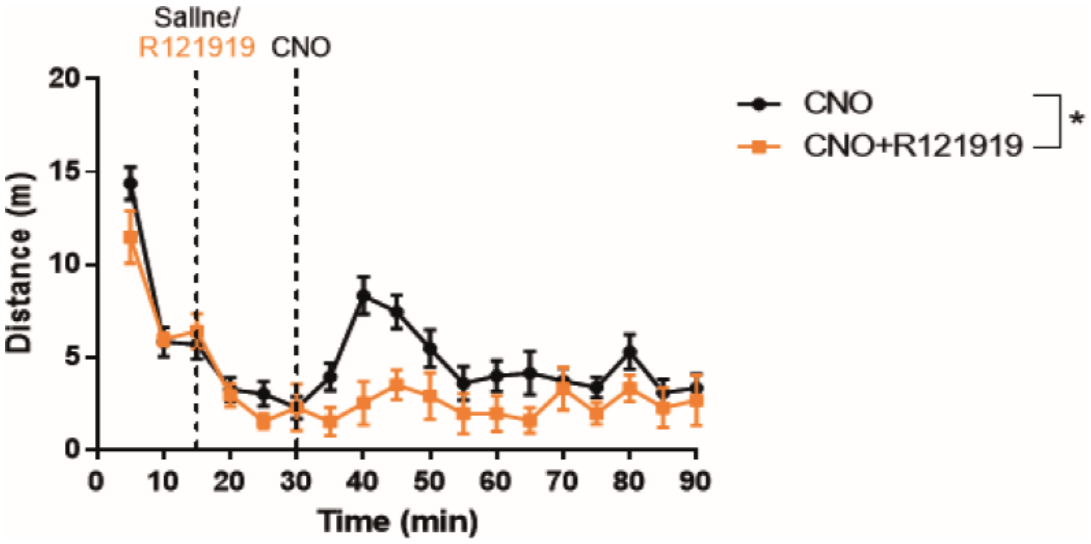

Fig 30. CRHR1 antagonist R121919 blocks CNO-induced increase in locomotor activity

Mice were injected with AAV_8-hSyn-DIO-hM3Dq-mCherry in the IPACL and subjected to a 90 min open field test which they were allowed to freely explore. Mice were injected either 10 mg/kg of R121919 or saline 15 min after the first entry to the arena. At 30 min, both groups received 5 mg/kg of CNO, and were allowed to explore the arena until the end of the test. The result showed that there is an increased locomotor activity in the pure CNO group while CNO + R121919 remained unaffected (Repeat measured two- way ANOVA, $F_{1,17} = 5.10$, $p = 0.03$). Value represent mean ± SEM, * $p < 0.05$.

In addition to the locomotor effect observed in the open field, our data showed that R121919 reversed the maladaptive behaviour in the open field. R121919 animals also entered the centre less compared to the CNO animals while there was no difference on the time spent in the centre zone (Fig 31a). No differences were observed in the elevated plus maze comparing the two groups (Fig 31b). In the dark light box, R121919 reduced transitions into the lit zone without affecting the time spent in the lit zone (Fig 31c). cFos expression was assessed in the SN showing that R121919 indeed blocked the CRH triggered activation in the SN after activation of IPACL CRH neurons by CNO administration (Fig 31d).

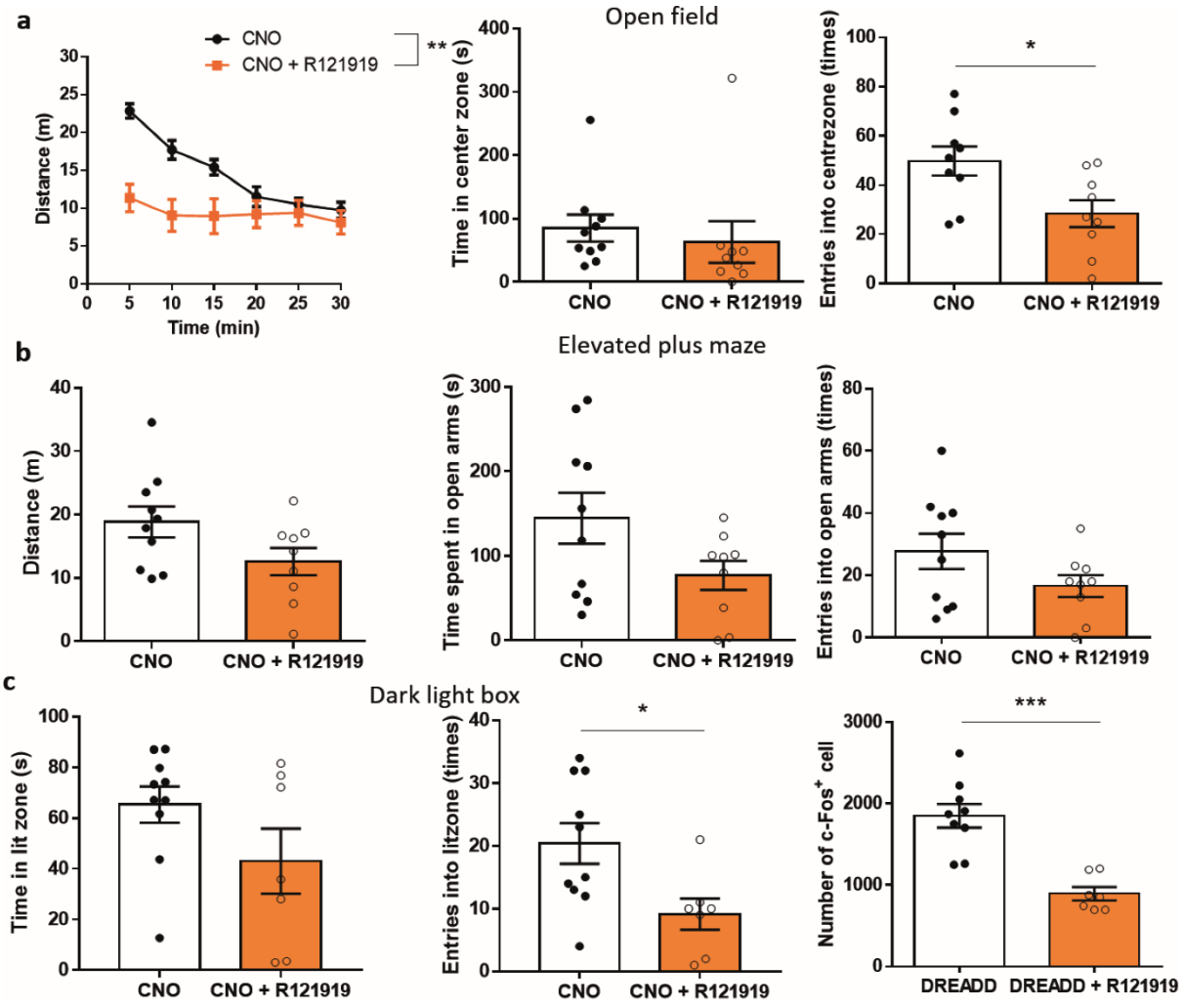

Fig 31. CRHR1 antagonist R121919 blocked CNO induced arousal behaviour

(a) In the open field the CNO + R121919 group showed lower locomotor activity (Repeated measured two-way ANOVA, $F_{1,17} = 8.97$, $p = 0.0081$) and showed less entries into the centre zone ($p = 0.017$, t = 2.66) but no changes in time spent in the centre zone ($p = 0.57$, t = 0.56) compared to the CNO group. (b) In the elevated plus maze no difference in activity, time spent in the open arms and entries into the open arms were observed

(Distance, $p = 0.073$, t = 1.9; time spent in open arms, $p = 0.075$, t = 1.89; entries in to open arms, $p = 0.12$, t = 1.62). (c) CNO+R121919 animals made less transitions into the lit zone ($p = 0.022$, t = 2.54) but do not spend less time in the lit zone ($p = 0.12$, t = 1.64). (d) CNO+R121919 animals have less cFos positive cells in the SN indicating the activation of neurons following CNO administration is blocked by CRHR1 antagonist R121919 ($p < 0.0001$, t = 5.29). Value represent mean ± SEM, * $p < 0.05$, *** $p < 0.0001$.

Moreover, in the CPP, R121919 was able to revert the place aversion compared to the CNO group which avoided the CNO paired chamber (Fig 32b and c). Overall, these results suggested that CRH itself is essential for triggering of aversive responses. These results also indicated that the aversive responses triggered by activation of CRH neurons in the IPACL was CRHR1 dependent.

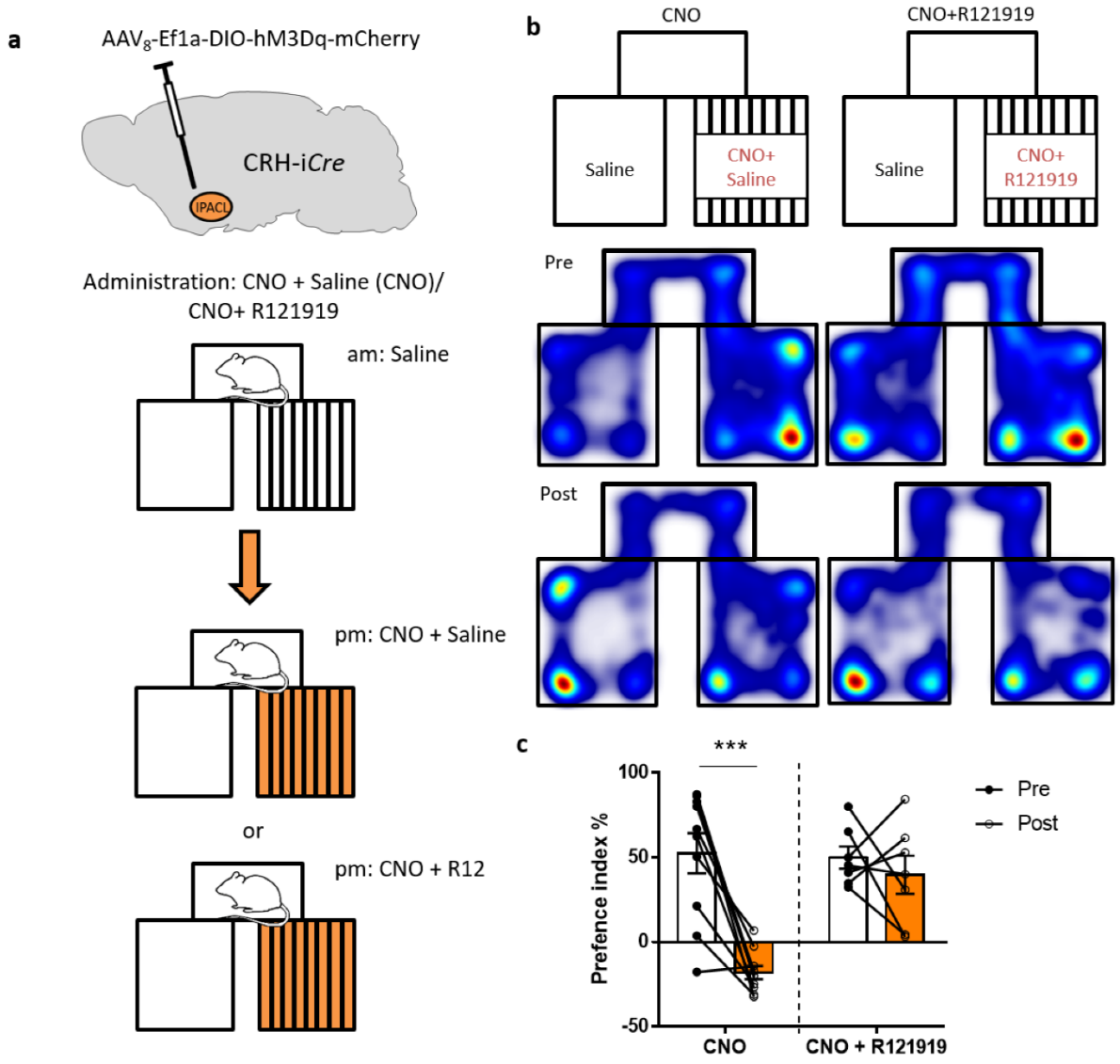

Fig 32. The CRHR1 antagonist R121919 is sufficient to block CNO-induced place aversion

(a) Scheme displaying virus injection and conditioned place preference paradigm. Gq-DREADD or control virus was injected in the IPACL. Both groups of animals were paired with saline in the morning. In the afternoon one group was paired with CNO and the other group with CNO+R121919 (b) Heat map showing the initial preference of the mice indicating that both groups of animals preferred the mosaic chamber. The DREADD-expressing animals showed place aversion by avoiding the chamber paired with CNO while the antagonist treated animals maintained the initial preference. (c) Calculated preference index indicating the DREADD-expressing animals avoided the CNO-paired chamber indicating place aversion after activating the CRHR1 neurons of IPACL (Two-way ANOVA, Bonferroni's multiple comparison, $p < 0.0001$, $t = 5.94$). Value represent mean ± SEM, *** $p < 0.0001$.

4.8 Globus pallidus CRHR1 neurons are involved in anxiety circuits

4.8.1 CRHR1 is strongly expressed in neurons of the globus pallidus

The results indicated that CRH neurons from IPACL have only limited synaptic contacts with CRHR1 neurons in the SN. This raises the question where the terminals of IPACL CRH neurons release the peptide and on which CRH receptors it is acting. Previous studies have demonstrated that there is strong expression of CRHR1 neurons in telencephalic structures related to the basal ganglia including the patches of the striatum and globus pallidus external (GPe). To investigate the identity and properties of these a staining for PV were performed in the GPe identifying 60% of colocalization between CRHR1 neurons and PV neurons. In the other way around there are 80% of PV neurons colocalizing with CRHR1 neurons (Fig 33a-c).

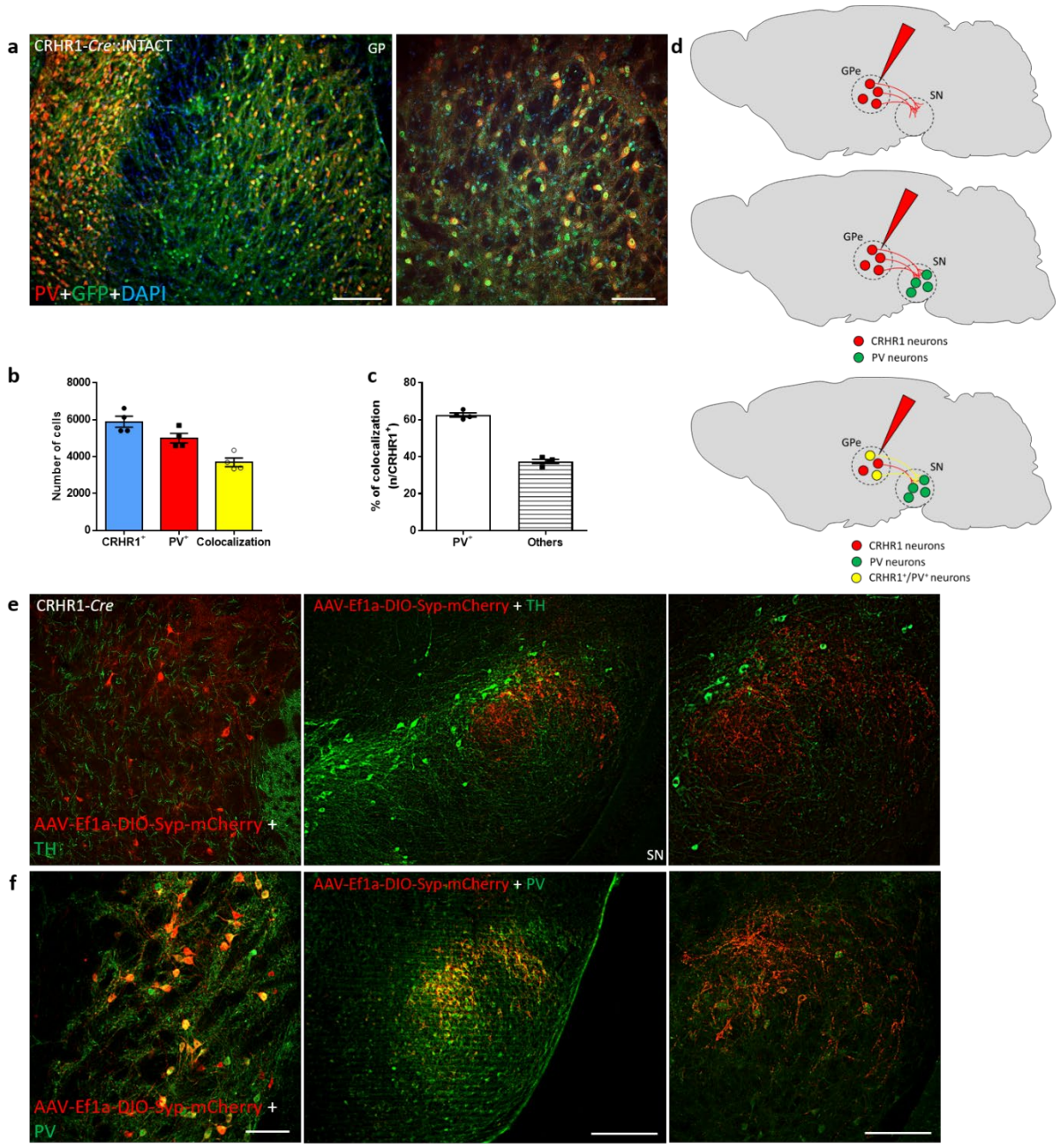

Fig 33. Characterization of Globus pallidus CRHR1 neurons projecting to the SN

(a) Representative image showing nuclei of CRHR1 neurons in the globus pallidus colocalizing with PV. (b) Representative image showing GPe CRHR1 neurons sending projections toward the SN, enlarged images showed CRHR1 neurons projecting to PV neurons. (c) Quantification of different cell types in the GPe demonstrating 60% of the CRHR1 neurons are PV positive. (d) Scheme showing virus injection plans and projections of different neurons in the GPe to the SN. (e)(f) CRHR1 neurons in the GPe are PV positive and innervated PV neurons in the SN. Value represent mean ± SEM, scale bar = 200 μm.

4.8.2 Parvalbumin positive CRHR1 neurons in the globus pallidus project into the SN

Since there are numerous reports demonstrating strong connections between striatal structures and the SN we would like to see where exactly those CRHR1 neurons project. We injected AAV-Ef1a-Syp-mCherry virus into the GPe of CRHR1-Cre mice and found strong projections into the SN. We further performed a PV staining in the SN and were able to identify the targets of CRHR1 projections in the SN as PV neurons. PV neurons are mostly described as local projecting interneurons. However, CRHR1-PV neurons in the GPe are seemingly long-range projecting neurons. Next, we wanted to understand what the functional impact of this projection is.

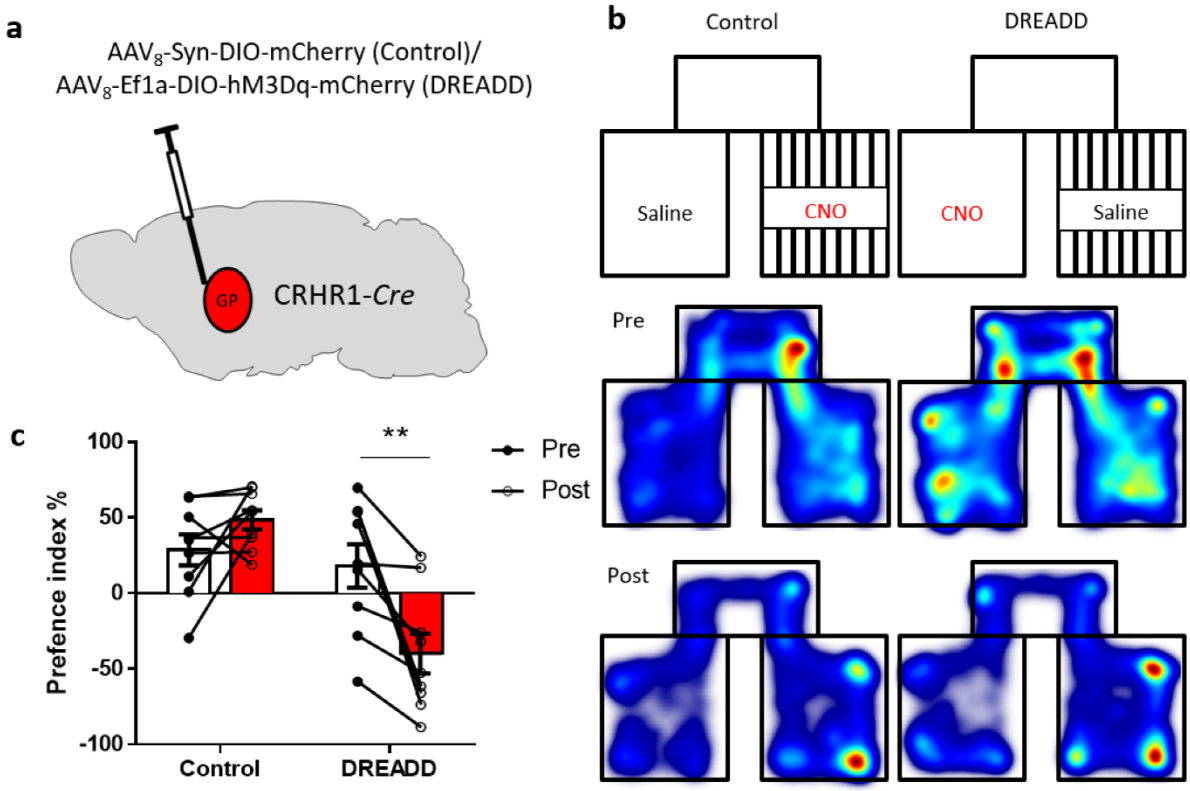

Fig 34. CRHR1 neurons in the GPe also trigger place aversion

(a) Scheme displaying virus injection and conditioned place preference paradigm. hM3Dq-DREADD or control virus was injected in the GPe. (b) Heat map showing the initial preference of the mice which control groups preferred the mosaic chamber and DREADD-expressing animals preferred the other. The DREADD-expressing animals showed place aversion by avoiding the CNO-paired chamber while the control animals maintained the intimal preference. (c) Preference index showing that DREADD-expressing animals avoided the CNO-paired chamber indicating place aversion after activating the CRHR1 neurons in the GPe (Two-way ANOVA, Bonferroni's multiple comparison test, $p = 0.006$, $t = 3.59$). Value represent mean ± SEM, ** $p < 0.01$.

4.8.3 Activation of CRHR1 neurons in the GPe contributes to place aversion and increases arousal

Cre-dependent DREADD virus (AAV$_8$-hSyn-DIO-hM3Dq-mCherry) was injected into the GPe of CRHR1-*Cre* mice in order to understand the consequence of activating these PV positive CRHR1 cells (Fig 34a). In the condition place preference test, DREADD-expressing mice showed strong aversion against the chamber paired with CNO compared to control mice (Fig 34b and c).

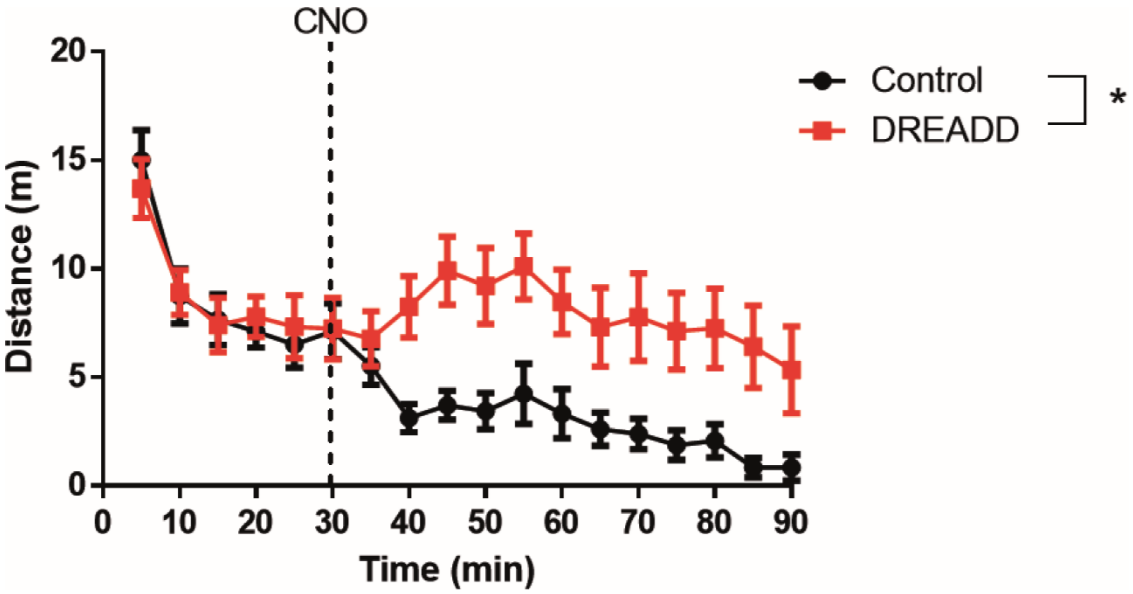

Fig 35. Activation of GPe CRHR1 neurons results in increased locomotor activity

Mice were subjected for 90 min to the open field test with CNO administration at 30 min. DREADD-expressing mice showed increased locomotor activity compared o control mice similar to effect of activating CRH neurons in the IPACL (Repeat measured two-way ANOVA, $F_{1,16} = 7.4$, $p = 0.014$). Value represent mean ± SEM, * $p < 0.05$.

Mice were subjected to the same tests used earlier. DREADD-expressing mice showed increased locomotor activity (Fig. 35) and delayed habituation in the open field test with overall increased locomotor activity as well as longer time spent in the centre zone (Fig 36a). Compared to control mice, DREADD-expressing mice did not show alterations in the

elevated plus maze with regards to locomotor, entries into the open arms or time spent in them (Fig 36b). However, DREADD-expressing mice presented with more entries into the lit zone in the dark light box but did not differ from control mice in the time spent in the lit zone (Fig 36c).

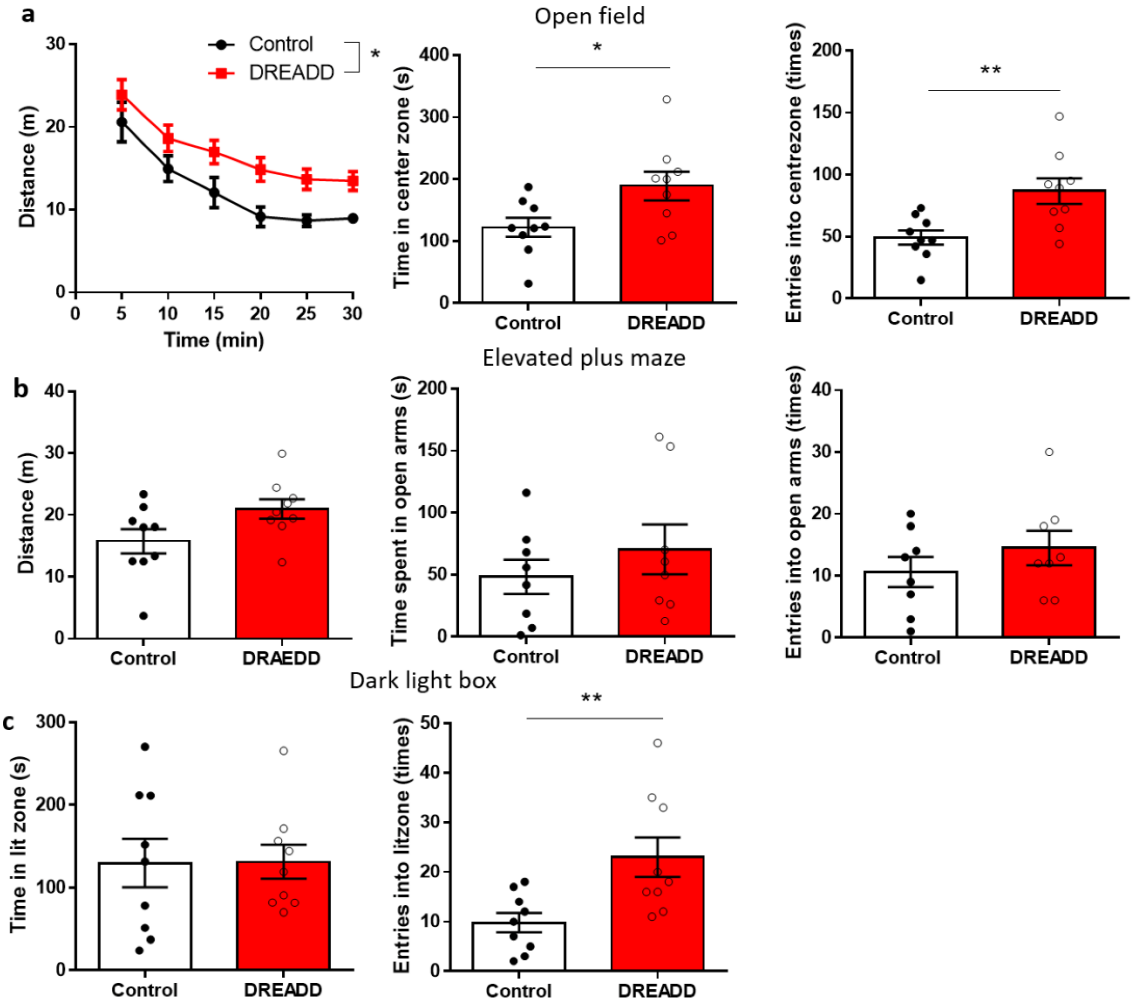

Fig 36. Activation of CRHR1 neurons in the GPe contributes to behavioural arousal

(a) DREADD-expressing mice showed maladaptive behaviour in the open field test indicated by higher locomotor activity (Repeat measured two-way ANOVA, $F_{1,14} = 6.54$, $p = 0.022$), more time spent in the centre zone ($p = 0.027$, t = 2.43) and more transitions into the centre zone ($p = 0.006$, t = 3.15). (b) DREADD-expressing animals were undistinguishable from control mice in the elevated plus maze (Distance, $p = 0.05$, t = 2.04; time in open arms, $p = 0.38$, t = 0.9; entries into open arms, $p = 0.31$, t = 1.05). (c) In the dark-light box DREADD-expressing animals made more transitions into the lit compartment compared to control mice ($p = 0.009$, t = 2.94) without staying more time in the lit zone ($p = 0.95$, t = 0.04). Value represent mean ± SEM, * $p < 0.05$, ** $p < 0.01$, *** $p < 0.0001$.

cFos expression was inspected in the GPe, showing that there were more cFos positive cells in the GPe of the DREADD-expressing animals compared to the control animals, indicating the successful activation of CRHR1 neuron in the GPe (Fig 37).

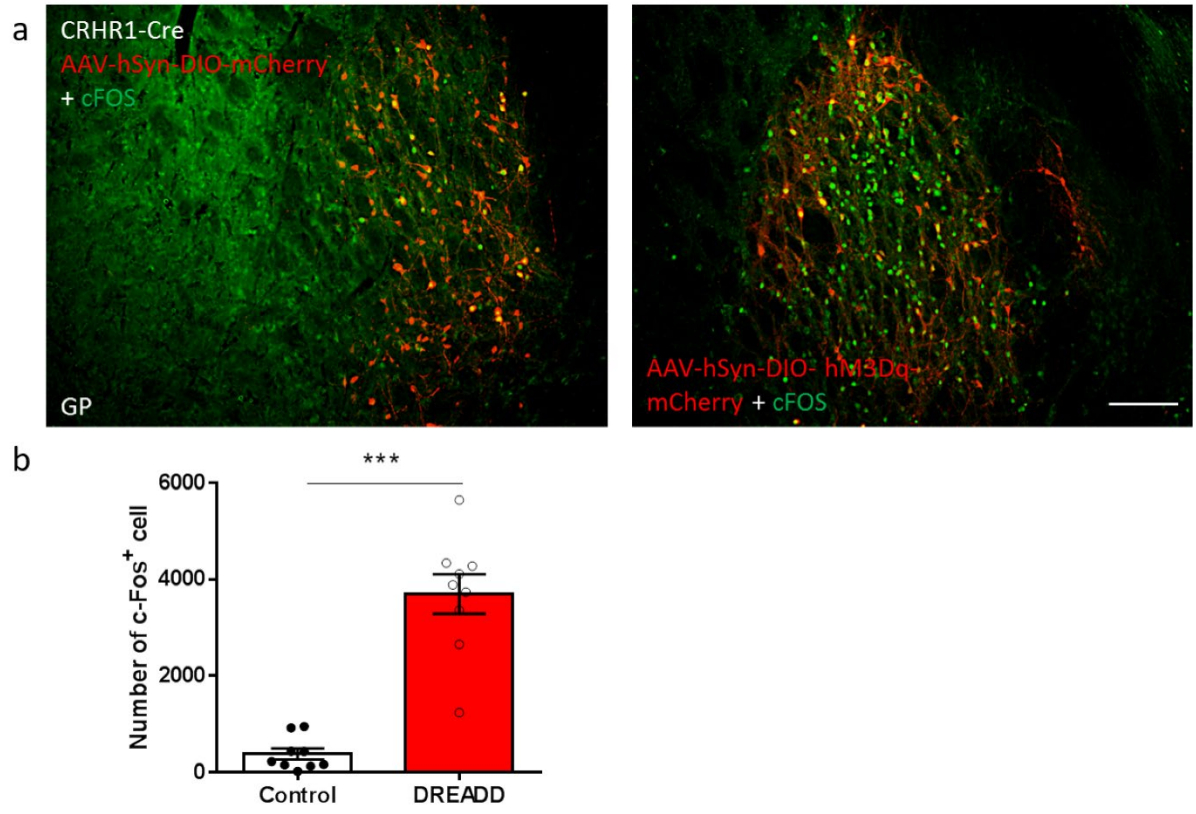

Fig 37. CNO activation of CRHR1 neurons induces cFos expression in the GPe

(a) Comparing cFos expressing in control and DREADD-expressing animals revealed the CNO mediated activation of CRHR1 neurons in the GPe. Scale bar = 200 μm. (b) Quantification of cFos positive cells in the GPe indicating the activation of GPe CRHR1 neurons following CNO-based activation ($p < 0.0001$, t = 7.81). Value represent mean ± SEM, *** $p < 0.0001$.

4.8.4 Activation of terminals of GPe CRHR1 neurons in the SN is sufficient to trigger place aversion

In order to understand whether the axon terminals of CRHR1 neurons projecting from the GPe to the SN are contributing to the behaviour outcomes, we injected *Cre*-dependent ChR2 (AAV5-Ef1a-DIO-ChR2-EYFP) or GFP (AAV5-Ef1a-DIO-EYFP) expressing virus in the GPe of CRHR1::*Cre* animals (Fig 38a and b). We subjected these mice to a real time place preference test. Mice expressing ChR2 in the GPe avoided the chamber in which the ChR2 was activated by light indicating their aversion against that chamber. This is in line with the DREADD-based activation of CRHR1 neurons in the GPe, suggesting activation of CRHR1 terminals in the SN is sufficient to trigger place aversion (Fig 38c-f). cFos expression in the SN was significantly increased in the ChR2 group compared to the control group (Fig 38b).

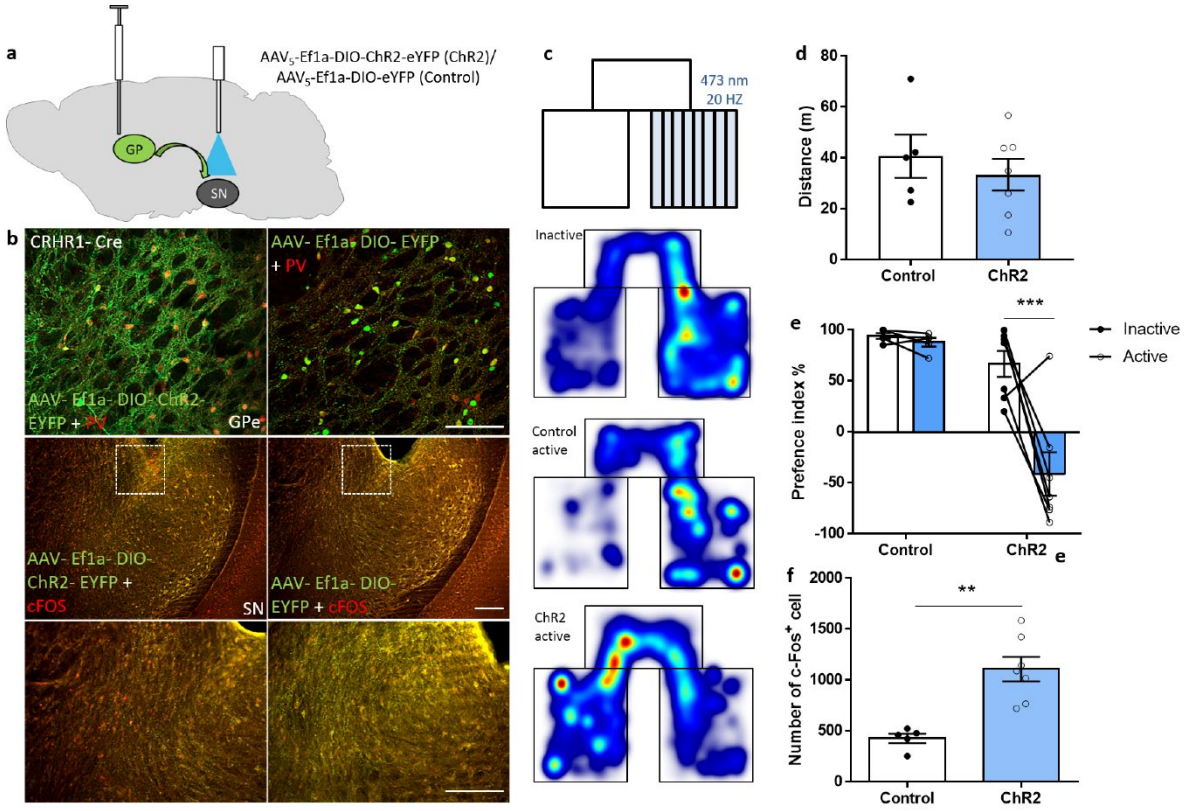

Fig 38. Activation terminals of GPe CRHR1 neurons in the SN triggers place aversion

(a) Scheme displaying virus injection and placement of optic fibres. ChR2 or control virus were injected in the GPe followed by the implantation of the optic fibres in the SN. (b) Representative images of coronal brain sections from virus injected animals showing that labelled cells are CRHR1 and PV double positive neurons.

Staining of cFos in the SN showed more cFos positive cells in the ChR2 animals compared to control. (c) Heat map showing the initial preference (Inactive) of the mice which both groups preferred the black chamber. The ChR2 animals showed place aversion by avoiding the light chamber while the control animals maintained the initial preference. (d) No difference in locomotor activity was observed between two groups ($p = 0.49$, $t = 0.71$). (e) The ChR2 animals avoided the light chamber indicating place aversion after activating the terminals of IPACL CRH neurons in the SN (Two-way ANOVA, Bonferroni's multiple comparison test, $p < 0.0001$, $t = 5.56$). (f) There are significantly more cFos positive cells in the SN of the ChR2 animals demonstrating the successful activation of GPe CRHR1 neurons with light ($p = 0.001$, $t = 4.56$). Value represent mean ± SEM, *** $p < 0.0001$. Scale bar = 200 μm.

5. Discussion

After the complete failure of CRH receptor antagonist in clinical trials [253], the approaches that scientists pursued to develop treatments for patients suffering from psychiatric diseases has been questioned. In the case of CRH, one of the main questions is how and where the neuropeptide and its receptors act in the CNS. Numerous studies have demonstrated that CRH expression in the rodent brain is restricted to certain regions [254]. In contrast, CRH receptors are ubiquitously expressed throughout the brain. A study also showed deleting CRHR1 in hippocampus and cortex has distinctly different behaviour outcomes compare with the one in ventral midbrain [250]. This gave us the hint that understanding the connection of CRH- and CRH receptor expressing neurons in different brain regions might be one important aspect that is still missing in order to develop new clinical interventions based on the CRH/CRHRs system. In addition, our previous study suggests that CRH in projection neurons of the BNST and CeA affects anxiety-like behaviours via interaction with CRHR1 expressed on midbrain dopaminergic neurons [243].

The starting point of this study was to unravel the biological identity of CRHR1 neurons in the ventral midbrain which would provide some hints on functional aspects of these cells. There are several studies using immunohistochemistry or single cell RNA sequencing to specify the cell populations in the ventral midbrain. These studies indicate that there are three main neuronal populations in the region: dopaminergic, GABAergic and glutamatergic neurons [255,256]. We went one step further concentrating on CRHR1 cells. From our results we were able to clarify that CRHR1 neurons in the ventral mid brain are heterogenic and basically comprise the three main populations of neurons. At this point we can roughly separate them into dopaminergic, GABAergic and glutamatergic neurons which also has been described in the literatures and confirmed by many others [257,258].

One of the questions investigated in this study is the connectivity of CRH and CRHR1 neurons. Since there are little to none CRH positive neurons in the ventral midbrain, this raises the question from where and how CRH is transported and released in the midbrain. With the help of different anterograde and retrograde tracers, we revealed the main sites of CRH expressing neurons projecting into the ventral midbrain. There are specific differences between the VTA and SN. The main site of CRH input to the VTA originates in the BNST. Furthermore, we were able to further define that lateral posterior part (BSTLP) as the main

sub region of the BNST projecting to the VTA. Analysis of our anterograde tracing results with a Pearson-correlation test (relative fluorescence strength of projection compare to injection site) showed that the VTA is associated with regions such as NAc and PAG. These connections have been shown earlier by studies on rewarding behaviour [259-262]. Besides its strong implication in rewarding behaviour, the VTA has recently been shown to be involved in other anxiety-related behaviours [263,264]. Further studies concentrating on the connectivity of VTA and anxiety-related brain regions will shed more light on the role of the VTA in circuits of emotions.

The SN is traditionally thought to be involved in motor-related behaviours especially in the field of Parkinson's disease [265-267]. The connectivity of the SN has been studied by many groups. However, the connectivity of CRH neurons and the SN is largely unknown [268-271]. To our surprise, the main inputs of CRH neurons into SN are from CeA and IPACL. Projections from the CeA have been published in previous publications. In contrast, the IPACL has never been identified as a major origin of SN afferents. Direct comparison of CeA with the IPACL, shows that they both contain CRH positive neurons which are GABAergic. In order to understand the differences in connectivity between these two regions and the SN, two anterograde tracing viruses with different colours were injected in these regions. From our results, we were able to distinguish the anatomical difference of the projections. In general, CeA CRH neurons project into various different brain regions. In case of the SN, the main input from the CeA is found in the lateral part of the structure. In contrast, IPACL CRH neurons project to the medial and lateral part of the SN with more CRH terminals found in the medial part.

The IPAC, is described as a part of the central division of extended amygdala. It is rostrally directly continuous with the caudomedial shell of the accumbens and caudally with the central amygdaloid nucleus [272]. With the help of CLARITY, we were able to show that CRH neurons in the lateral part of the IPAC, share the interconnection with CeA CRH neurons. IPAC connects with diverse brain regions including the basolateral amygdala [273], the paraventricular nucleus of the thalamus [274], the lateral hypothalamic area [275], the ventral tegmental area [276,277] and the parafacial zone [273]. In contrast, IPACL CRH neurons projections are less diverse; they project to the SN and have rather local projection to the IPACM. A detailed investigation of the IPACL neurons revealed the heterogeneity of SN projection areas. CRH terminals are innervating both dopaminergic and GABAergic cells which increases the complexity of this circuit. Exact quantification was not possible but

qualitatively it appears that there are slightly more projections innervating dopaminergic neurons.

It is still a mystery how and where CRH is released upon an adverse or stressful event. One of the aims of this study was to investigate whether there is a direct synaptic connection established between CRH and CRHR1 neurons. A direct synaptic connection between CRH and CRHR1 neurons would represent as strong hint that CRH is released from the axon terminal and CRHR1 neurons at the post-synapse will be the direct site of action. Therefore, rabies tracing experiments were conducted. The first experiment using CRHR1-*Cre* animals was only able to label a limited number of cells in the brain. The main finding was that there are connections between striatum and the SN, which can be related to the striatonigral pathway. Besides the striatum, minor connections were found between the SN and the CeA, BNST as well as the IPACL. This result suggested that there is rather sparse direct synaptic connection between IPACL CRH neurons and SN CRHR1 neurons.

CRHR1 neurons constitute only a subset of GABAergic and dopaminergic neurons in the SN. In order to interrogate the synaptic contact of IPACL CRH neurons with GABAergic (PV) and dopaminergic neurons in the SN, rabies-based tracings were conducted using PV-*Cre* and Dat-*Cre*ERT^2 animals. These experiments showed that the main projections targeting the SN PV positive neurons are originate from PV positive neurons in the GPe. Cells were also detected in the CeA which is in line with the result of anterograde tracing. For IPALC, the signal was way weaker compared to the GPe or the CeA, suggesting that terminals of the CRH neurons have only sparse synaptic contacts with PV positive and dopaminergic neurons.

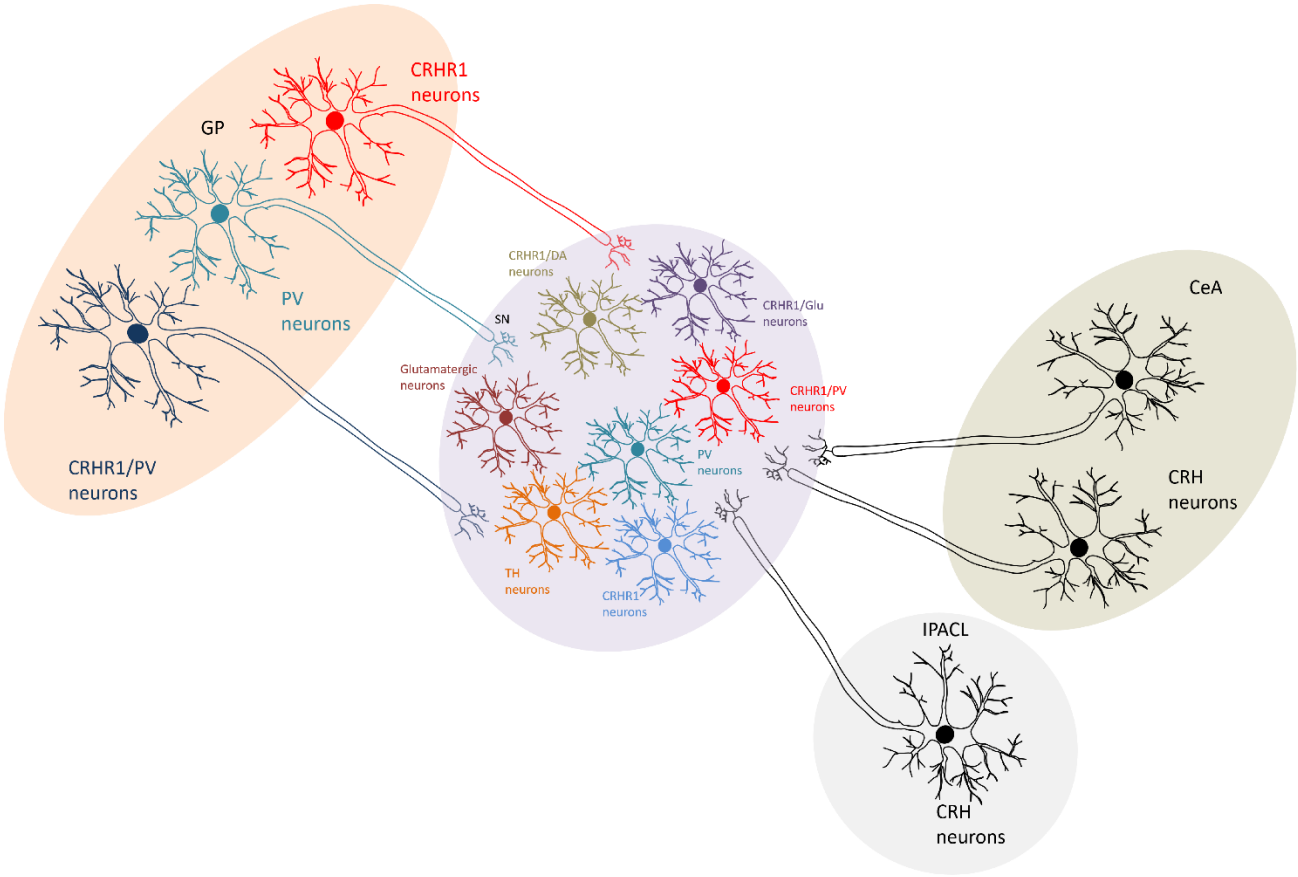

Fig 39. Connectivity of the SN with the extended amygdala and GPe

Different anterograde and retrograde tracing methods, revealed the connection map of the SN with regions of the extended amygdala including IPACL and CeA as well as GPe. IPACL CRH neurons send long-range projections into the SN, both in the medial and lateral part of the region. CRH axon terminals are innervating the SN but seemingly establish only sparse connections with GABAergic, dopaminergic or CRHR1 neurons. From the CeA, CRH neurons are mainly projecting to the lateral part of the SN and where they have direct synaptic connections with CRHR1 neurons as well as GABAergic neurons. GPe PV neurons also show strong projections into the SN, having connections with dopaminergic, GABAergic and CRHR1 neurons.

Since the IPACL is part of the extended amygdala, it is suspected to play a role in the regulation of stress-related behaviour. In addition, it was associated with disgust behaviour in mice recently [278]. However, the function of IPACL CRH neurons has not been investigated so far. To understand the function of IPACL CRH neurons, these cells were specifically activated using Cre-dependent DREADD. Interestingly, activation of CRH neurons in the IPACL generated a strong arousal response and place aversion. This result suggests that IPACL CRH neurons are able to trigger aversive responses. A similar experiment activating CRHR1 neurons in the SN was conducted, which revealed that DREADD-expressing mice

show anxiogenic behaviour but otherwise are indistinguishable from control animals. Since the SN is a heterogenic region composed of different subtypes of neurons mainly consist of DA neurons in the SNc and GABAergic neurons in the SNr which both to some extent express CRHR1. Therefore, activating different types of CRHR1 neurons in the SN might result in inhibition of each other. This results in the lack of behavioural phenotype of DREADD-based activation of CRHR1 neurons in the SN.

An important question that was addressed in this study is whether CRH is contributing to the behavioural outcomes following activation of IPACL CRH neurons. The effects on locomotor activity itself suggests the hypothesis that CRH is released upon activation of CRH neurons in the IPACL [279]. To address this question, the same DREADD experiment was performed in the IPACL, but comparing CNO + saline with CNO + R121919 [280]. From our results, we were able to see the ablation of arousal and place aversion behaviours when CRHR1 was blocked by systemic administration of R121919, indicating the direct contribution of CRH and CRHR1 to the observed behaviours.

The results from activation of SN CRHR1 neurons raised the question where CRH is released and affects the behavioural outcomes we had observed. The SN is strongly interconnected with structures of basal ganglia including striatum and the GPe [281,282], which also contain CRHR1 expressing neurons. To test the projection of CRHR1 neurons present in these structures tracing experiments were performed in the striatum and the GPe using CRHR1-*Cre* mice. Strong CRHR1 expression was detected in the GPe while at the same time those CRHR1 neurons project to the SN. Characterisation of the CRHR1 neurons in the GPe revealed that CRHR1 neurons are mainly PV neurons which is consistent with previous studies [283]. Further characterization, revealed that PV neurons send long range projection onto PV neurons in the SN which opens up the possibility of presynaptic CRHR1 receptors in the SN as potential mediator of CRH released from the IPACL into the SN. Therefore, the functional role of this circuit was explicitly addressed. Activation of CRHR1 neurons in the GPe had similar effects as activating CRH neurons in the IPACL which was further confirmed by optogenetic activation of axon terminals of the CRHR1 neurons. The GPe has previously been characterized with respect to its involvement in reward and also anxiety-related behaviours. CRHR1 neurons in the GPe have been linked with rewarding behaviour in studies investigating the connection of GPe and lateral hanebula, which demonstrate that GPe projections into the lateral hanebula are reward related. In another study, it was demonstrated that dopaminergic and glutamatergic projections into the GPe from the VTA also contribute

to reward behaviour in mice [284-287]. Recent studies suggests that activation of GPe PV neurons leads to increased locomotor activity [288] and activation of GPe CRHR1 neurons leads to anxiogenic behaviour with the contribution of CRH neurons projecting from CeA and PVN [289]. This study proposes that CRHR1 neurons in the GPe are involved in place aversion and arousal behaviour, on top of that, there is evidence that CRHR1 PV positive long-range projecting neurons contribute to this behavioural outcome. Rabies virus-mediated tracing demonstrated a direct synaptic connection between GPe and SN while the IPACL and the SN showed only limited direct contact.

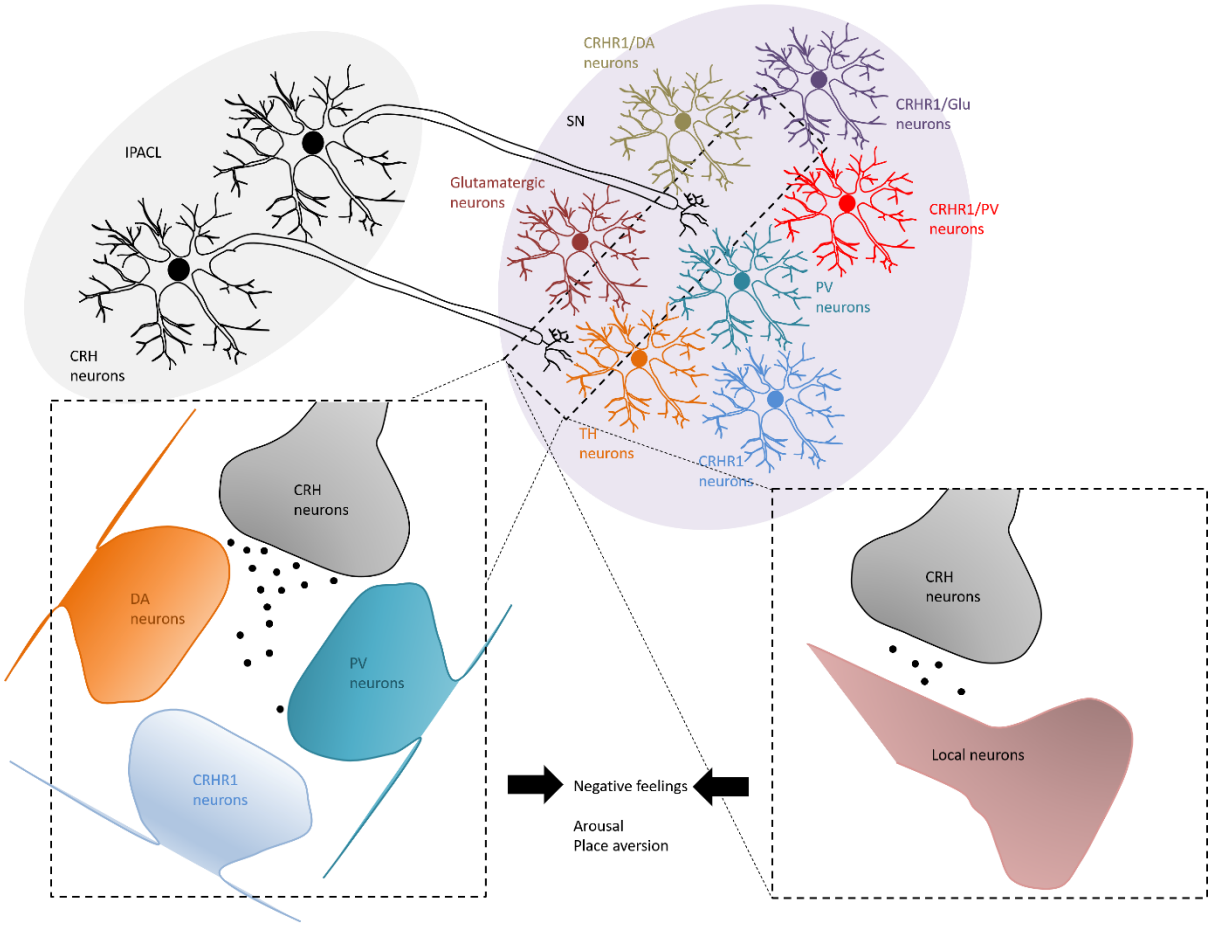

Fig 40. CRH projecting neurons in the IPACL trigger aversive behaviours

CRH neurons in the IPACL project into the SN, however, the neurons show limited direct synaptic connection to local SN neurons. Here we hypothesized that CRH neurons after activation will release CRH in the region of the SN which contains different types of neurons. The released CRH will be picked up by local neurons as a neuromodulator even without synaptic connections. Since local GABA/PV, DA/TH and glutamatergic neurons are also expressing CRHR1, we are unable to rule out the role of local CRHR1 neurons. CRH as

neuromodulator triggers the aversive behaviour which can be blocked by systemic administration of CRHR1 antagonist R121919.

In conclusion, this study demonstrates that CRH expressing neurons in the IPACL send long range projections into the SN. Furthermore, CRHR1 expressing neurons in the GPe also project into the SN. In addition, we are able to describe the function of IPACL CRH and GPe CRHR1 neurons upon activation. From these results, we can conclude that CRH is the main trigger of aversive responses in the extended amygdala and CRHR1 in the GPe is also a key component. In this study we were unable to directly proof that that there are presynaptic CRH receptors located on axon terminals of GPe neurons in the SN due to technical limitations. However, in the future it will be inevitable to demonstrate the presence of presynaptic CRHR1 and its involvement in the regulation of behaviour by CRH released from IPACL neurons in the SN.

Beyond the results presented in this study, there are other CRH circuits in the brain that showed the similar functional implication of CRH involving in regulating aversive responses. For instance, CRH was found engaging the Locus Coeruleus (LC) noradrenergic system that mediates stress-induced anxiety. Endogenous CRH inputs from the amygdala into LC increase tonic LC activity, inducing anxiety-like behaviours [290]. Furthermore, activation of CRH neurons in the amygdala abolished the increasing serotonergic activity in dorsal raphe nucleus (DRv) neurons and ameliorated stress-induced anhedonia in susceptible rats [291]. Another paper suggests CRH is strongly modulated by early-life adversity in the amygdala which resulted in aberrant expression of CRH in the amygdala and increased connectivity of the nucleus accumbens (NAc) with fear/anxiety regions, disrupting the function of NAc of pleasure and reward [292]. In contrast, reward decreases anxiety-like behaviour and stress-hormone surge induced by acute activation of PVN CRH neurons or repeated stress challenge. Repeated stress upregulates glutamatergic transmission and induces an N-methyl-D-aspartate receptor (NMDAR)-dependent burst-firing pattern in PVN CRH neurons which can be abolished by reward consumption [79]. Since different CRH/CRHR1 circuits contribute differentially to behaviour and even have opposite effects [250], further understanding of the CRH/CRHR1 neurocircuits provides an entry point for the development of more accurate drug delivery. Selective targeting of specific CRH/CRHR1 circuits might open up novel avenues for therapeutic intervention in different psychiatric disorders.

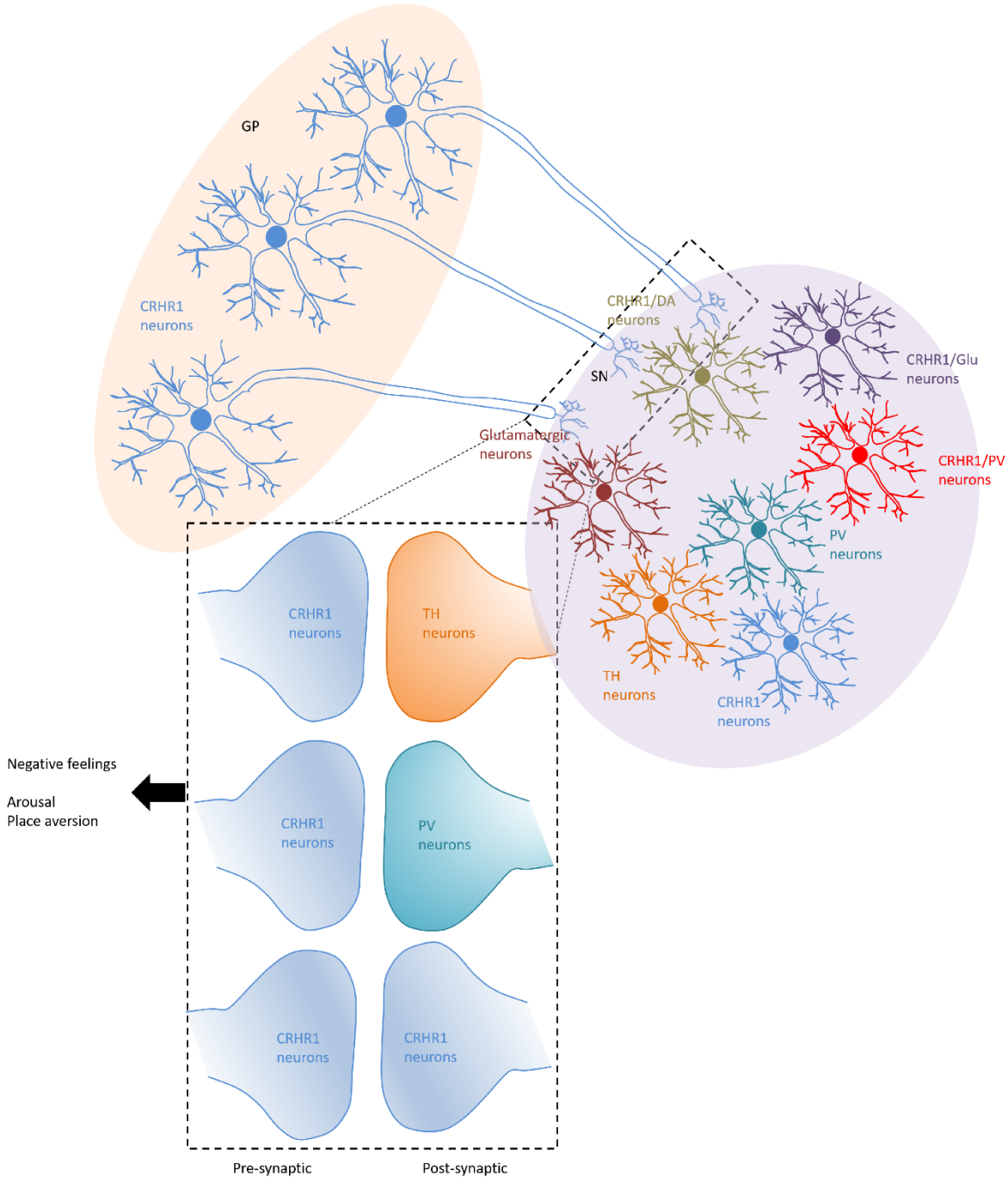

Fig 41. CRHR1 from GPe mediating aversive behavior

Besides the local CRHR1 neurons in the SN, there are PV positive CRHR1 neurons projecting from the GPe which have strong connections with local neurons in the SN. Since there is no proof that local neurons are directly involved in the arousal and aversive behaviour, we suspect those CRHR1 neurons from the GPe are the neurons that receive CRH signaling from the IPACL. In this study, there was no direct evidence of the pre-synaptic CRHR1 in the GPe, however, evidence of pre-synaptic CRHR1 has been shown in other publication modulating the excitatory signals in the hippocampal CA3 [293,294].

A next step in this study would be using Cre virus (AAV_8-Cre) in the SN or GPe of CRHR1-floxed animals together with DREADD-based activation of IPACL CRH neurons. This should provide information with regards to the site where CRH is released to activate CRHR1 following stimulation in the IPACL. With more bioinformatics support, we hope we are able to describe the populations of both CRH and CRHR1 neurons in more detail in the future. To understand the functional circuits between the IPACL and the GPe, calcium imaging or electrophysiology will be a good assist. Calcium imaging will allow to monitor cell activity in freely moving animals during behavioural tests. Electrophysiological recording will provide information on synaptic activity and connectivity between structures. Since this study is mainly based on activation of the CRH/CRHR1 system, it is suggested to conduct future studies involving inhibition of the system in order to further understand the physiological role of this system in regulation of aversive responses. In the future it will be beneficial to develop a CRH sensor in order to detect the release of CRH as well as the binding of CRH to its receptors. This will provide insight into the question how CRH is triggered at the molecular level and how CRH in long-range projecting neurons reaches its target.

References

1 Kraepelin, E. Arbeitspsychologische untersuchungen. *Zeitschrift für die gesamte Neurologie und Psychiatrie* **70**, 230-240, doi:10.1007/BF02867530 (1921).

2 Spitzer, R. L., Endicott, J. & Robins, E. Clinical criteria for psychiatric diagnosis and DSM-III. *The American journal of psychiatry* **132**, 1187-1192, doi:10.1176/ajp.132.11.1187 (1975).

3 Crow, T. J. Molecular pathology of schizophrenia: more than one disease process? *British medical journal* **280**, 66-68, doi:10.1136/bmj.280.6207.66 (1980).

4 Andreasen, N. C. & Olsen, S. Negative v positive schizophrenia. Definition and validation. *Archives of general psychiatry* **39**, 789-794, doi:10.1001/archpsyc.1982.04290070025006 (1982).

5 Golden, C. J. *et al.* Cerebral ventricular size and neuropsychological impairment in young chronic schizophrenics. Measurement by the standardized Luria-Nebraska Neuropsychological Battery. *Archives of general psychiatry* **37**, 619-623, doi:10.1001/archpsyc.1980.01780190017001 (1980).

6 Hamilton, M. The assessment of anxiety states by rating. *The British journal of medical psychology* **32**, 50-55, doi:10.1111/j.2044-8341.1959.tb00467.x (1959).

7 Hamilton, M. A rating scale for depression. *Journal of neurology, neurosurgery, and psychiatry* **23**, 56-62, doi:10.1136/jnnp.23.1.56 (1960).

8 Hamilton, M. Development of a rating scale for primary depressive illness. *The British journal of social and clinical psychology* **6**, 278-296, doi:10.1111/j.2044-8260.1967.tb00530.x (1967).

9 Kovelman, J. A. & Scheibel, A. B. A neurohistological correlate of schizophrenia. *Biological psychiatry* **19**, 1601-1621 (1984).

10 Bogerts, B., Meertz, E. & Schonfeldt-Bausch, R. Basal ganglia and limbic system pathology in schizophrenia. A morphometric study of brain volume and shrinkage. *Archives of general psychiatry* **42**, 784-791, doi:10.1001/archpsyc.1985.01790310046006 (1985).

11 Weinberger, D. R., Berman, K. F. & Zec, R. F. Physiologic dysfunction of dorsolateral prefrontal cortex in schizophrenia. I. Regional cerebral blood flow evidence. *Archives of general psychiatry* **43**, 114-124, doi:10.1001/archpsyc.1986.01800020020004 (1986).

12 Kane, J., Honigfeld, G., Singer, J. & Meltzer, H. Clozapine for the treatment-resistant schizophrenic. A double-blind comparison with chlorpromazine. *Archives of general psychiatry* **45**, 789-796, doi:10.1001/archpsyc.1988.01800330013001 (1988).

13 Coccaro, E. F. *et al.* Serotonergic studies in patients with affective and personality disorders. Correlates with suicidal and impulsive aggressive behavior. *Archives of general psychiatry* **46**, 587-599, doi:10.1001/archpsyc.1989.01810070013002 (1989).

14 LeDoux, J. E. Emotion circuits in the brain. *Annual review of neuroscience* **23**, 155-184, doi:10.1146/annurev.neuro.23.1.155 (2000).

15 Phan, K. L., Wager, T., Taylor, S. F. & Liberzon, I. Functional neuroanatomy of emotion: a meta-analysis of emotion activation studies in PET and fMRI. *NeuroImage* **16**, 331-348, doi:10.1006/nimg.2002.1087 (2002).

16 Phillips, M. L., Drevets, W. C., Rauch, S. L. & Lane, R. Neurobiology of emotion perception I: The neural basis of normal emotion perception. *Biological psychiatry* **54**, 504-514, doi:10.1016/s0006-3223(03)00168-9 (2003).

17 Mayberg, H. S. *et al.* Deep brain stimulation for treatment-resistant depression. *Neuron* **45**, 651-660, doi:10.1016/j.neuron.2005.02.014 (2005).

18 Egan, M. F. *et al.* Effect of COMT Val108/158 Met genotype on frontal lobe function and risk for schizophrenia. *Proceedings of the National Academy of Sciences of the United States of America* **98**, 6917-6922, doi:10.1073/pnas.111134598 (2001).

19 Purves, K. L. *et al.* A major role for common genetic variation in anxiety disorders. *Molecular psychiatry*, doi:10.1038/s41380-019-0559-1 (2019).

20 Ward, J. *et al.* The genomic basis of mood instability: identification of 46 loci in 363,705 UK Biobank participants, genetic correlation with psychiatric disorders, and association with gene expression and function. *Molecular psychiatry*, doi:10.1038/s41380-019-0439-8 (2019).
21 Stahl, E. A. *et al.* Genome-wide association study identifies 30 loci associated with bipolar disorder. *Nature genetics* **51**, 793-803, doi:10.1038/s41588-019-0397-8 (2019).
22 Coleman, J. R. I., Gaspar, H. A., Bryois, J. & Breen, G. The Genetics of the Mood Disorder Spectrum: Genome-wide Association Analyses of More Than 185,000 Cases and 439,000 Controls. *Biological psychiatry*, doi:10.1016/j.biopsych.2019.10.015 (2019).
23 Wray, N. R. *et al.* Genome-wide association analyses identify 44 risk variants and refine the genetic architecture of major depression. *Nature genetics* **50**, 668-681, doi:10.1038/s41588-018-0090-3 (2018).
24 Flint, J. & Ideker, T. The great hairball gambit. *PLoS genetics* **15**, e1008519, doi:10.1371/journal.pgen.1008519 (2019).
25 Flint, J. & Kendler, K. S. The genetics of major depression. *Neuron* **81**, 484-503, doi:10.1016/j.neuron.2014.01.027 (2014).
26 Deisseroth, K. Optogenetics. *Nature methods* **8**, 26-29, doi:10.1038/nmeth.f.324 (2011).
27 Fenno, L., Yizhar, O. & Deisseroth, K. The development and application of optogenetics. *Annual review of neuroscience* **34**, 389-412, doi:10.1146/annurev-neuro-061010-113817 (2011).
28 Yizhar, O., Fenno, L. E., Davidson, T. J., Mogri, M. & Deisseroth, K. Optogenetics in neural systems. *Neuron* **71**, 9-34, doi:10.1016/j.neuron.2011.06.004 (2011).
29 D'Souza, D. Post-traumatic stress disorder--a scar for life. *Br J Clin Pract* **49**, 309-313 (1995).
30 Holsboer, F. & Barden, N. Antidepressants and hypothalamic-pituitary-adrenocortical regulation. *Endocr Rev* **17**, 187-205, doi:10.1210/edrv-17-2-187 (1996).
31 Sherman, J. E. & Kalin, N. H. ICV-CRH alters stress-induced freezing behavior without affecting pain sensitivity. *Pharmacology, biochemistry, and behavior* **30**, 801-807, doi:10.1016/0091-3057(88)90103-7 (1988).
32 Murakami, K., Akana, S., Dallman, M. F. & Ganong, W. F. Correlation between the stress-induced transient increase in corticotropin-releasing hormone content of the median eminence of the hypothalamus and adrenocorticotropic hormone secretion. *Neuroendocrinology* **49**, 233-241, doi:10.1159/000125122 (1989).
33 Berger, M., Krieg, C., Bossert, S., Schreiber, W. & von Zerssen, D. Past and present strategies of research on the HPA-axis in psychiatry. *Acta psychiatrica Scandinavica. Supplementum* **341**, 112-125, doi:10.1111/j.1600-0447.1988.tb08557.x (1988).
34 Amsterdam, J. D., Maislin, G., Gold, P. & Winokur, A. The assessment of abnormalities in hormonal responsiveness at multiple levels of the hypothalamic-pituitary-adrenocortical axis in depressive illness. *Psychoneuroendocrinology* **14**, 43-62, doi:10.1016/0306-4530(89)90055-3 (1989).
35 Kalin, N. H., Sherman, J. E. & Takahashi, L. K. Antagonism of endogenous CRH systems attenuates stress-induced freezing behavior in rats. *Brain research* **457**, 130-135, doi:10.1016/0006-8993(88)90064-9 (1988).
36 Furutani, Y. *et al.* Cloning and sequence analysis of cDNA for ovine corticotropin-releasing factor precursor. *Nature* **301**, 537-540, doi:10.1038/301537a0 (1983).
37 Jingami, H. *et al.* Cloning and sequence analysis of cDNA for rat corticotropin-releasing factor precursor. *FEBS letters* **191**, 63-66, doi:10.1016/0014-5793(85)80994-7 (1985).
38 Robinson, B. G., D'Angio, L. A., Jr., Pasieka, K. B. & Majzoub, J. A. Preprocorticotropin releasing hormone: cDNA sequence and in vitro processing. *Molecular and cellular endocrinology* **61**, 175-180, doi:10.1016/0303-7207(89)90128-7 (1989).
39 Roche, P. J., Crawford, R. J., Fernley, R. T., Tregear, G. W. & Coghlan, J. P. Nucleotide sequence of the gene coding for ovine corticotropin-releasing factor and regulation of its

mRNA levels by glucocorticoids. *Gene* **71**, 421-431, doi:10.1016/0378-1119(88)90059-5 (1988).

40 Seasholtz, A. F., Bourbonais, F. J., Harnden, C. E. & Camper, S. A. Nucleotide sequence and expression of the mouse corticotropin-releasing hormone gene. *Molecular and cellular neurosciences* **2**, 266-273, doi:10.1016/1044-7431(91)90054-r (1991).

41 Thompson, R. C., Seasholtz, A. F., Douglass, J. O. & Herbert, E. The rat corticotropin-releasing hormone gene. *Annals of the New York Academy of Sciences* **512**, 1-11, doi:10.1111/j.1749-6632.1987.tb24947.x (1987).

42 Hook, V. *et al.* Proteases for processing proneuropeptides into peptide neurotransmitters and hormones. *Annual review of pharmacology and toxicology* **48**, 393-423, doi:10.1146/annurev.pharmtox.48.113006.094812 (2008).

43 Montecucchi, P. C., Anastasi, A., de Castiglione, R. & Erspamer, V. Isolation and amino acid composition of sauvagine. An active polypeptide from methanol extracts of the skin of the South American frog Phyllomedusa sauvagei. *International journal of peptide and protein research* **16**, 191-199 (1980).

44 Montecucchi, P. C. & Henschen, A. Amino acid composition and sequence analysis of sauvagine, a new active peptide from the skin of Phyllomedusa sauvagei. *International journal of peptide and protein research* **18**, 113-120, doi:10.1111/j.1399-3011.1981.tb02047.x (1981).

45 Vaughan, J. *et al.* Urocortin, a mammalian neuropeptide related to fish urotensin I and to corticotropin-releasing factor. *Nature* **378**, 287-292, doi:10.1038/378287a0 (1995).

46 van den Pol, A. N. Neuropeptide transmission in brain circuits. *Neuron* **76**, 98-115, doi:10.1016/j.neuron.2012.09.014 (2012).

47 Cummings, S., Elde, R., Ells, J. & Lindall, A. Corticotropin-releasing factor immunoreactivity is widely distributed within the central nervous system of the rat: an immunohistochemical study. *The Journal of neuroscience : the official journal of the Society for Neuroscience* **3**, 1355-1368 (1983).

48 Merchenthaler, I., Vigh, S., Petrusz, P. & Schally, A. V. Immunocytochemical localization of corticotropin-releasing factor (CRF) in the rat brain. *The American journal of anatomy* **165**, 385-396, doi:10.1002/aja.1001650404 (1982).

49 Sakanaka, M., Shibasaki, T. & Lederis, K. Corticotropin releasing factor-like immunoreactivity in the rat brain as revealed by a modified cobalt-glucose oxidase-diaminobenzidine method. *The Journal of comparative neurology* **260**, 256-298, doi:10.1002/cne.902600209 (1987).

50 Sawchenko, P. E. & Swanson, L. W. Localization, colocalization, and plasticity of corticotropin-releasing factor immunoreactivity in rat brain. *Federation proceedings* **44**, 221-227 (1985).

51 Itoi, K. *et al.* Visualization of corticotropin-releasing factor neurons by fluorescent proteins in the mouse brain and characterization of labeled neurons in the paraventricular nucleus of the hypothalamus. *Endocrinology* **155**, 4054-4060, doi:10.1210/en.2014-1182 (2014).

52 Kono, J. *et al.* Distribution of corticotropin-releasing factor neurons in the mouse brain: a study using corticotropin-releasing factor-modified yellow fluorescent protein knock-in mouse. *Brain structure & function* **222**, 1705-1732, doi:10.1007/s00429-016-1303-0 (2017).

53 Taniguchi, H. *et al.* A resource of Cre driver lines for genetic targeting of GABAergic neurons in cerebral cortex. *Neuron* **71**, 995-1013, doi:10.1016/j.neuron.2011.07.026 (2011).

54 Chen, Y., Bender, R. A., Frotscher, M. & Baram, T. Z. Novel and transient populations of corticotropin-releasing hormone-expressing neurons in developing hippocampus suggest unique functional roles: a quantitative spatiotemporal analysis. *The Journal of neuroscience : the official journal of the Society for Neuroscience* **21**, 7171-7181, doi:10.1523/jneurosci.21-18-07171.2001 (2001).

55 Kubota, Y. *et al.* Selective coexpression of multiple chemical markers defines discrete populations of neocortical GABAergic neurons. *Cerebral cortex (New York, N.Y. : 1991)* **21**, 1803-1817, doi:10.1093/cercor/bhq252 (2011).
56 Majzoub, J. A. & Karalis, K. P. Placental corticotropin-releasing hormone: function and regulation. *American journal of obstetrics and gynecology* **180**, S242-246, doi:10.1016/s0002-9378(99)70708-8 (1999).
57 Bale, T. L. & Vale, W. W. CRF and CRF receptors: role in stress responsivity and other behaviors. *Annual review of pharmacology and toxicology* **44**, 525-557, doi:10.1146/annurev.pharmtox.44.101802.121410 (2004).
58 Koob, G. F. Brain stress systems in the amygdala and addiction. *Brain research* **1293**, 61-75, doi:10.1016/j.brainres.2009.03.038 (2009).
59 Binder, E. B. & Nemeroff, C. B. The CRF system, stress, depression and anxiety-insights from human genetic studies. *Molecular psychiatry* **15**, 574-588, doi:10.1038/mp.2009.141 (2010).
60 Cain, D. W. & Cidlowski, J. A. Immune regulation by glucocorticoids. *Nature reviews. Immunology* **17**, 233-247, doi:10.1038/nri.2017.1 (2017).
61 Herman, J. P. *et al.* Regulation of the Hypothalamic-Pituitary-Adrenocortical Stress Response. *Comprehensive Physiology* **6**, 603-621, doi:10.1002/cphy.c150015 (2016).
62 Kuo, T., McQueen, A., Chen, T. C. & Wang, J. C. Regulation of Glucose Homeostasis by Glucocorticoids. *Advances in experimental medicine and biology* **872**, 99-126, doi:10.1007/978-1-4939-2895-8_5 (2015).
63 Gillespie, C. F. & Nemeroff, C. B. Hypercortisolemia and depression. *Psychosomatic medicine* **67 Suppl 1**, S26-28, doi:10.1097/01.psy.0000163456.22154.d2 (2005).
64 Lesch, K. P., Laux, G., Schulte, H. M., Pfuller, H. & Beckmann, H. Corticotropin and cortisol response to human CRH as a probe for HPA system integrity in major depressive disorder. *Psychiatry research* **24**, 25-34, doi:10.1016/0165-1781(88)90136-9 (1988).
65 Smith, M. A. *et al.* The corticotropin-releasing hormone test in patients with posttraumatic stress disorder. *Biological psychiatry* **26**, 349-355, doi:10.1016/0006-3223(89)90050-4 (1989).
66 Asan, E. *et al.* The corticotropin-releasing factor (CRF)-system and monoaminergic afferents in the central amygdala: investigations in different mouse strains and comparison with the rat. *Neuroscience* **131**, 953-967, doi:10.1016/j.neuroscience.2004.11.040 (2005).
67 Sirinathsinghji, D. J., Rees, L. H., Rivier, J. & Vale, W. Corticotropin-releasing factor is a potent inhibitor of sexual receptivity in the female rat. *Nature* **305**, 232-235, doi:10.1038/305232a0 (1983).
68 Tazi, A. *et al.* Behavioral activation by CRF: evidence for the involvement of the ventral forebrain. *Life sciences* **41**, 41-49, doi:10.1016/0024-3205(87)90554-6 (1987).
69 Koob, G. F. *et al.* The role of corticotropin-releasing factor in behavioural responses to stress. *Ciba Foundation symposium* **172**, 277-289; discussion 290-275, doi:10.1002/9780470514368.ch14 (1993).
70 Nguyen, A. Q., Dela Cruz, J. A., Sun, Y., Holmes, T. C. & Xu, X. Genetic cell targeting uncovers specific neuronal types and distinct subregions in the bed nucleus of the stria terminalis. *The Journal of comparative neurology* **524**, 2379-2399, doi:10.1002/cne.23954 (2016).
71 Berridge, C. W. & Dunn, A. J. Corticotropin-releasing factor elicits naloxone sensitive stress-like alterations in exploratory behavior in mice. *Regulatory peptides* **16**, 83-93, doi:10.1016/0167-0115(86)90196-5 (1986).
72 Britton, D. R., Koob, G. F., Rivier, J. & Vale, W. Intraventricular corticotropin-releasing factor enhances behavioral effects of novelty. *Life sciences* **31**, 363-367, doi:10.1016/0024-3205(82)90416-7 (1982).
73 Heinrichs, S. C., Menzaghi, F., Merlo Pich, E., Britton, K. T. & Koob, G. F. The role of CRF in behavioral aspects of stress. *Annals of the New York Academy of Sciences* **771**, 92-104, doi:10.1111/j.1749-6632.1995.tb44673.x (1995).

74 Sherman, J. E. & Kalin, N. H. The effects of ICV-CRH on novelty-induced behavior. *Pharmacology, biochemistry, and behavior* **26**, 699-703, doi:10.1016/0091-3057(87)90599-5 (1987).
75 Swerdlow, N. R., Geyer, M. A., Vale, W. W. & Koob, G. F. Corticotropin-releasing factor potentiates acoustic startle in rats: blockade by chlordiazepoxide. *Psychopharmacology* **88**, 147-152, doi:10.1007/bf00652231 (1986).
76 Lee, Y. & Davis, M. Role of the septum in the excitatory effect of corticotropin-releasing hormone on the acoustic startle reflex. *The Journal of neuroscience : the official journal of the Society for Neuroscience* **17**, 6424-6433, doi:10.1523/jneurosci.17-16-06424.1997 (1997).
77 Sahuque, L. L. *et al.* Anxiogenic and aversive effects of corticotropin-releasing factor (CRF) in the bed nucleus of the stria terminalis in the rat: role of CRF receptor subtypes. *Psychopharmacology* **186**, 122-132, doi:10.1007/s00213-006-0362-y (2006).
78 Liang, K. C. *et al.* Corticotropin-releasing factor: long-lasting facilitation of the acoustic startle reflex. *The Journal of neuroscience : the official journal of the Society for Neuroscience* **12**, 2303-2312, doi:10.1523/jneurosci.12-06-02303.1992 (1992).
79 Yuan, Y. *et al.* Reward Inhibits Paraventricular CRH Neurons to Relieve Stress. *Current biology : CB* **29**, 1243-1251.e1244, doi:10.1016/j.cub.2019.02.048 (2019).
80 Koutmani, Y. *et al.* CRH Promotes the Neurogenic Activity of Neural Stem Cells in the Adult Hippocampus. *Cell reports* **29**, 932-945.e937, doi:10.1016/j.celrep.2019.09.037 (2019).
81 Chen, R., Lewis, K. A., Perrin, M. H. & Vale, W. W. Expression cloning of a human corticotropin-releasing-factor receptor. *Proceedings of the National Academy of Sciences of the United States of America* **90**, 8967-8971, doi:10.1073/pnas.90.19.8967 (1993).
82 Chang, C. P., Pearse, R. V., 2nd, O'Connell, S. & Rosenfeld, M. G. Identification of a seven transmembrane helix receptor for corticotropin-releasing factor and sauvagine in mammalian brain. *Neuron* **11**, 1187-1195, doi:10.1016/0896-6273(93)90230-o (1993).
83 Vita, N. *et al.* Primary structure and functional expression of mouse pituitary and human brain corticotrophin releasing factor receptors. *FEBS letters* **335**, 1-5, doi:10.1016/0014-5793(93)80427-v (1993).
84 Perrin, M. *et al.* Identification of a second corticotropin-releasing factor receptor gene and characterization of a cDNA expressed in heart. *Proceedings of the National Academy of Sciences of the United States of America* **92**, 2969-2973, doi:10.1073/pnas.92.7.2969 (1995).
85 Hsu, S. Y. & Hsueh, A. J. Human stresscopin and stresscopin-related peptide are selective ligands for the type 2 corticotropin-releasing hormone receptor. *Nature medicine* **7**, 605-611, doi:10.1038/87936 (2001).
86 Polymeropoulos, M. H., Torres, R., Yanovski, J. A., Chandrasekharappa, S. C. & Ledbetter, D. H. The human corticotropin-releasing factor receptor (CRHR) gene maps to chromosome 17q12-q22. *Genomics* **28**, 123-124, doi:10.1006/geno.1995.1118 (1995).
87 Vamvakopoulos, N. C. & Sioutopoulou, T. O. Human corticotropin-releasing hormone receptor gene (CRHR) is located on the long arm of chromosome 17 (17q12-qter). *Chromosome research : an international journal on the molecular, supramolecular and evolutionary aspects of chromosome biology* **2**, 471-473, doi:10.1007/bf01552870 (1994).
88 Burrows, H. L., Seasholtz, A. F. & Camper, S. A. Localization of the corticotropin-releasing hormone receptor gene on mouse chromosome 11. *Mammalian genome : official journal of the International Mammalian Genome Society* **6**, 55-56, doi:10.1007/bf00350896 (1995).
89 Teli, T. *et al.* Structural domains determining signalling characteristics of the CRH-receptor type 1 variant R1beta and response to PKC phosphorylation. *Cellular signalling* **20**, 40-49, doi:10.1016/j.cellsig.2007.08.014 (2008).
90 Markovic, D. & Grammatopoulos, D. K. Focus on the splicing of secretin GPCRs transmembrane-domain 7. *Trends in biochemical sciences* **34**, 443-452, doi:10.1016/j.tibs.2009.06.002 (2009).

91 Chen, A. *et al.* Mouse corticotropin-releasing factor receptor type 2alpha gene: isolation, distribution, pharmacological characterization and regulation by stress and glucocorticoids. *Molecular endocrinology (Baltimore, Md.)* **19**, 441-458, doi:10.1210/me.2004-0300 (2005).
92 Van Pett, K. *et al.* Distribution of mRNAs encoding CRF receptors in brain and pituitary of rat and mouse. *The Journal of comparative neurology* **428**, 191-212, doi:10.1002/1096-9861(20001211)428:2<191::aid-cne1>3.0.co;2-u (2000).
93 Kühne, C. *et al.* Visualizing corticotropin-releasing hormone receptor type 1 expression and neuronal connectivities in the mouse using a novel multifunctional allele. *The Journal of comparative neurology* **520**, 3150-3180, doi:10.1002/cne.23082 (2012).
94 Hillhouse, E. W. & Grammatopoulos, D. K. The molecular mechanisms underlying the regulation of the biological activity of corticotropin-releasing hormone receptors: implications for physiology and pathophysiology. *Endocr Rev* **27**, 260-286, doi:10.1210/er.2005-0034 (2006).
95 Lesh, J. S., Burrows, H. L., Seasholtz, A. F. & Camper, S. A. Mapping of the mouse corticotropin-releasing hormone receptor 2 gene (Crhr2) to chromosome 6. *Mammalian genome : official journal of the International Mammalian Genome Society* **8**, 944-945, doi:10.1007/s003359900644 (1997).
96 Catalano, R. D., Kyriakou, T., Chen, J., Easton, A. & Hillhouse, E. W. Regulation of corticotropin-releasing hormone type 2 receptors by multiple promoters and alternative splicing: identification of multiple splice variants. *Molecular endocrinology (Baltimore, Md.)* **17**, 395-410, doi:10.1210/me.2002-0302 (2003).
97 Kishimoto, T., Pearse, R. V., 2nd, Lin, C. R. & Rosenfeld, M. G. A sauvagine/corticotropin-releasing factor receptor expressed in heart and skeletal muscle. *Proceedings of the National Academy of Sciences of the United States of America* **92**, 1108-1112, doi:10.1073/pnas.92.4.1108 (1995).
98 Valdenaire, O., Giller, T., Breu, V., Gottowik, J. & Kilpatrick, G. A new functional isoform of the human CRF2 receptor for corticotropin-releasing factor. *Biochimica et biophysica acta* **1352**, 129-132, doi:10.1016/s0167-4781(97)00047-x (1997).
99 Kostich, W. A., Chen, A., Sperle, K. & Largent, B. L. Molecular identification and analysis of a novel human corticotropin-releasing factor (CRF) receptor: the CRF2gamma receptor. *Molecular endocrinology (Baltimore, Md.)* **12**, 1077-1085, doi:10.1210/mend.12.8.0145 (1998).
100 Chen, A. M. *et al.* A soluble mouse brain splice variant of type 2alpha corticotropin-releasing factor (CRF) receptor binds ligands and modulates their activity. *Proceedings of the National Academy of Sciences of the United States of America* **102**, 2620-2625, doi:10.1073/pnas.0409583102 (2005).
101 Lovenberg, T. W., Chalmers, D. T., Liu, C. & De Souza, E. B. CRF2 alpha and CRF2 beta receptor mRNAs are differentially distributed between the rat central nervous system and peripheral tissues. *Endocrinology* **136**, 4139-4142, doi:10.1210/endo.136.9.7544278 (1995).
102 Regev, L., Ezrielev, E., Gershon, E., Gil, S. & Chen, A. Genetic approach for intracerebroventricular delivery. *Proceedings of the National Academy of Sciences of the United States of America* **107**, 4424-4429, doi:10.1073/pnas.0907059107 (2010).
103 Henckens, M. J., Deussing, J. M. & Chen, A. Region-specific roles of the corticotropin-releasing factor-urocortin system in stress. *Nature reviews. Neuroscience* **17**, 636-651, doi:10.1038/nrn.2016.94 (2016).
104 McQueen, M. B. *et al.* Combined analysis from eleven linkage studies of bipolar disorder provides strong evidence of susceptibility loci on chromosomes 6q and 8q. *American journal of human genetics* **77**, 582-595, doi:10.1086/491603 (2005).
105 Segurado, R. *et al.* Genome scan meta-analysis of schizophrenia and bipolar disorder, part III: Bipolar disorder. *American journal of human genetics* **73**, 49-62, doi:10.1086/376547 (2003).

106 Levinson, D. F. The genetics of depression: a review. *Biological psychiatry* **60**, 84-92, doi:10.1016/j.biopsych.2005.08.024 (2006).
107 Smoller, J. W. *et al.* Association of a genetic marker at the corticotropin-releasing hormone locus with behavioral inhibition. *Biological psychiatry* **54**, 1376-1381, doi:10.1016/s0006-3223(03)00598-5 (2003).
108 Smoller, J. W. *et al.* The corticotropin-releasing hormone gene and behavioral inhibition in children at risk for panic disorder. *Biological psychiatry* **57**, 1485-1492, doi:10.1016/j.biopsych.2005.02.018 (2005).
109 Gu, J., Sadler, L., Daiger, S., Wells, D. & Wagner, M. Dinucleotide repeat polymorphism at the CRH gene. *Human molecular genetics* **2**, 85, doi:10.1093/hmg/2.1.85 (1993).
110 Bradley, R. G. *et al.* Influence of child abuse on adult depression: moderation by the corticotropin-releasing hormone receptor gene. *Archives of general psychiatry* **65**, 190-200, doi:10.1001/archgenpsychiatry.2007.26 (2008).
111 Polanczyk, G. *et al.* Protective effect of CRHR1 gene variants on the development of adult depression following childhood maltreatment: replication and extension. *Archives of general psychiatry* **66**, 978-985, doi:10.1001/archgenpsychiatry.2009.114 (2009).
112 DeYoung, C. G., Cicchetti, D. & Rogosch, F. A. Moderation of the association between childhood maltreatment and neuroticism by the corticotropin-releasing hormone receptor 1 gene. *Journal of child psychology and psychiatry, and allied disciplines* **52**, 898-906, doi:10.1111/j.1469-7610.2011.02404.x (2011).
113 Dunlop, B. W. *et al.* Corticotropin-Releasing Factor Receptor 1 Antagonism Is Ineffective for Women With Posttraumatic Stress Disorder. *Biological psychiatry* **82**, 866-874, doi:10.1016/j.biopsych.2017.06.024 (2017).
114 Tyrka, A. R. *et al.* Interaction of childhood maltreatment with the corticotropin-releasing hormone receptor gene: effects on hypothalamic-pituitary-adrenal axis reactivity. *Biological psychiatry* **66**, 681-685, doi:10.1016/j.biopsych.2009.05.012 (2009).
115 Ressler, K. J. *et al.* Polymorphisms in CRHR1 and the serotonin transporter loci: gene x gene x environment interactions on depressive symptoms. *American journal of medical genetics. Part B, Neuropsychiatric genetics : the official publication of the International Society of Psychiatric Genetics* **153b**, 812-824, doi:10.1002/ajmg.b.31052 (2010).
116 Keck, M. E. *et al.* Combined effects of exonic polymorphisms in CRHR1 and AVPR1B genes in a case/control study for panic disorder. *American journal of medical genetics. Part B, Neuropsychiatric genetics : the official publication of the International Society of Psychiatric Genetics* **147b**, 1196-1204, doi:10.1002/ajmg.b.30750 (2008).
117 Weber, H. *et al.* Allelic variation in CRHR1 predisposes to panic disorder: evidence for biased fear processing. *Molecular psychiatry* **21**, 813-822, doi:10.1038/mp.2015.125 (2016).
118 Licinio, J. *et al.* Association of a corticotropin-releasing hormone receptor 1 haplotype and antidepressant treatment response in Mexican-Americans. *Molecular psychiatry* **9**, 1075-1082, doi:10.1038/sj.mp.4001587 (2004).
119 Liu, Z. *et al.* Association study of corticotropin-releasing hormone receptor1 gene polymorphisms and antidepressant response in major depressive disorders. *Neuroscience letters* **414**, 155-158, doi:10.1016/j.neulet.2006.12.013 (2007).
120 Liu, Z. *et al.* Negative life events and corticotropin-releasing-hormone receptor1 gene in recurrent major depressive disorder. *Scientific reports* **3**, 1548, doi:10.1038/srep01548 (2013).
121 Cruceanu, C. *et al.* Rare susceptibility variants for bipolar disorder suggest a role for G protein-coupled receptors. *Molecular psychiatry* **23**, 2050-2056, doi:10.1038/mp.2017.223 (2018).
122 O'Connell, C. P. *et al.* Antidepressant Outcomes Predicted by Genetic Variation in Corticotropin-Releasing Hormone Binding Protein. *The American journal of psychiatry* **175**, 251-261, doi:10.1176/appi.ajp.2017.17020172 (2018).

123 Griebel, G. & Holsboer, F. Neuropeptide receptor ligands as drugs for psychiatric diseases: the end of the beginning? *Nature reviews. Drug discovery* **11**, 462-478, doi:10.1038/nrd3702 (2012).
124 Sanders, J. & Nemeroff, C. The CRF System as a Therapeutic Target for Neuropsychiatric Disorders. *Trends in pharmacological sciences* **37**, 1045-1054, doi:10.1016/j.tips.2016.09.004 (2016).
125 Zobel, A. W. *et al.* Effects of the high-affinity corticotropin-releasing hormone receptor 1 antagonist R121919 in major depression: the first 20 patients treated. *Journal of psychiatric research* **34**, 171-181, doi:10.1016/s0022-3956(00)00016-9 (2000).
126 Held, K. *et al.* Treatment with the CRH1-receptor-antagonist R121919 improves sleep-EEG in patients with depression. *Journal of psychiatric research* **38**, 129-136, doi:10.1016/s0022-3956(03)00076-1 (2004).
127 Künzel, H. E. *et al.* Treatment of depression with the CRH-1-receptor antagonist R121919: endocrine changes and side effects. *Journal of psychiatric research* **37**, 525-533, doi:10.1016/s0022-3956(03)00070-0 (2003).
128 Binneman, B. *et al.* A 6-week randomized, placebo-controlled trial of CP-316,311 (a selective CRH1 antagonist) in the treatment of major depression. *The American journal of psychiatry* **165**, 617-620, doi:10.1176/appi.ajp.2008.07071199 (2008).
129 Coric, V. *et al.* Multicenter, randomized, double-blind, active comparator and placebo-controlled trial of a corticotropin-releasing factor receptor-1 antagonist in generalized anxiety disorder. *Depression and anxiety* **27**, 417-425, doi:10.1002/da.20695 (2010).
130 Spierling, S. R. & Zorrilla, E. P. Don't stress about CRF: assessing the translational failures of CRF(1)antagonists. *Psychopharmacology* **234**, 1467-1481, doi:10.1007/s00213-017-4556-2 (2017).
131 Kirchhoff, V. D., Nguyen, H. T., Soczynska, J. K., Woldeyohannes, H. & McIntyre, R. S. Discontinued psychiatric drugs in 2008. *Expert opinion on investigational drugs* **18**, 1431-1443, doi:10.1517/13543780903184591 (2009).
132 Dunlop, B. W. *et al.* Evaluation of a corticotropin releasing hormone type 1 receptor antagonist in women with posttraumatic stress disorder: study protocol for a randomized controlled trial. *Trials* **15**, 240, doi:10.1186/1745-6215-15-240 (2014).
133 Zorrilla, E. P., Heilig, M., de Wit, H. & Shaham, Y. Behavioral, biological, and chemical perspectives on targeting CRF(1) receptor antagonists to treat alcoholism. *Drug and alcohol dependence* **128**, 175-186, doi:10.1016/j.drugalcdep.2012.12.017 (2013).
134 Kwako, L. E. *et al.* The corticotropin releasing hormone-1 (CRH1) receptor antagonist pexacerfont in alcohol dependence: a randomized controlled experimental medicine study. *Neuropsychopharmacology : official publication of the American College of Neuropsychopharmacology* **40**, 1053-1063, doi:10.1038/npp.2014.306 (2015).
135 Schwandt, M. L. *et al.* The CRF1 Antagonist Verucerfont in Anxious Alcohol-Dependent Women: Translation of Neuroendocrine, But not of Anti-Craving Effects. *Neuropsychopharmacology : official publication of the American College of Neuropsychopharmacology* **41**, 2818-2829, doi:10.1038/npp.2016.61 (2016).
136 Lynch, G., Gall, C., Mensah, P. & Cotman, C. W. Horseradish peroxidase histochemistry: a new method for tracing efferent projections in the central nervous system. *Brain research* **65**, 373-380, doi:10.1016/0006-8993(74)90229-7 (1974).
137 Kristensson, K. & Olsson, Y. Retrograde axonal transport of protein. *Brain research* **29**, 363-365, doi:10.1016/0006-8993(71)90044-8 (1971).
138 Reiner, A. *et al.* Pathway tracing using biotinylated dextran amines. *J Neurosci Methods* **103**, 23-37, doi:10.1016/s0165-0270(00)00293-4 (2000).
139 Veenman, C. L., Reiner, A. & Honig, M. G. Biotinylated dextran amine as an anterograde tracer for single- and double-labeling studies. *J Neurosci Methods* **41**, 239-254, doi:10.1016/0165-0270(92)90089-v (1992).

140 Aransay, A., Rodriguez-Lopez, C., Garcia-Amado, M., Clasca, F. & Prensa, L. Long-range projection neurons of the mouse ventral tegmental area: a single-cell axon tracing analysis. *Front Neuroanat* **9**, 59, doi:10.3389/fnana.2015.00059 (2015).
141 Coude, D., Parent, A. & Parent, M. Single-axon tracing of the corticosubthalamic hyperdirect pathway in primates. *Brain structure & function* **223**, 3959-3973, doi:10.1007/s00429-018-1726-x (2018).
142 Gerfen, C. R. & Sawchenko, P. E. An anterograde neuroanatomical tracing method that shows the detailed morphology of neurons, their axons and terminals: immunohistochemical localization of an axonally transported plant lectin, Phaseolus vulgaris leucoagglutinin (PHA-L). *Brain research* **290**, 219-238, doi:10.1016/0006-8993(84)90940-5 (1984).
143 Shink, E., Bevan, M. D., Bolam, J. P. & Smith, Y. The subthalamic nucleus and the external pallidum: two tightly interconnected structures that control the output of the basal ganglia in the monkey. *Neuroscience* **73**, 335-357, doi:10.1016/0306-4522(96)00022-x (1996).
144 Smith, Y., Bevan, M. D., Shink, E. & Bolam, J. P. Microcircuitry of the direct and indirect pathways of the basal ganglia. *Neuroscience* **86**, 353-387, doi:10.1016/s0306-4522(98)00004-9 (1998).
145 Gerfen, C. R. & Sawchenko, P. E. A method for anterograde axonal tracing of chemically specified circuits in the central nervous system: combined Phaseolus vulgaris-leucoagglutinin (PHA-L) tract tracing and immunohistochemistry. *Brain research* **343**, 144-150, doi:10.1016/0006-8993(85)91168-0 (1985).
146 Raju, D. V. & Smith, Y. Anterograde axonal tract tracing. *Current protocols in neuroscience* **Chapter 1**, Unit 1.14, doi:10.1002/0471142301.ns0114s37 (2006).
147 Pieribone, V. A., Aston-Jones, G. & Bohn, M. C. Adrenergic and non-adrenergic neurons in the C1 and C3 areas project to locus coeruleus: a fluorescent double labeling study. *Neuroscience letters* **85**, 297-303, doi:10.1016/0304-3940(88)90582-4 (1988).
148 Van Bockstaele, E. J., Wright, A. M., Cestari, D. M. & Pickel, V. M. Immunolabeling of retrogradely transported Fluoro-Gold: sensitivity and application to ultrastructural analysis of transmitter-specific mesolimbic circuitry. *J Neurosci Methods* **55**, 65-78, doi:10.1016/0165-0270(94)90042-6 (1994).
149 Wessendorf, M. W. Fluoro-Gold: composition, and mechanism of uptake. *Brain research* **553**, 135-148, doi:10.1016/0006-8993(91)90241-m (1991).
150 Yoshida, J., Polley, E. H., Nyhus, L. M. & Donahue, P. E. Labeling of nerve cells in the dorsal motor nucleus of the vagus of rats by retrograde transport of Fluoro-Gold. *Brain research* **455**, 1-8, doi:10.1016/0006-8993(88)90106-0 (1988).
151 Naumann, T., Peterson, G. M. & Frotscher, M. Fine structure of rat septohippocampal neurons: II. A time course analysis following axotomy. *The Journal of comparative neurology* **325**, 219-242, doi:10.1002/cne.903250207 (1992).
152 Katz, L. C., Burkhalter, A. & Dreyer, W. J. Fluorescent latex microspheres as a retrograde neuronal marker for in vivo and in vitro studies of visual cortex. *Nature* **310**, 498-500, doi:10.1038/310498a0 (1984).
153 Schofield, B. R. Retrograde axonal tracing with fluorescent markers. *Current protocols in neuroscience* **Chapter 1**, Unit 1.17, doi:10.1002/0471142301.ns0117s43 (2008).
154 Ramoa, A. S., Campbell, G. & Shatz, C. J. Transient morphological features of identified ganglion cells in living fetal and neonatal retina. *Science (New York, N.Y.)* **237**, 522-525, doi:10.1126/science.3603038 (1987).
155 Voigt, T., LeVay, S. & Stamnes, M. A. Morphological and immunocytochemical observations on the visual callosal projections in the cat. *The Journal of comparative neurology* **272**, 450-460, doi:10.1002/cne.902720312 (1988).

156 Huettner, J. E. & Baughman, R. W. Primary culture of identified neurons from the visual cortex of postnatal rats. *The Journal of neuroscience : the official journal of the Society for Neuroscience* **6**, 3044-3060 (1986).
157 Coulombe, J. N. & Bronner-Fraser, M. Cholinergic neurones acquire adrenergic neurotransmitters when transplanted into an embryo. *Nature* **324**, 569-572, doi:10.1038/324569a0 (1986).
158 Britto, L. R., Keyser, K. T., Hamassaki, D. E. & Karten, H. J. Catecholaminergic subpopulation of retinal displaced ganglion cells projects to the accessory optic nucleus in the pigeon (Columba livia). *The Journal of comparative neurology* **269**, 109-117, doi:10.1002/cne.902690109 (1988).
159 Buhl, E. H., Schwerdtfeger, W. K., Germroth, P. & Singer, W. Combining retrograde tracing, intracellular injection, anterograde degeneration and electron microscopy to reveal synaptic links. *J Neurosci Methods* **29**, 241-250, doi:10.1016/0165-0270(89)90148-9 (1989).
160 Katz, L. C. & Iarovici, D. M. Green fluorescent latex microspheres: a new retrograde tracer. *Neuroscience* **34**, 511-520, doi:10.1016/0306-4522(90)90159-2 (1990).
161 Luppi, P. H., Fort, P. & Jouvet, M. Iontophoretic application of unconjugated cholera toxin B subunit (CTb) combined with immunohistochemistry of neurochemical substances: a method for transmitter identification of retrogradely labeled neurons. *Brain research* **534**, 209-224, doi:10.1016/0006-8993(90)90131-t (1990).
162 Zin-Ka-Ieu, S., Roger, M. & Arnault, P. Direct contacts between fibers from the ventrolateral thalamic nucleus and frontal cortical neurons projecting to the striatum: a light-microscopy study in the rat. *Anatomy and embryology* **197**, 77-87, doi:10.1007/s004290050121 (1998).
163 Llewellyn-Smith, I. J., Martin, C. L., Arnolda, L. F. & Minson, J. B. Tracer-toxins: cholera toxin B-saporin as a model. *J Neurosci Methods* **103**, 83-90, doi:10.1016/s0165-0270(00)00298-3 (2000).
164 Krout, K. E., Belzer, R. E. & Loewy, A. D. Brainstem projections to midline and intralaminar thalamic nuclei of the rat. *The Journal of comparative neurology* **448**, 53-101, doi:10.1002/cne.10236 (2002).
165 Schofield, C. L., Field, R. A. & Russell, D. A. Glyconanoparticles for the colorimetric detection of cholera toxin. *Analytical chemistry* **79**, 1356-1361, doi:10.1021/ac061462j (2007).
166 Panchuk-Voloshina, N. *et al.* Alexa dyes, a series of new fluorescent dyes that yield exceptionally bright, photostable conjugates. *The journal of histochemistry and cytochemistry : official journal of the Histochemistry Society* **47**, 1179-1188, doi:10.1177/002215549904700910 (1999).
167 Conte, W. L., Kamishina, H. & Reep, R. L. Multiple neuroanatomical tract-tracing using fluorescent Alexa Fluor conjugates of cholera toxin subunit B in rats. *Nature protocols* **4**, 1157-1166, doi:10.1038/nprot.2009.93 (2009).
168 Gerfen, C. R. & Sawchenko, P. E. An anterograde neuroanatomical tracing method that shows the detailed morphology of neurons, their axons and terminals: Immunohistochemical localization of an axonally transported plant lectin, Phaseolus vulgaris-leucoagglutinin (PHA-L). *Brain research* **1645**, 42-45, doi:10.1016/j.brainres.2015.12.040 (2016).
169 Schwab, M. E., Javoy-Agid, F. & Agid, Y. Labeled wheat germ agglutinin (WGA) as a new, highly sensitive retrograde tracer in the rat brain hippocampal system. *Brain research* **152**, 145-150, doi:10.1016/0006-8993(78)90140-3 (1978).
170 Schmued, L. C. & Fallon, J. H. Fluoro-Gold: a new fluorescent retrograde axonal tracer with numerous unique properties. *Brain research* **377**, 147-154, doi:10.1016/0006-8993(86)91199-6 (1986).
171 Stoeckel, K., Schwab, M. & Thoenen, H. Role of gangliosides in the uptake and retrograde axonal transport of cholera and tetanus toxin as compared to nerve growth factor and

wheat germ agglutinin. *Brain research* **132**, 273-285, doi:10.1016/0006-8993(77)90421-8 (1977).

172 Gerfen, C. R., Paletzki, R. & Heintz, N. GENSAT BAC cre-recombinase driver lines to study the functional organization of cerebral cortical and basal ganglia circuits. *Neuron* **80**, 1368-1383, doi:10.1016/j.neuron.2013.10.016 (2013).

173 Castle, M. J., Gershenson, Z. T., Giles, A. R., Holzbaur, E. L. & Wolfe, J. H. Adeno-associated virus serotypes 1, 8, and 9 share conserved mechanisms for anterograde and retrograde axonal transport. *Human gene therapy* **25**, 705-720, doi:10.1089/hum.2013.189 (2014).

174 Castle, M. J., Perlson, E., Holzbaur, E. L. & Wolfe, J. H. Long-distance axonal transport of AAV9 is driven by dynein and kinesin-2 and is trafficked in a highly motile Rab7-positive compartment. *Molecular therapy : the journal of the American Society of Gene Therapy* **22**, 554-566, doi:10.1038/mt.2013.237 (2014).

175 Zingg, B. *et al.* AAV-Mediated Anterograde Transsynaptic Tagging: Mapping Corticocollicular Input-Defined Neural Pathways for Defense Behaviors. *Neuron* **93**, 33-47, doi:10.1016/j.neuron.2016.11.045 (2017).

176 Wu, Z., Asokan, A. & Samulski, R. J. Adeno-associated virus serotypes: vector toolkit for human gene therapy. *Molecular therapy : the journal of the American Society of Gene Therapy* **14**, 316-327, doi:10.1016/j.ymthe.2006.05.009 (2006).

177 Kaplitt, M. G. *et al.* Safety and tolerability of gene therapy with an adeno-associated virus (AAV) borne GAD gene for Parkinson's disease: an open label, phase I trial. *Lancet (London, England)* **369**, 2097-2105, doi:10.1016/s0140-6736(07)60982-9 (2007).

178 Ojala, D. S., Amara, D. P. & Schaffer, D. V. Adeno-associated virus vectors and neurological gene therapy. *The Neuroscientist : a review journal bringing neurobiology, neurology and psychiatry* **21**, 84-98, doi:10.1177/1073858414521870 (2015).

179 Murlidharan, G., Samulski, R. J. & Asokan, A. Biology of adeno-associated viral vectors in the central nervous system. *Frontiers in molecular neuroscience* **7**, 76, doi:10.3389/fnmol.2014.00076 (2014).

180 Tervo, D. G. *et al.* A Designer AAV Variant Permits Efficient Retrograde Access to Projection Neurons. *Neuron* **92**, 372-382, doi:10.1016/j.neuron.2016.09.021 (2016).

181 Kremer, E. J., Boutin, S., Chillon, M. & Danos, O. Canine adenovirus vectors: an alternative for adenovirus-mediated gene transfer. *Journal of virology* **74**, 505-512, doi:10.1128/jvi.74.1.505-512.2000 (2000).

182 Soudais, C., Laplace-Builhe, C., Kissa, K. & Kremer, E. J. Preferential transduction of neurons by canine adenovirus vectors and their efficient retrograde transport in vivo. *FASEB journal : official publication of the Federation of American Societies for Experimental Biology* **15**, 2283-2285, doi:10.1096/fj.01-0321fje (2001).

183 Soudais, C., Skander, N. & Kremer, E. J. Long-term in vivo transduction of neurons throughout the rat CNS using novel helper-dependent CAV-2 vectors. *FASEB journal : official publication of the Federation of American Societies for Experimental Biology* **18**, 391-393, doi:10.1096/fj.03-0438fje (2004).

184 Schwarz, L. A. *et al.* Viral-genetic tracing of the input-output organization of a central noradrenaline circuit. *Nature* **524**, 88-92, doi:10.1038/nature14600 (2015).

185 Finke, S. & Conzelmann, K. K. Replication strategies of rabies virus. *Virus research* **111**, 120-131, doi:10.1016/j.virusres.2005.04.004 (2005).

186 Klingen, Y., Conzelmann, K. K. & Finke, S. Double-labeled rabies virus: live tracking of enveloped virus transport. *Journal of virology* **82**, 237-245, doi:10.1128/jvi.01342-07 (2008).

187 Ugolini, G. Specificity of rabies virus as a transneuronal tracer of motor networks: transfer from hypoglossal motoneurons to connected second-order and higher order central nervous system cell groups. *The Journal of comparative neurology* **356**, 457-480, doi:10.1002/cne.903560312 (1995).

188 Wickersham, I. R. *et al.* Monosynaptic restriction of transsynaptic tracing from single, genetically targeted neurons. *Neuron* **53**, 639-647, doi:10.1016/j.neuron.2007.01.033 (2007).
189 Wickersham, I. R., Finke, S., Conzelmann, K. K. & Callaway, E. M. Retrograde neuronal tracing with a deletion-mutant rabies virus. *Nature methods* **4**, 47-49, doi:10.1038/nmeth999 (2007).
190 Callaway, E. M. Transneuronal circuit tracing with neurotropic viruses. *Current opinion in neurobiology* **18**, 617-623, doi:10.1016/j.conb.2009.03.007 (2008).
191 Wall, N. R., Wickersham, I. R., Cetin, A., De La Parra, M. & Callaway, E. M. Monosynaptic circuit tracing in vivo through Cre-dependent targeting and complementation of modified rabies virus. *Proceedings of the National Academy of Sciences of the United States of America* **107**, 21848-21853, doi:10.1073/pnas.1011756107 (2010).
192 Mebatsion, T., Konig, M. & Conzelmann, K. K. Budding of rabies virus particles in the absence of the spike glycoprotein. *Cell* **84**, 941-951, doi:10.1016/s0092-8674(00)81072-7 (1996).
193 Young, J. A., Bates, P. & Varmus, H. E. Isolation of a chicken gene that confers susceptibility to infection by subgroup A avian leukosis and sarcoma viruses. *Journal of virology* **67**, 1811-1816 (1993).
194 Federspiel, M. J., Bates, P., Young, J. A., Varmus, H. E. & Hughes, S. H. A system for tissue-specific gene targeting: transgenic mice susceptible to subgroup A avian leukosis virus-based retroviral vectors. *Proceedings of the National Academy of Sciences of the United States of America* **91**, 11241-11245, doi:10.1073/pnas.91.23.11241 (1994).
195 Marshel, J. H., Mori, T., Nielsen, K. J. & Callaway, E. M. Targeting single neuronal networks for gene expression and cell labeling in vivo. *Neuron* **67**, 562-574, doi:10.1016/j.neuron.2010.08.001 (2010).
196 Hagendorf, N. & Conzelmann, K. K. Recombinant Fluorescent Rabies Virus Vectors for Tracing Neurons and Synaptic Connections. *Cold Spring Harbor protocols* **2015**, pdb.top089391, doi:10.1101/pdb.top089391 (2015).
197 Dodt, H. U. *et al.* Ultramicroscopy: three-dimensional visualization of neuronal networks in the whole mouse brain. *Nature methods* **4**, 331-336, doi:10.1038/nmeth1036 (2007).
198 Erturk, A. *et al.* Three-dimensional imaging of solvent-cleared organs using 3DISCO. *Nature protocols* **7**, 1983-1995, doi:10.1038/nprot.2012.119 (2012).
199 Becker, K., Jahrling, N., Saghafi, S., Weiler, R. & Dodt, H. U. Chemical clearing and dehydration of GFP expressing mouse brains. *PloS one* **7**, e33916, doi:10.1371/journal.pone.0033916 (2012).
200 Renier, N. *et al.* iDISCO: a simple, rapid method to immunolabel large tissue samples for volume imaging. *Cell* **159**, 896-910, doi:10.1016/j.cell.2014.10.010 (2014).
201 Pan, C. *et al.* Shrinkage-mediated imaging of entire organs and organisms using uDISCO. *Nature methods* **13**, 859-867, doi:10.1038/nmeth.3964 (2016).
202 Qi, Y. *et al.* FDISCO: Advanced solvent-based clearing method for imaging whole organs. *Science advances* **5**, eaau8355, doi:10.1126/sciadv.aau8355 (2019).
203 Ke, M. T., Fujimoto, S. & Imai, T. SeeDB: a simple and morphology-preserving optical clearing agent for neuronal circuit reconstruction. *Nature neuroscience* **16**, 1154-1161, doi:10.1038/nn.3447 (2013).
204 Kuwajima, T. *et al.* ClearT: a detergent- and solvent-free clearing method for neuronal and non-neuronal tissue. *Development (Cambridge, England)* **140**, 1364-1368, doi:10.1242/dev.091844 (2013).
205 Hama, H. *et al.* Scale: a chemical approach for fluorescence imaging and reconstruction of transparent mouse brain. *Nature neuroscience* **14**, 1481-1488, doi:10.1038/nn.2928 (2011).
206 Susaki, E. A. *et al.* Whole-brain imaging with single-cell resolution using chemical cocktails and computational analysis. *Cell* **157**, 726-739, doi:10.1016/j.cell.2014.03.042 (2014).

207 Tainaka, K. *et al.* Whole-body imaging with single-cell resolution by tissue decolorization. *Cell* **159**, 911-924, doi:10.1016/j.cell.2014.10.034 (2014).
208 Susaki, E. A. *et al.* Advanced CUBIC protocols for whole-brain and whole-body clearing and imaging. *Nature protocols* **10**, 1709-1727, doi:10.1038/nprot.2015.085 (2015).
209 Tomer, R., Ye, L., Hsueh, B. & Deisseroth, K. Advanced CLARITY for rapid and high-resolution imaging of intact tissues. *Nature protocols* **9**, 1682-1697, doi:10.1038/nprot.2014.123 (2014).
210 Chung, K. *et al.* Structural and molecular interrogation of intact biological systems. *Nature* **497**, 332-337, doi:10.1038/nature12107 (2013).
211 Treweek, J. B. *et al.* Whole-body tissue stabilization and selective extractions via tissue-hydrogel hybrids for high-resolution intact circuit mapping and phenotyping. *Nature protocols* **10**, 1860-1896, doi:10.1038/nprot.2015.122 (2015).
212 Yang, B. *et al.* Single-cell phenotyping within transparent intact tissue through whole-body clearing. *Cell* **158**, 945-958, doi:10.1016/j.cell.2014.07.017 (2014).
213 Yu, T. *et al.* Elevated-temperature-induced acceleration of PACT clearing process of mouse brain tissue. *Scientific reports* **7**, 38848, doi:10.1038/srep38848 (2017).
214 Murray, E. *et al.* Simple, Scalable Proteomic Imaging for High-Dimensional Profiling of Intact Systems. *Cell* **163**, 1500-1514, doi:10.1016/j.cell.2015.11.025 (2015).
215 Wan, P. *et al.* Evaluation of seven optical clearing methods in mouse brain. *Neurophotonics* **5**, 035007, doi:10.1117/1.NPh.5.3.035007 (2018).
216 Davis, M., Walker, D. L., Miles, L. & Grillon, C. Phasic vs sustained fear in rats and humans: role of the extended amygdala in fear vs anxiety. *Neuropsychopharmacology : official publication of the American College of Neuropsychopharmacology* **35**, 105-135, doi:10.1038/npp.2009.109 (2010).
217 Phelps, E. A. Emotion and cognition: insights from studies of the human amygdala. *Annual review of psychology* **57**, 27-53, doi:10.1146/annurev.psych.56.091103.070234 (2006).
218 Choi, D. C. *et al.* Prelimbic cortical BDNF is required for memory of learned fear but not extinction or innate fear. *Proceedings of the National Academy of Sciences of the United States of America* **107**, 2675-2680, doi:10.1073/pnas.0909359107 (2010).
219 Sotres-Bayon, F. & Quirk, G. J. Prefrontal control of fear: more than just extinction. *Current opinion in neurobiology* **20**, 231-235, doi:10.1016/j.conb.2010.02.005 (2010).
220 Milad, M. R. & Quirk, G. J. Neurons in medial prefrontal cortex signal memory for fear extinction. *Nature* **420**, 70-74, doi:10.1038/nature01138 (2002).
221 Dias, B. G., Banerjee, S. B., Goodman, J. V. & Ressler, K. J. Towards new approaches to disorders of fear and anxiety. *Current opinion in neurobiology* **23**, 346-352, doi:10.1016/j.conb.2013.01.013 (2013).
222 Alheid, G. F. *et al.* The neuronal organization of the supracapsular part of the stria terminalis in the rat: the dorsal component of the extended amygdala. *Neuroscience* **84**, 967-996, doi:10.1016/s0306-4522(97)00560-5 (1998).
223 Lebow, M. A. & Chen, A. Overshadowed by the amygdala: the bed nucleus of the stria terminalis emerges as key to psychiatric disorders. *Molecular psychiatry* **21**, 450-463, doi:10.1038/mp.2016.1 (2016).
224 Ciocchi, S. *et al.* Encoding of conditioned fear in central amygdala inhibitory circuits. *Nature* **468**, 277-282, doi:10.1038/nature09559 (2010).
225 Gungor, N. Z., Yamamoto, R. & Pare, D. Optogenetic study of the projections from the bed nucleus of the stria terminalis to the central amygdala. *Journal of neurophysiology* **114**, 2903-2911, doi:10.1152/jn.00677.2015 (2015).
226 Sanford, C. A. *et al.* A Central Amygdala CRF Circuit Facilitates Learning about Weak Threats. *Neuron* **93**, 164-178, doi:10.1016/j.neuron.2016.11.034 (2017).
227 Jolkkonen, E. & Pitkanen, A. Intrinsic connections of the rat amygdaloid complex: projections originating in the central nucleus. *The Journal of comparative neurology* **395**, 53-72 (1998).

228 Day, H. E., Curran, E. J., Watson, S. J., Jr. & Akil, H. Distinct neurochemical populations in the rat central nucleus of the amygdala and bed nucleus of the stria terminalis: evidence for their selective activation by interleukin-1beta. *The Journal of comparative neurology* **413**, 113-128 (1999).
229 Kang-Park, M., Kieffer, B. L., Roberts, A. J., Siggins, G. R. & Moore, S. D. Interaction of CRF and kappa opioid systems on GABAergic neurotransmission in the mouse central amygdala. *The Journal of pharmacology and experimental therapeutics* **355**, 206-211, doi:10.1124/jpet.115.225870 (2015).
230 Cai, H., Haubensak, W., Anthony, T. E. & Anderson, D. J. Central amygdala PKC-delta(+) neurons mediate the influence of multiple anorexigenic signals. *Nature neuroscience* **17**, 1240-1248, doi:10.1038/nn.3767 (2014).
231 Janak, P. H. & Tye, K. M. From circuits to behaviour in the amygdala. *Nature* **517**, 284-292, doi:10.1038/nature14188 (2015).
232 Pego, J. M. *et al.* Dissociation of the morphological correlates of stress-induced anxiety and fear. *The European journal of neuroscience* **27**, 1503-1516, doi:10.1111/j.1460-9568.2008.06112.x (2008).
233 Ventura-Silva, A. P. *et al.* Stress shifts the response of the bed nucleus of the stria terminalis to an anxiogenic mode. *The European journal of neuroscience* **36**, 3396-3406, doi:10.1111/j.1460-9568.2012.08262.x (2012).
234 Mazzone, C. M. *et al.* Acute engagement of Gq-mediated signaling in the bed nucleus of the stria terminalis induces anxiety-like behavior. *Molecular psychiatry* **23**, 143-153, doi:10.1038/mp.2016.218 (2018).
235 Ventura-Silva, A. P., Borges, S., Sousa, N., Rodrigues, A. J. & Pego, J. M. Amygdalar corticotropin-releasing factor mediates stress-induced anxiety. *Brain research* **1729**, 146622, doi:10.1016/j.brainres.2019.146622 (2020).
236 Pomrenze, M. B. *et al.* A Corticotropin Releasing Factor Network in the Extended Amygdala for Anxiety. *The Journal of neuroscience : the official journal of the Society for Neuroscience* **39**, 1030-1043, doi:10.1523/jneurosci.2143-18.2018 (2019).
237 Asok, A. *et al.* Optogenetic silencing of a corticotropin-releasing factor pathway from the central amygdala to the bed nucleus of the stria terminalis disrupts sustained fear. *Molecular psychiatry* **23**, 914-922, doi:10.1038/mp.2017.79 (2018).
238 Kim, S. Y. *et al.* Diverging neural pathways assemble a behavioural state from separable features in anxiety. *Nature* **496**, 219-223, doi:10.1038/nature12018 (2013).
239 Jennings, J. H. *et al.* Distinct extended amygdala circuits for divergent motivational states. *Nature* **496**, 224-228, doi:10.1038/nature12041 (2013).
240 Dong, H. W., Petrovich, G. D., Watts, A. G. & Swanson, L. W. Basic organization of projections from the oval and fusiform nuclei of the bed nuclei of the stria terminalis in adult rat brain. *The Journal of comparative neurology* **436**, 430-455 (2001).
241 Dong, H. W. & Swanson, L. W. Projections from bed nuclei of the stria terminalis, posterior division: implications for cerebral hemisphere regulation of defensive and reproductive behaviors. *The Journal of comparative neurology* **471**, 396-433, doi:10.1002/cne.20002 (2004).
242 Sun, N. & Cassell, M. D. Intrinsic GABAergic neurons in the rat central extended amygdala. *The Journal of comparative neurology* **330**, 381-404, doi:10.1002/cne.903300308 (1993).
243 Dedic, N. *et al.* Chronic CRH depletion from GABAergic, long-range projection neurons in the extended amygdala reduces dopamine release and increases anxiety. *Nature neuroscience* **21**, 803-807, doi:10.1038/s41593-018-0151-z (2018).
244 Füzesi, T., Daviu, N., Wamsteeker Cusulin, J. I., Bonin, R. P. & Bains, J. S. Hypothalamic CRH neurons orchestrate complex behaviours after stress. *Nature communications* **7**, 11937, doi:10.1038/ncomms11937 (2016).

245 Anderson, D. J. & Adolphs, R. A framework for studying emotions across species. *Cell* **157**, 187-200, doi:10.1016/j.cell.2014.03.003 (2014).
246 Chrousos, G. P. Regulation and dysregulation of the hypothalamic-pituitary-adrenal axis. The corticotropin-releasing hormone perspective. *Endocrinol Metab Clin North Am* **21**, 833-858 (1992).
247 McEwen, B. S. & Stellar, E. Stress and the individual. Mechanisms leading to disease. *Arch Intern Med* **153**, 2093-2101 (1993).
248 Madisen, L. *et al.* A robust and high-throughput Cre reporting and characterization system for the whole mouse brain. *Nature neuroscience* **13**, 133-140, doi:10.1038/nn.2467 (2010).
249 Mo, A. *et al.* Epigenomic Signatures of Neuronal Diversity in the Mammalian Brain. *Neuron* **86**, 1369-1384, doi:10.1016/j.neuron.2015.05.018 (2015).
250 Refojo, D. *et al.* Glutamatergic and dopaminergic neurons mediate anxiogenic and anxiolytic effects of CRHR1. *Science (New York, N.Y.)* **333**, 1903-1907, doi:10.1126/science.1202107 (2011).
251 Hippenmeyer, S. *et al.* A developmental switch in the response of DRG neurons to ETS transcription factor signaling. *PLoS Biol* **3**, e159, doi:10.1371/journal.pbio.0030159 (2005).
252 Engblom, D. *et al.* Glutamate receptors on dopamine neurons control the persistence of cocaine seeking. *Neuron* **59**, 497-508, doi:10.1016/j.neuron.2008.07.010 (2008).
253 Spierling, S. R. & Zorrilla, E. P. Don't stress about CRF: assessing the translational failures of CRF1antagonists. *Psychopharmacology* **234**, 1467-1481, doi:10.1007/s00213-017-4556-2 (2017).
254 Deussing, J. M. & Chen, A. The Corticotropin-Releasing Factor Family: Physiology of the Stress Response. *Physiological reviews* **98**, 2225-2286, doi:10.1152/physrev.00042.2017 (2018).
255 Tiklová, K. *et al.* Single-cell RNA sequencing reveals midbrain dopamine neuron diversity emerging during mouse brain development. *Nature communications* **10**, 581, doi:10.1038/s41467-019-08453-1 (2019).
256 La Manno, G. *et al.* Molecular Diversity of Midbrain Development in Mouse, Human, and Stem Cells. *Cell* **167**, 566-580.e519, doi:10.1016/j.cell.2016.09.027 (2016).
257 Poulin, J. F., Gaertner, Z., Moreno-Ramos, O. A. & Awatramani, R. Classification of Midbrain Dopamine Neurons Using Single-Cell Gene Expression Profiling Approaches. *Trends in neurosciences* **43**, 155-169, doi:10.1016/j.tins.2020.01.004 (2020).
258 Korotkova, T. M., Ponomarenko, A. A., Brown, R. E. & Haas, H. L. Functional diversity of ventral midbrain dopamine and GABAergic neurons. *Molecular neurobiology* **29**, 243-259, doi:10.1385/mn:29:3:243 (2004).
259 Pignatelli, M. & Bonci, A. Spiraling Connectivity of NAc-VTA Circuitry. *Neuron* **97**, 261-262, doi:10.1016/j.neuron.2017.12.046 (2018).
260 Omelchenko, N. & Sesack, S. R. Periaqueductal gray afferents synapse onto dopamine and GABA neurons in the rat ventral tegmental area. *Journal of neuroscience research* **88**, 981-991, doi:10.1002/jnr.22265 (2010).
261 Sartor, G. C. & Aston-Jones, G. Regulation of the ventral tegmental area by the bed nucleus of the stria terminalis is required for expression of cocaine preference. *The European journal of neuroscience* **36**, 3549-3558, doi:10.1111/j.1460-9568.2012.08277.x (2012).
262 Stamatakis, A. M. *et al.* Amygdala and bed nucleus of the stria terminalis circuitry: Implications for addiction-related behaviors. *Neuropharmacology* **76 Pt B**, 320-328, doi:10.1016/j.neuropharm.2013.05.046 (2014).
263 Cha, J. *et al.* Hyper-reactive human ventral tegmental area and aberrant mesocorticolimbic connectivity in overgeneralization of fear in generalized anxiety disorder. *The Journal of neuroscience : the official journal of the Society for Neuroscience* **34**, 5855-5860, doi:10.1523/jneurosci.4868-13.2014 (2014).

264 Small, K. M., Nunes, E., Hughley, S. & Addy, N. A. Ventral tegmental area muscarinic receptors modulate depression and anxiety-related behaviors in rats. *Neuroscience letters* **616**, 80-85, doi:10.1016/j.neulet.2016.01.057 (2016).
265 Fearnley, J. M. & Lees, A. J. Ageing and Parkinson's disease: substantia nigra regional selectivity. *Brain : a journal of neurology* **114 (Pt 5)**, 2283-2301, doi:10.1093/brain/114.5.2283 (1991).
266 Becker, G., Seufert, J., Bogdahn, U., Reichmann, H. & Reiners, K. Degeneration of substantia nigra in chronic Parkinson's disease visualized by transcranial color-coded real-time sonography. *Neurology* **45**, 182-184, doi:10.1212/wnl.45.1.182 (1995).
267 Gibb, W. R. & Lees, A. J. Anatomy, pigmentation, ventral and dorsal subpopulations of the substantia nigra, and differential cell death in Parkinson's disease. *Journal of neurology, neurosurgery, and psychiatry* **54**, 388-396, doi:10.1136/jnnp.54.5.388 (1991).
268 Triarhou, L. C., Norton, J. & Ghetti, B. Synaptic connectivity of tyrosine hydroxylase immunoreactive nerve terminals in the striatum of normal, heterozygous and homozygous weaver mutant mice. *Journal of neurocytology* **17**, 221-232, doi:10.1007/bf01674209 (1988).
269 Ibáñez-Sandoval, O. *et al.* Electrophysiological and Morphological Characteristics and Synaptic Connectivity of Tyrosine Hydroxylase-Expressing Neurons in Adult Mouse Striatum. *The Journal of Neuroscience* **30**, 6999-7016, doi:10.1523/jneurosci.5996-09.2010 (2010).
270 Wictorin, K. Anatomy and connectivity of intrastriatal striatal transplants. *Progress in neurobiology* **38**, 611-639, doi:10.1016/0301-0082(92)90044-f (1992).
271 Galiñanes, G. L., Taravini, I. R. E. & Gustavo Murer, M. Dopamine-Dependent Periadolescent Maturation of Corticostriatal Functional Connectivity in Mouse. *The Journal of Neuroscience* **29**, 2496-2509, doi:10.1523/jneurosci.4421-08.2009 (2009).
272 Alheid, G. F., Shammah-Lagnado, S. J. & Beltramino, C. A. The interstitial nucleus of the posterior limb of the anterior commissure: a novel layer of the central division of extended amygdala. *Annals of the New York Academy of Sciences* **877**, 645-654, doi:10.1111/j.1749-6632.1999.tb09294.x (1999).
273 Shammah-Lagnado, S. J., Alheid, G. F. & Heimer, L. Striatal and central extended amygdala parts of the interstitial nucleus of the posterior limb of the anterior commissure: evidence from tract-tracing techniques in the rat. *The Journal of comparative neurology* **439**, 104-126, doi:10.1002/cne.1999 (2001).
274 Li, S. & Kirouac, G. J. Projections from the paraventricular nucleus of the thalamus to the forebrain, with special emphasis on the extended amygdala. *The Journal of comparative neurology* **506**, 263-287, doi:10.1002/cne.21502 (2008).
275 Otake, K. & Nakamura, Y. Possible pathways through which neurons of the shell of the nucleus accumbens influence the outflow of the core of the nucleus accumbens. *Brain Dev* **22 Suppl 1**, S17-26, doi:10.1016/s0387-7604(00)00142-x (2000).
276 Hasue, R. H. & Shammah-Lagnado, S. J. Origin of the dopaminergic innervation of the central extended amygdala and accumbens shell: a combined retrograde tracing and immunohistochemical study in the rat. *The Journal of comparative neurology* **454**, 15-33, doi:10.1002/cne.10420 (2002).
277 Ogawa, S. K., Cohen, J. Y., Hwang, D., Uchida, N. & Watabe-Uchida, M. Organization of monosynaptic inputs to the serotonin and dopamine neuromodulatory systems. *Cell reports* **8**, 1105-1118, doi:10.1016/j.celrep.2014.06.042 (2014).
278 Tanaka, D. H., Li, S., Mukae, S. & Tanabe, T. Genetic Access to Gustatory Disgust-Associated Neurons in the Interstitial Nucleus of the Posterior Limb of the Anterior Commissure in Male Mice. *Neuroscience* **413**, 45-63, doi:10.1016/j.neuroscience.2019.06.021 (2019).
279 Clements, S., Schreck, C. B., Larsen, D. A. & Dickhoff, W. W. Central administration of corticotropin-releasing hormone stimulates locomotor activity in juvenile chinook salmon (Oncorhynchus tshawytscha). *General and comparative endocrinology* **125**, 319-327, doi:10.1006/gcen.2001.7707 (2002).

280 Gutman, D. A., Owens, M. J., Thrivikraman, K. V. & Nemeroff, C. B. Persistent anxiolytic affects after chronic administration of the CRF_1 receptor antagonist R121919 in rats. *Neuropharmacology* **60**, 1135-1141, doi:10.1016/j.neuropharm.2010.10.004 (2011).
281 Farassat, N. *et al.* In vivo functional diversity of midbrain dopamine neurons within identified axonal projections. *eLife* **8**, doi:10.7554/eLife.48408 (2019).
282 Rizzi, G. & Tan, K. R. Synergistic Nigral Output Pathways Shape Movement. *Cell reports* **27**, 2184-2198.e2184, doi:10.1016/j.celrep.2019.04.068 (2019).
283 Hunt, A. J. *et al.* Paraventricular hypothalamic and amygdalar CRF neurons synapse in the external globus pallidus. *Brain Structure and Function* **223**, 2685-2698, doi:10.1007/s00429-018-1652-y (2018).
284 Hong, S. & Hikosaka, O. The globus pallidus sends reward-related signals to the lateral habenula. *Neuron* **60**, 720-729, doi:10.1016/j.neuron.2008.09.035 (2008).
285 Smith, K. S., Tindell, A. J., Aldridge, J. W. & Berridge, K. C. Ventral pallidum roles in reward and motivation. *Behavioural brain research* **196**, 155-167, doi:10.1016/j.bbr.2008.09.038 (2009).
286 Wickens, J. Toward an anatomy of disappointment: reward-related signals from the globus pallidus. *Neuron* **60**, 530-531, doi:10.1016/j.neuron.2008.11.002 (2008).
287 Parker, J. G. *et al.* Attenuating GABA(A) receptor signaling in dopamine neurons selectively enhances reward learning and alters risk preference in mice. *The Journal of neuroscience : the official journal of the Society for Neuroscience* **31**, 17103-17112, doi:10.1523/jneurosci.1715-11.2011 (2011).
288 Pamukcu, A. *et al.* Parvalbumin(+) and Npas1(+) Pallidal Neurons Have Distinct Circuit Topology and Function. *The Journal of neuroscience : the official journal of the Society for Neuroscience* **40**, 7855-7876, doi:10.1523/jneurosci.0361-20.2020 (2020).
289 Hunt, A. J., Jr. *et al.* Paraventricular hypothalamic and amygdalar CRF neurons synapse in the external globus pallidus. *Brain Struct Funct* **223**, 2685-2698, doi:10.1007/s00429-018-1652-y (2018).
290 McCall, J. G. *et al.* CRH Engagement of the Locus Coeruleus Noradrenergic System Mediates Stress-Induced Anxiety. *Neuron* **87**, 605-620, doi:10.1016/j.neuron.2015.07.002 (2015).
291 Prakash, N. *et al.* Serotonergic Plasticity in the Dorsal Raphe Nucleus Characterizes Susceptibility and Resilience to Anhedonia. *The Journal of neuroscience : the official journal of the Society for Neuroscience* **40**, 569-584, doi:10.1523/jneurosci.1802-19.2019 (2020).
292 Birnie, M. T. *et al.* Plasticity of the Reward Circuitry After Early-Life Adversity: Mechanisms and Significance. *Biological psychiatry* **87**, 875-884, doi:10.1016/j.biopsych.2019.12.018 (2020).
293 Gunn, B. G. *et al.* The Endogenous Stress Hormone CRH Modulates Excitatory Transmission and Network Physiology in Hippocampus. *Cerebral cortex (New York, N.Y. : 1991)* **27**, 4182-4198, doi:10.1093/cercor/bhx103 (2017).
294 Williams, C. L., Buchta, W. C. & Riegel, A. C. CRF-R2 and the heterosynaptic regulation of VTA glutamate during reinstatement of cocaine seeking. *The Journal of neuroscience : the official journal of the Society for Neuroscience* **34**, 10402-10414, doi:10.1523/jneurosci.0911-13.2014 (2014).

6. Supplements

6.1 Curriculum Vitae

SIMON CHANG

EDUCATION

PhD STUDENT IN GRADUATE SCHOOL OF SYSTEMIC NEUROSCIENCES SEP 2016 - PRESENT

Department of stress Neurobiology and Neurogenetics
Max Planck Institute of Psychiatry, Munich, Germany

- Research interest in CRH system, neurogenetics and stress related disorders

MASTER OF SCIENCES (M.Sc.) SEP 2014 - JAN 2016

Graduate Institute of Biomedical Sciences Division of Physiology and Pharmacology
Chang Gung University, Taoyuan, Taiwan

- Research interests in stress related disorders and neurogenetics

BACHELOR OF SCIENCES (B.Sc.) JUN 2012 - JUN 2014

Department of Biomedical Sciences
Chang Gung University, Taoyuan, Taiwan

- Intern student and research assistant in Functional Neuroscience Lab

RESEARCH EXPERIENCE

PhD student in Graduate school of Systemic Neurosciences
September 2016 — present
Department of stress Neurobiology and Neurogenetics, Max Planck Institute of Psychiatry, Munich, Germany

- **Working on the project "Characterization of CRH/ CRH receptors neurocircuitries and their relationship with stress" (advised by Dr. Jan Deussing)**
  - Designing and performing of experiments
  - Mapping of CRH/ CRH neurocircuitries
  - Involved in the genetic analysis and pathway finding
  - In charge of data analysing and explaining

Master's student and Research Assistant, Functional Neuroscience Lab September 2014 — January 2016
Graduate Institute of Biomedical Sciences Division of Physiology and Pharmacology, Chang Gung University

- **Working on the project "Neuropsin inactivation has protective effects on depressive-like behaviours and memory impairments induced by chronic stress" (advised by Dr. Guo-Jen Huang)**
  - Designing and performing of experiments; project leader
  - Designed a set of chronic stress models
  - Involved in the genetic analysis and pathway finding
  - In charge of data analysing and explaining

- **International collaboration in the project "Molecular signatures of major depression" with Dr. Jonathan Flint (Welcome Trust Human Genetic Centre, University of Oxford, UK)**
  - Performer and designer of animal experiments as one of the main project leaders
  - Developed a new model of chronic repeated stress
  - Involved in data analysing of qPCR
  - Involved in sample preparation and data analysis of next generation sequencing

Intern student and Research Assistant, Functional Neuroscience Lab September 2012 — September 2014
Department of Biomedical Sciences, Chang Gung University

- **Investigating the role of neuropsin in PTSD** (advised by Dr. Guo-Jen Huang)
  - Designing and performing of experiments
  - Developed a PTSD animal model
  - Performed different types of animal behaviour tests (open field, elevated plus maze and water maze)
  - Involved in analysing and identifying differences between neuropsin wild type and knockout mice after experience of traumatic stress.
- **Investigating the role of *Cyp11a1* KO mice in stress** (advised by Dr. Guo-Jen Huang)
  - Team leader and advisor for two members (Ju Yu Tong and Sheng Yuan Hung)
  - Co-performer of the experiment
  - In charge of data analysis and explanation

SKILLS & TECHNIQUES

Languages:
Fluent in English and Chinese (native)

Scientific techniques

- Different types of animal behaviour testing; including anxiety, learning/memory and motor function
- Histology and immunohistochemistry
- Genetic screening of mice
- Isolation of RNA and analysis by transcriptional profiling such as qPCR, *in situ* hybridization
- DNA extraction for next generation sequencing
- Statistical analysis and data explanation of animal behaviour tests and qPCR
- Basic analysis of sequencing data
- Animal surgery and viral vector packing

Other skills:
Very good in communicating with team members and cooperating with different research groups.

AWARDS & HONOURS

Best poster prize, 2019 FENS-Hertie winter school – awarded by Dr. Johannes Graeff and Dr. Dominique de Quervain

Mifek Kirschner young scientists award 2017 – awarded by Prof. Dr. Alon Chen, Max Planck Institute of Psychiatry, Munich, Germany

First place in poster presentation (oral) 2016 – awarded by Prof. Dr. Jin-Chung Chen, Graduate institute of Biomedical Sciences, Chang Gung University

Award of excellent in poster competition (oral) 2014 – awarded by Dr. Sze-Cheng Lo, Department of Biomedical Sciences, Chang Gung University

6.2 List of publications

Peer reviewed journal

Chang S*, Bok P*, Tsai CY, Sun CP, Liu H, Deussing JM, Huang GJ. NPTX2 is a key component in the regulation of anxiety. ***Neuropsychopharmacology*** 2018 Aug; 43(9):1943-1953. * First author

Dedic N, Kühne C, Jakovcevski M, Hartmann J, Genewsky AJ, Gomes KS, Anderzhanova E, Pöhlmann ML, **Chang S**, Kolarz A, Vogl AM, Dine J, Metzger MW, Schmid B, Almada RC, Ressler KJ, Wotjak CT, Grinevich V, Chen A, Schmidt MV, Wurst W, Refojo D, Deussing JM. Chronic CRH depletion from GABAergic, long-range projection neurons in the extended amygdala reduces dopamine release and increases anxiety. ***Nat Neurosci***. 2018 Jun;21(6):803-807.

Chang S*, Bok P, Sun C-P, Edwards A, Huang G-J. Neuropsin inactivation has protective effects against depressive-like behaviours and memory impairment induced by chronic stress. ***PLoS Genetics*** 2016; 12(10): e1006356. * First author

Cai N, Li Y, **Chang S**, Liang J, Lin C, Zhang X, Liang L, Hu J, Chan W, Kendler KS, Malinauskas T, Huang GJ, Li Q, Mott R, Flint J. Genetic control over mtDNA and Its relationship to major depressive disorder. ***Current Biology*** 2015 Dec 21;25(24):3170-77.

Cai N*, **Chang S***, Li Y*, Li Q, Hu J, Liang J, Song L, Kretzschmar W, Gan X, Nicod J, Rivera M, Deng H, Du B, Li K, Sang W, Gao J, Gao S, Ha B, Ho HY, Hu C, Hu J, Hu Z, Huang G, Jiang G, Jiang T,Jin W, Li G, Li K, Li Y, Li Y, Li Y, Lin YT, Liu L, Liu T, Liu Y, Liu Y, Lu Y, Lv L, Meng H, Qian P, Sang H, Shen J, Shi J, Sun J, Tao M, Wang G, Wang G, Wang J, Wang L, Wang X, Wang X, Yang H,Yang L, Yin Y, Zhang J, Zhang K, Sun N, Zhang W, Zhang X, Zhang Z, Zhong H, Breen G, Wang J,Marchini J, Chen Y, Xu Q, Xu X, Mott R, Huang GJ, Kendler K, Flint J. Molecular signatures of major depression. ***Current Biology*** 2015 May 4;25(9):1146-56. *Co-first author

Poster presentation

Chang S, Jan M Deussing et.al. Characterization of CRH/CRH receptor neurocircuitries and their involvement in stress

FENS 2018 Forum, Berlin, Germany.

Chang S, Huang GJ. Neuronal Pentraxin II as a key component in the regulation of anxiety

SFN Neuroscience 2016, San Diego, USA.

Chang S, Huang GJ. Neuropsin inactivation has protective effects against depressive-like behaviours and memory impairment induced by chronic stress.

FENS 2016 Forum, Copenhagen, Denmark.

Chang S, Huang GJ. Neuropsin provides a protecting effect and impaired PTSD-like behaviour.

FENS 2013 Regional meeting, Prague, Czech Republic.

6.3 Acknowledgements

I would like to thank Jan, my supervisor, for your unconditional support toward this study and allowing me to try out all the different possibilities. With your great sense of humour and useful comments makes this path toward my PhD full of colours and energies. Together we are able to create plenty of fun even the obstacle seemed so hard to crack, this will forever be an unforgettable period of time in my life.

I would also like to dedicate my great thanks to Carsten and Prof Dr. Wolfgang Wurst. Both of you have really great patience in listening to all my struggles in the TAC meeting and provided many useful information that shaped this project in a good way without doubt.

Thanks to many friends in the institute which I will not list all the names. I will always remember all the warmth and helps that you all provided during all the good and bad time. Among of the friends, I must mention the unconditioned supports from Chu-Lan who helped me to settle in Munich and also provided all the professional assists in this story. Without Na and Lianyuan we would not have our beautiful sequencing data in this study and thanks for having patience with all my questions and requests.

There are few colleagues I would like to mention in order to give them my greatest respect and say a big thank you: Laura, you are such a smart student and colleague, without your help it might be impossible to have all the CLARITY setup and running properly. All the jokes and complaints we shared will always be a memory, it is my pleasure to be able to work together with you.

Claudia, always sharing all the information, happiness and sadness with me, you are a great colleague who taught me a lot and always being there reminding me that sometimes rules might also be useful. I know sometimes I do have too many complaints but you are still there consulting me without any condition.

Mira, I will always miss all your jokes and all the knowledge that you shared with me. You are one of the great examples that hard working and perfection leads to something amazing. It is also a great pleasure for me to worked with you.

My great thanks also go to all our collaborators that helped us to make this story complete and wonderful. To all the technical service and to Stefi and Sarbrina of GEMM that make my life easier with all the hard works and of course all the laughter.

Of course, to all the people who once made my life difficult, obstacle will only make me stronger and I will keep breaking it down. I learned a lot during these years facing all the bad thigs and think into a positive way. For this I also cast my thanks to you all.

Before going to the end, thanks all the mice that gave their lives in this study, I am sorry you can't have a better life but you guys/girls are the best. Rest in peace and I hope you have a better next life.

In the end, love might not solve all the problems but without love there are only problems left. Federica, it is amazing to find a person in my life that is able to understand all the weird thoughts coming out from my mind. Someone who can always ease my temper while things are going wrong and all your wonderful supports make my life complete. I will definitely remember all the expertise and great scientific supports that you provided.

6.4 List of contributions

All experiments were conducted by Simon Chang besides the FACS which was carried out by Dr. Rossella Di Giaimo in Max Planck Institute of Psychiatry.

Dr. Chu-Lan Lao provided the virus used for rabies tracing from LMU.

Prof Dr. Karl-Klaus Conzelmann provided the rabies virus from LMU.

Single-nuclei sequencing data was analysed by Dr. Na Cai and Lianyuan Huang from Helmholtz pioneer campus.

Federica Fermani provided great assist in setting up optogenetic facility in Max Planck Institute of Psychiatry.

Laura Sotillos provided assist of setting up CLARITY facility in Max Planck Institute of Psychiatry.

6.5 Eidesstattliche Versicherung/Affidavit

Hiermit versichere ich an Eides statt, dass ich die vorliegende Dissertation „EXTENDED AMYGDALA CRH CIRCUITS TRIGGER AVERSIVE RESPONSES“ selbstständig angefertigt habe, mich außer der angegebenen keiner

weiteren Hilfsmittel bedient und alle Erkenntnisse, die aus dem Schrifttum ganz oder

annähernd übernommen sind, als solche kenntlich gemacht und nach ihrer Herkunft unter

Bezeichnung der Fundstelle einzeln nachgewiesen habe.

I hereby confirm that the dissertation “Extended Amygdala CRH circuits trigger aversive responses” is the result of my own work and

that I have only used sources or materials listed and specified in the dissertation.

München, den Unterschrift

Munich, 10.09.2021 Simon Chang